UNDERSTANDING HOW THE TRAFFICKING OF CYTOKINETIC ENZYMES IS REGULATED DURING MITOTIC EXIT IN *SACCHAROMYCES CEREVISIAE*

BY

CHIN CHEEN FEI

B.SC. (Hons), UTAR

A THESIS SUBMITTED

FOR THE DEGREE OF PHD OF SCIENCE

DEPARTMENT OF BIOCHEMISTRY

NATIONAL UNIVERSITY OF SINGAPORE

2014

DECLARATION

I hereby declare that the thesis is my original work and it has been written by me in its entirety. I have duly acknowledged all the sources of information which have been used in the thesis.

This thesis has also not been submitted for any degree in any university previously.

CHIN CHEEN FEI

31 MARCH 2014

Acknowledgement

First and foremost, I would like to acknowledge and extend my heartfelt gratitude to my PhD supervisor, Dr. Yeong Foong May for her encouragement, scientific insights, stimulating discussions, and great patience throughout my study. Her enthusiasm for science was contagious and motivational. Without her continuous guidance, the completion of this dissertation would not have been possible. I am also very grateful for her support of my attendance at scientific conferences that allowed me to present our work to the scientific community.

I am indebted to my colleague, Ms. Chew YuanYuan for her excellent technical support, encouragement and for sharing the laughter throughout my study. It has always been a great pleasure working with her in the lab. I would also like to extend my sincere gratitude to Ms. Beryl Augustine and Mr. Lee WeiRen for their insightful discussion and technical assistance to the work in this thesis.

Special thanks to Mr. Tan KaiQuan for his time and insightful comments in proof reading this thesis. I also owe my appreciation to all ex-YFM lab members who had contributed to the work in this dissertation.

I am grateful to the Ministry of Education (MOE), Singapore and Yong Loo Lin School of Medicine, National University of Singapore (NUS) for the scholarship and research funding. In addition, special thanks to Genetic Society of America (GSA), American Society for Cell Biology (ASCB) and Department of Biochemistry (NUS) for providing the scientific conference

travel fellowships that granted me opportunity to interact with excellent scientists that share my passion in science.

Last but not least, I owe my deepest appreciation to my parents and siblings for their love and continuous support to pursue my dream in science.

Publications

Research Articles

1. Chin CF, Bennett AM, Ma WK, Mark C. Hall and Yeong FM. Dependence of Chs2 ER export on dephosphorylation by cytoplasmic Cdc14 ensures that septum formation follows mitosis. *Molecular Biology of the Cell*. 2012 Jan;23(1):45-58. PMID:22072794

2. Chin CF, Onishi M, Chew YY, Lee WR, Augustine B, and Yeong FM. Continuous endocytosis of cytokinetic enzymes maintains mitotic spindle integrity during mitotic exit. (Manuscript in preparation).

International Conference Abstracts

1. Chin CF and FM Yeong, "Regulation of Chs2p trafficking at the end of mitosis". The Genetics Society of America Conferences (2010). The Genetics Society of America. (Yeast Genetics and Molecular Biology Meeting, 27 Jul - 1 Aug 2010, University of British Columbia, Vancouver, Canada). Chin CF awarded travel award from the Yeast Genetics and Molecular Biology Meeting organizers. Poster presentation.

2. Chin CF, Beryl Augustine and FM Yeong, "Cell Cycle Regulated Chs2p Endocytosis at the end of mitosis". *Molecular Biology of the Cell* (2012). (2012 American Society for Cell Biology (ASCB) Annual Meeting, San Francisco, CA-USA). Chin CF awarded travel fellowship from the ASCB meeting organizers and Department of Biochemistry,NUS. Poster presentation.

3. Beryl Augustine, Chin CF, and FM Yeong, "Clathrin Mediated Endocytosis of Chs2p at the end of Mitosis". *Molecular Biology of the Cell* (2012). (2012 American Society for Cell Biology (ASCB) Annual Meeting, San Francisco, CA-USA). Poster presentation.

4. Chin CF, Bennett AM, Ma WK, Mark C. Hall and Yeong FM. Chs2 Dephosphorylation and ER Export during Mitotic Exit are Controlled by Spatial-temporal Regulation of Cdc14 Phosphatase. Mass Spec 2013 - New Horizons in MS Hyphenated Techniques and Analyses (6-7 March 2013- Biopolis Singapore). Poster presentation.

5. Chin CF, Onishi M, Chew YY, Lee WR, Augustine B, and Yeong FM. Defects in endocytosis of chitin synthases alter AMR constriction dynamics during cytokinesis". The EMBO Meeting, 21- 24 September, 2013, Amsterdam, Netherlands. Poster presentation.

Table of Contents

Summary

Cytokinesis is the final step of cell division cycle in which a dividing cell undergoes physical separation to form two progeny cells. The splitting of the cell is usually restrained until completion of nuclear division. In budding yeast, cytokinesis is accomplished by the spatio-temporal coordination of acto-myosin ring constriction (AMR) and septation. The primary septum in yeast is synthesized by a transmembrane protein, chitin synthase II (Chs2p). During metaphase-anaphase transition, Chs2p is retained in the endoplasmic reticulum due to its N-terminal phosphorylation of 4 Cdk1 perfect sites by mitotic cyclin dependent kinase, Cdk1p. At the end of mitosis, destruction of mitotic cyclins and activation of Mitotic Exit Network (MEN) triggers Chs2p ER export. Chs2p is then delivered to the division site to lay down the primary septum. The roles of Chs2p in regulating primary septum formation and facilitating AMR constriction are well documented in many studies. Nevertheless, the underlying mechanism that is responsible for the timely Chs2p ER export is yet to be elucidated. Here, this study shows that Chs2p is a novel substrate for Cdc14p phosphatase (the ultimate effector of the MEN). At late telophase, Chs2p ER export requires the direct reversal of the inhibitory Cdk1 phosphorylation by cytoplasmic localization of Cdc14p. Timely MEN dependent Cdc14p cytoplasmic localization at the end of mitosis ensures Chs2p ER export and septum formation invariably occurs only after completion of chromosome segregation.

Upon arrival at division site, Chs2p is rapidly internalized through clathrin-mediated endocytosis (CME) and targeted to vacuole for degradation.

However, the key factor that triggers Chs2p internalization remains unrevealed. The data from this study indicate that the timely retrieval of Chs2p from division site is regulated by evolutionarily conserved proteins, yeast casein kinases, Yck1/2p. In the absence of Yck1/2p activity, Chs2p endocytosis is severely compromised. Mutagenesis study revealed that Yck1/2- phospho-deficient mutant, Chs2p-(15S-to-15A)-YFP failed to be internalized during mitotic exit. Coincidentally, Yck1p/2p colocalized with Chs2p at the division site during mitotic exit. These results suggest that Yck1/2p dependent phosphorylation on Chs2p might serve as a signal for Chs2p endocytosis at the correct time. This study is the first to show that Yck1/2p controls the endocytosis of the cell cycle regulated cargo, Chs2p, which is involved in facilitating AMR constriction during mitotic exit.

At late mitosis, it has been previously shown that the Chs2p localizes to the division site before spindle disassembly, and subsequent cytokinesis. The deposition of primary septum by Chs2p at the neck has been demonstrated to provide mechanical support for AMR constriction. Therefore, this raises the question of how cells coordinate the constriction of AMR at the division site to ensure spindle disassembly precedes AMR constriction. In this study, we establish that cells coordinate these two events by regulating the continuous endocytosis of cytokinetic enzymes - Chs2p, Chs3p and Fks1p at the division site. Failure to endocytose cytokinetic enzymes at late mitosis results in a thickened cell wall, aberrant septation and mitotic spindle breakage. Interestingly, defective endocytosis of cytokinetic enzymes causes premature AMR constriction that leads to spindle breakage. As a consequence of mitotic

spindle breakage, the spindle fails to reassemble in the subsequent round of cell division.

Collectively, the evidence gathered in this study has provided a new perspective on how the cell coordinates the protein trafficking of cytokinetic enzymes with late mitotic events. Upon chromosome segregation, MEN dependent mitotic kinase destruction and Cdc14p release into the cytoplasm permits Chs2p ER export to the division site and prior to spindle disassembly. The neck localization of Chs2p deposits the primary septum and facilitates the constriction of AMR. This mechanism regulates the timely delivery of Chs2p to the division site to ensure physical separation of the mother-daughter cells is prohibited prior to chromosome segregation. In parallel to Chs2p division site localization, a signal for endocytosis retrieval of Chs2p is imposed by Yck1/2p. Concurrently, Chs3p and Fks1p are also internalized through CME in a continuous manner prior to spindle disassembly and AMR constriction. The timely turnover of cytokinetic enzymes at the division site is crucial in maintaining spindle integrity by preventing premature AMR constriction during mitotic exit.

List of Tables

List of Figures

Abbreviations

AMR	Actomyosin Ring
aMT	Astral Microtubule
APC	Anaphase-Promoting Complex
Cdk	Cyclin Dependent Kinase
CME	Clathrin Mediated Endocytosis
COPII	Coat Protein Complex II
C-terminal	Carboxyl Terminal
DMSO	Dimethyl Sulfoxide
ECFP	Enhanced Cyan Fluorescent Protein
EDTA	Ethylenediaminetetraacetic acid
ER	Endoplasmic Reticulum
Gal	Galactose
GFP	Green Fluorescent Protein
Glu	Glucose
GPCR	G-Protein Coupled Receptor
GST	Gluthatione S-transferase
HIS	Histidine
HPH1	Hygromycin
ipMT	Interpolar Microtubule
KAN	Geneticin G418
kMT	Kinetochore Microtubule
LatB	Latrunculin B
LEU	Leucine
MCC	Mitotic Checkpoint Complex
mCHERRY	monomeric Cherry Fluorescent Protein

MEN	Mitotic Exit Network
MT	Microtubule
MTOC	Microtubule Organizing Center
NAT	Nourseothricin
Noc	Nocodazole
N-terminal	Amino Terminal
PAGE	Polyacrylamide gel electrophoresis
PBS	Phosphate Buffered Saline
PCR	Polymerase Chain Reaction
PM	Plasma Membrane
PMSF	Phenyl Methane Sulfonyl Fluoride
PS	Primary Septum
Raf	Raffinose
REDSTAR	Redstar Fluorescent Protein
RER	Rough Endoplasmic Reticulum
RFP	Red Fluorescent Protein
RT	Room Temperature
SC	Synthetic Complete
SD	Standard Deviation
SEM	Standard Error of the Mean
SPB	Spindle Pole Body
SS	Secondary Septum
TBE	Tris-Borate-EDTA
TCA	Trichloroacetic Acid
TGN	Trans-Golgi Network
TRP	Tryptophan
ts	temperature sensitive

URA	Uracil
YFP	Yellow Fluorescent Protein
YP	Yeast Extract
YPD	Yeast Extract-Peptone-Dextrose

Chapter 1 Introduction

1.1 Overview of the study

The cell division cycle is a fundamental mechanism of cell reproduction in all living organisms, from unicellular prokaryotic and eukaryotic cells to the multicellular mammals. The concept -'*Omnis cellula e cellula'* (every cell originates from another pre-existing cell) was postulated by the German pathologist Rudolf Virchow in 1855. Virchows's cell theory laid the conceptual foundation for eukaryotic cell-division cycle (Schultz, 2008).

Eukaryotic cell division cycle comprises 4 main phases, namely, G1 (Gap1), S (Synthesis), G2 (Gap2) and M (Mitosis) phase (Bähler, 2005). The last phase of the cell division cycle, M-phase, is the stage where a cell segregates its duplicated chromosomes to form two genetically identical daughter cells. M-phase is further categorized into four distinct stages, namely, prophase, metaphase, anaphase and telophase. At the end of mitosis (telophase), the dividing cell undergoes cytokinesis that physically splits the cells apart to form progeny cells. In animal and fungal cells, cytokinesis involves an acto-myosin ring (AMR) constriction that drives the formation of a cleavage furrow and membrane ingression at the midbody [reviewed in (Balasubramanian et al., 2004)].

In budding yeast, cytokinesis is tightly coordinated with other mitotic events to ensure that cells undergo physical separation after chromosome segregation. As a cell enters mitosis, it starts to accumulate mitotic cyclins such as Clb2p (homolog of mammalian cyclin B) (Fitch et al., 1992). Association of Clb2p with Cdk1p forms the Clb2p-Cdk1p complex that acts to promote mitotic entry by triggering events such as mitotic spindle assembly and chromosome condensation. After nuclear division, destruction of mitotic cyclins and

inactivation of mitotic kinase (mitotic exit) trigger the execution of the final event of the cell division cycle- cytokinesis.

At telophase, cytokinesis is accomplished by the spatio-temporal coordination of AMR constriction and centripetal deposition of primary septum (PS) by chitin synthase II (Chs2p) (Schmidt et al., 2002; VerPlank and Li, 2005). During mitotic exit, actin-cytoskeleton reorganization leads to the realignment of actin cables to the division site [reviewed in (Bi and Park, 2012a)] . The realignment of actin cables targets the exocytosis of Chs2p via COP II secretory pathway from the endoplasmic reticulum (ER) to the division site to lay down the primary septum (Chuang and Schekman, 1996; VerPlank and Li, 2005; Zhang et al., 2006). After the formation of the primary septum, Fks1p (catalytic subunit of β-1,3-glucan synthase) together with Chs3p (chitin synthase III) synthesizes the glucan-mannan rich secondary septum next to the ingressing primary septum [reviewed in (Weiss, 2012)] . The primary septum and secondary septum form a tri-laminar structure that physically partitions the cytoplasm of the mother-daughter cells. Subsequently, Chs2p and Chs3p are endocytosed from the division site in a Sla2p-dependent manner (Chin et al., 2011; Chuang and Schekman, 1996; Ziman et al., 1998). Finally, the separation of mother-daughter cells is achieved through the digestion of PS by the chitinase, Cts1p (Kuranda MJ, 1991).

The execution of cytokinesis has to be coordinated with other late mitotic events such as spindle disassembly. Upon Chs2p arrival at the neck, the mitotic spindle is rapidly disassembled prior to cytokinesis. This observation

suggests that an intimate relationship might exist between these two biological processes.

The processes of the PS, SS formation and AMR constriction are well described in many studies. However, the molecular mechanism that regulates the timely export of the protein that synthesizes the primary septum, Chs2p from the ER to the division site during mitotic exit remains unexplored. The processes of septum formation, cytokinesis and spindle disassembly are also contingent upon mitotic exit when the mitotic Cdk1p activity is destroyed. As all of these events occur during late mitosis, this raises the question of how cells coordinate cytokinesis and spindle disassembly to ensure spindle disassembly always precedes cytokinesis.

1.2 Cell division cycle in *Saccharomyces cerevisiae*

1.2.1 Yeast cell cycle regulation and cyclin-dependent kinases

Cell Division Cycle is a fundamental process for all living organisms for cell growth and reproduction. In early 1970s, the landmark genetic screen that was performed by Lee Hartwell isolated temperature sensitive mutant yeast strains that exhibited abnormalities in cell division cycle (*cdc*) (Hartwell, 1967). The most remarkable discovery in the screen was the identification of the *CDC28* (mammalian homolog-*CDK1*) gene that serves as a master regulator of the cell division that is conserved among the eukaryotic cells (Hartwell et al., 1970).

In eukaryotic cells, cell division cycle is divided into 4 main phases, G1 (Gap1), S (Synthesis), G2 (Gap2) and M (Mitosis) (Bähler, 2005). The progression of the cell through the cell cycle is tightly regulated by the oscillation of cyclin-Cdk (cyclin dependent kinase) activity. Association of the

phase specific cyclin with Cdk1p forms the cyclin-Cdk1 complex that drives the cell cycle progression. The oscillation of the kinase activities during cell cycle progression is controlled by the timely synthesis and destruction of cyclins, fluctuation of Cdks inhibitor (CKI) levels and by the antagonistic activity of phosphatases [reviewed in (Enserink and Kolodner, 2010)]. As the key research interest in this work is to understand the protein trafficking of cytokinetic enzymes at the end of mitosis, the literature review will mainly focus on mitosis.

1.2.2 Mitosis

Mitosis is a crucial process in cell division cycle in which a cell segregates its duplicated chromosomes to form two genetically identical progeny cells. This process is categorized into 4 main stages, prophase, metaphase, anaphase and telophase. In higher eukaryotic cells, dividing cells undergo open mitosis in which the nuclear envelope is disassembled prior to chromosome segregation in metaphase. Upon completion of chromosome segregation, nuclear envelope is reformed prior to cytokinesis. On the contrary, fungi cells such as budding yeast undergo a closed mitosis in which chromosome segregation takes place within an intact nucleus (De Souza and Osmani, 2007).

1.2.3 Mitotic entry

The entry into mitosis is driven by the activation of mitotic kinase, Cdk1p activity. During G2/M phase transition, Clb2p, the major mitotic cyclin that drives mitosis in budding yeast is gradually accumulates and binds to Cdk1p to form the mitotic kinase complex, Clb2p-Cdk1p. However, the mitotic kinase formed is inactive due to the inhibitory phosphorylation imposed by Swe1p (*Saccharomyces WEE1* homologue) kinase at the tyrosine-19 residue

of Cdk1p (Booher et al., 1993). To promote mitotic entry, activation of Clb2-Cdk1p complex is achieved through reversal phosphorylation by Mih1p (mammalian *CDC25* homologue) (Russell et al., 1989). Upon activation, Clb2p-Cdk1p complex drives early mitotic events such as mitotic spindle assembly and chromosome condensation (Enserink and Kolodner, 2010).

1.2.4 Mitotic exit

1.2.4.1 Destruction of mitotic cyclins during mitosis.

High Clb2p-Cdk1p activity drives mitotic progression until sister chromatids aligned at the metaphase plate [reviewed in (Wurzenberger and Gerlich, 2011). At this stage, cells are ready to progress to anaphase where chromosome segregation takes place. However, the degradation of the mitotic cyclins is a prerequisite for cells to exit from the mitosis. The destruction of mitotic cyclins requires the activity of E3 ubiquitin ligase- APC (Anaphase-Promoting Complex) which promotes mitotic kinase destruction though ubiquitination of mitotic cyclin, Clb2p. Ubiquitinated Clb2p then targeted for degradation via the 26S proteasome (Irniger et al., 1995).

Activity of the APC is regulated in a bi-phasic manner by binding to its activators, Cdc20p and its homologue Cdh1p (Yeong et al., 2000). The binding of Cdc20p to the APC is tightly regulated by the spindle assembly checkpoint (SAC) during mitosis. At metaphase, attachment of mitotic spindle to the chromosome alleviates the inhibitory signal that is imposed by SAC and triggers the activation of APC by its activator, Cdc20p [reviewed in (Peters, 2006)]. Activated APC^{Cdc20} targets securin, Pds1p (separase, Esp1p inhibitor) for 26S proteasome degradation through ubiquitination (Cohen-Fix et al.,

1996). Degradation of Pds1p leads to the liberation of Esp1p which in turn cleaves the cohesion complex that holds the sister chromatid together (Uhlmann et al., 2000). This promotes sister chromatid separation and triggers the onset of anaphase. Concurrently, APC^{Cdc20} also initiates the first wave of mitotic cyclin destruction leading to a 50% reduction of mitotic kinase activity (Yeong et al., 2000). Nevertheless, the activation of APC^{Cdc20} *per se* is inadequate to complete the destruction and inactivation of mitotic cyclins. Furthermore, reversal of phosphorylation of Cdk1p substrates is also essential for mitotic exit. Therefore, an additional regulatory network which involves an evolutionarily conserved phosphatase, Cdc14p, is required to complete the mitotic exit process in budding yeast.

1.2.4.2 Cdc14p Regulation

In budding yeast, Cdc14p (a dual specificity phosphatase) is the key player that mediates late mitotic events such as chromosome segregation, spindle elongation and cytokinesis. Cdc14p is sequestered in the nucleolus in most of the cell cycle stages through association with its nucleolar inhibitor, Net1p (Shou et al., 1999; Visintin et al., 1999). The activity of Cdc14p is controlled by two regulatory networks known as CdcFourteen Early Anaphase Release (FEAR) and Mitotic Exit Network (MEN) [reviewed in (Stegmeier and Amon, 2004)].

1.2.4.3 CdcFourteen Early Anaphase Release (FEAR)

During early anaphase, when mitotic activity is high, FEAR is triggered through the activation of Esp1p (separase) by APC^{Cdc20} dependent degradation of Pds1p (securin). Esp1p that is freed from Pds1p binds directly to an

evolutionarily conserved phosphatase, $PP2A^{Cdc55}$ and inhibits its activity (Queralt et al., 2006; Wang and Ng, 2006). However, the down regulation of PP2A-Cdc55p activity is independent of separase's proteolytic activity. Two PP2A interactors, Zds1p and Zds2p (zillion different screens) have been shown to physically interact with separase. Over-expression of Zds1p and Zds2p is sufficient to down regulate the $PP2A^{Cdc55}$ activity and permits Cdc14p nucleolar release. *zds1*Δ *zds2*Δ abolishes the separase driven nucleolar release of Cdc14p suggesting that Zds1p and Zds2p are downstream effectors of separase (Queralt and Uhlmann, 2008b). Nonetheless, the underlying mechanism of how separase contributes to down regulation of $PP2A^{Cdc55}$ remains unclear.

The reduction in $PP2A^{Cdc55}$ activity permits the phosphorylation of Net1p by Clb-Cdk1p (Azzam et al., 2004) and Polo-like kinase Cdc5p (Shou et al., 2002). This triggers the nucleolar release of Cdc14p to the nucleoplasm. Cdc14p in the nucleoplasm mediates spindle elongation by dephosphorylating spindle midzone proteins during early anaphase (Khmelinskii et al., 2007; Woodbury and Morgan, 2007). However, the release of Cdc14p to the nucleoplasm is transient due to the decline in Cdk1p activity that fails to sustain the Net1p phosphorylation during anaphase transition (Queralt et al., 2006). Furthermore, Cdc14p has been proposed to be involved in negative feedback loop that promotes its own nucleolar re-sequestration (Manzoni et al., 2010; Tomson et al., 2009; Visintin et al., 2008).

1.2.4.4 Mitotic Exit Network (MEN)

As cells progress to late anaphase, the second wave of mitotic cyclins destruction is dependent on the Mitotic Exit Network (MEN). The activation of this network is required to complete the inactivation of mitotic Cdk1p activity during mitotic exit. MEN is a Ras-like GTPase signalling cascade that consists of Tem1p (a GTPase), Lte1p (a GTP/GDP exchange factor), Cdc15p (Hippo-like kinase), Cdc5p (Polo-like kinase), Dbf2p/Dbf20p (Ser/Thr kinase), Mob1p (a kinase) and its ultimate effector Cdc14p (Ser/Thr phosphatase) (D'Amours and Amon, 2004).

During anaphase progression, Tem1p is concentrated at the daughter cell's spindle pole body (dSPB). Spindle elongation triggered by FEAR promotes the migration of the SPB into the daughter cell bringing Tem1p in close proximity to its GTP/GDP exchange factor, Lte1p that resides at the daughter cell cortex (Bardin et al., 2000; Pereira et al., 2000). However, the activation of Tem1p is negatively regulated by the GTPase activating protein (GAP), Bfa1p-Bub2p complex. In most stages of cell cycle, MEN is kept inactive by Bfa1p-Bub2p complex until mid-late anaphase where Cdc5p inhibits the complex component, Bfa1p through phosphorylation. Recently, a study from Queralt's group showed that Cdc5p dependent phosphorylation of Bfa1p is negatively regulated by the counteracting activity of $PP2A^{Cdc55}$ (Baro et al., 2013). As mentioned in previous section, FEAR activation contributes to the down-regulation of $PP2A^{Cdc55}$ activity. The inhibition of the $PP2A^{Cdc55}$ activity tips the kinase-phosphatase balance towards the Cdc5p and promotes the phosphorylation of Bfa1p. The alleviation of the Bfa1p inhibitory signal on MEN permits the activation of Tem1p. GTP-bound Tem1p then activates the

Cdc15p kinase through direct interaction, which in turn activates the downstream kinase Dbf2p (Jaspersen et al., 1998; Lee et al., 2001; Mah et al., 2001). Association of Dbf2p with Mob1p forms a kinase complex that promotes full-blown nucleolar release of Cdc14p to the cytoplasm. Concurrently, Dbf2p-Mob1p kinase complex also mediates Cdc14p cytoplasm retention by phosphorylating the Cdc14p nuclear localization signals (NLS) (Mohl et al., 2009).

MEN triggered Cdc14p released into the cytoplasm then increases the transcription of Sic1p (a Cdk1p inhibitor) through the dephosphorylation of the *SIC1* transcription factor Swi5p (Visintin et al., 1998). Concurrently, Cdc14p also dephosphorylates Cdh1p. Activated APC^{Cdh1} coupled with Sic1p accumulation causes the further inactivation of mitotic kinase activity, which drives cells to enter G1 phase (Visintin et al., 1998). Besides its role in mediating mitotic kinase destruction, Cdc14p cytoplasm release also promotes execution of mitotic exit events such as spindle disassembly, nuclear division and cytokinesis.

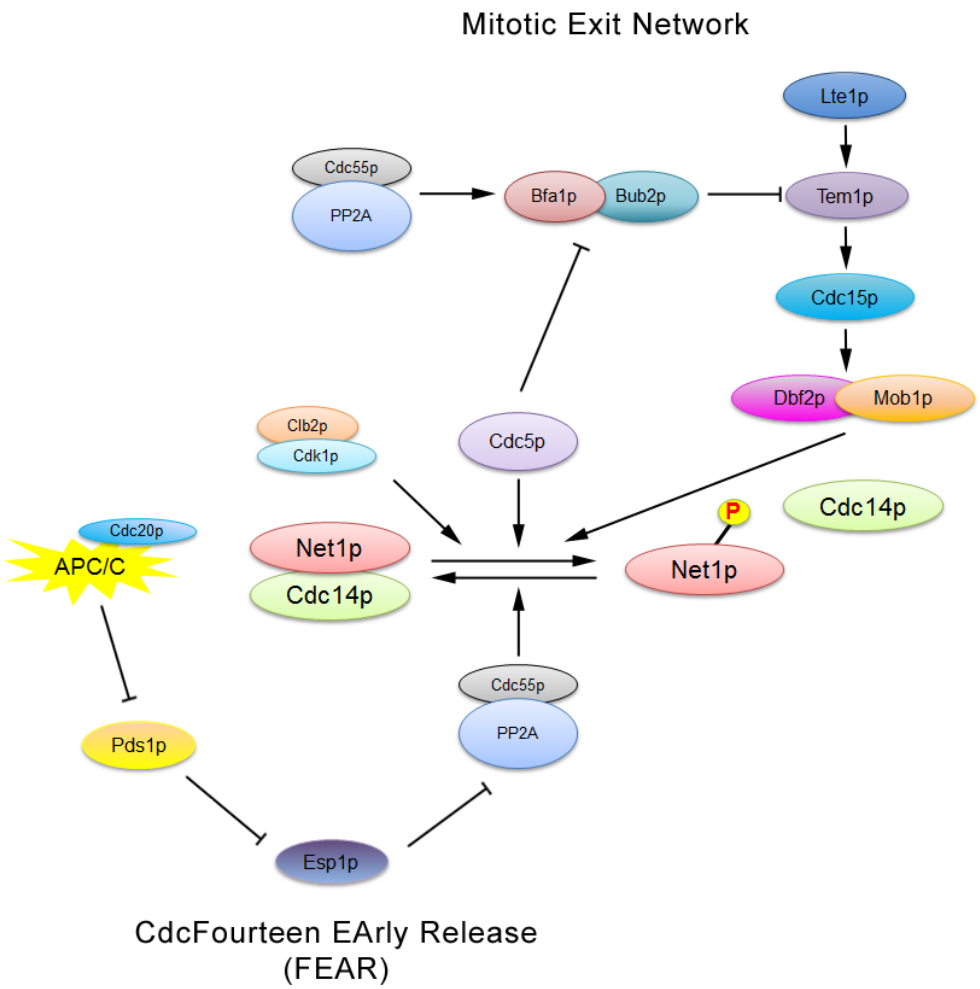

Figure 1.1 A schematic diagram of Cdc14p regulation in budding yeast. The spatio-temporal localization of Cdc14p is regulated by FEAR and MEN. At the onset of anaphase, activation of separase, Esp1p, contributes to the down regulation of $PP2A^{Cdc55}$. The reduction $PP2A^{Cdc55}$ activity promotes the phosphorylation of Net1p by Clb-Cdk1p and Cdc5p that eventually triggers the nucleolar release of Cdc14p to nucleoplasm. FEAR dependent Cdc14p nucleoplasm localization mediates the spindle elongation that lead to activation of Tem1p by Lte1p. This contributes activation of MEN cascade. The component of MEN, Dbf2p-Mob1p complex maintains Cdc14p cytoplasmic localization by phosphorylating Cdc14p NLS (see text for details).

1.2.5 Mitotic spindle microtubules dynamics

The spindle is a highly dynamic structure that changes its morphogenesis in a cell cycle regulated fashion. In budding yeast, spindle microtubules (MTs) are assembled from α-tubulin and β-tubulin heterodimers [reviewed in (Winey and Bloom, 2012)]. Assembly of spindle microtubules is initiated during G1-S-phase transition where the yeast Microtubule Organizing Center (MTOC) - spindle pole bodies are duplicated.

Upon duplication of the SPB, nuclear microtubules that emanate from both SPBs are nucleated together with additional motor proteins forming the bipolar mitotic spindle. Mitotic spindles are comprised of 3 types of MTs, astral MTs (aMTs), interpolar MTs (ipMTs) and kinetochore MTs (kMTs). These MTs work together to regulate many biological processes in the cell. For instance, aMTs that radiate from the SPB toward cell cortex are crucial in nuclear positioning. kMTs drive the chromosome segregation by providing the pushing and pulling force to separate the chromosomes to opposite spindle poles [reviewed in (Civelekoglu-Scholey and Scholey, 2010)]. On the other hand, ipMTs that emanate from the opposite spindle poles overlap and interdigitate in the middle of spindle to form the spindle midzone. The ipMTs are vital in providing the structural stability to the overall spindle structure, whereas spindle midzone plays an important role in chromosome segregation through generating forces required for spindle elongation (Glotzer, 2009).

During metaphase, faithful attachment of the microtubules to chromosome kinetochores, inactivates the spindle assembly checkpoint and triggers the dissociation of Cdc20p from the mitotic checkpoint complex (MCC) and

Mad2p-Cdc20p complex as a result of SAC inactivation [(Hardwick et al., 2000; Lau and Murray, 2012), reviewed in (Yu, 2002)]. Released Cdc20p in turn activates the APC complex and eventually lead to initiation of mitotic exit [reviewed in (Foley and Kapoor, 2013)]. At the onset of anaphase, Cdc14p release to the nucleoplasm stabilizes anaphase spindle through dephosphorylating Ask1p (a component of Dam1 complex) and Sli15p (a component of inner centromere-like protein (INCENP)-Aurora complex, Sli15p-Ipl1p). The dephosphorylated Ask1p and Sli15p-Ipl1p by then translocates from the kinetochores to the spindle, which in turn recruits kinetochore protein, Slk19p to the spindle midzone (Higuchi and Uhlmann, 2005; Pereira and Schiebel, 2003). In parallel, Ase1p is also dephosphorylated by Cdc14p. Dephosphorylated Ase1p together with Slk19p forms the functional midzone and promotes spindle elongation (Khmelinskii et al., 2007). Likewise, reversal of Cin8p phosphorylation by Cdc14p also promotes the spindle elongation during anaphase transition (Avunie-Masala et al., 2011).

As cell progresses through anaphase, activation of MEN leads to binding of APC to its cofactor Cdh1p. Activated APC^{Cdh1} in turn promotes mitotic spindle disassembly by targeting the microtubule cross-linking proteins that are involved in mitotic spindle stabilization such as Cin8p, Ase1p and Fin1p for proteosomal degradation (Hildebrandt and Hoyt, 2001; Juang et al., 1997; Woodbury and Morgan, 2007). The alternate pathway to trigger disassembly of the mitotic spindle is through aurora kinase B, Ipl1p and microtubule plus-end binding protein, Bim1p interaction (Tirnauer et al., 1999; Zimniak et al., 2009). At anaphase, Bim1p localizes to the microtubule plus ends to promote the stability of the midzone (Gardner et al., 2008). Phosphorylation of Bim1p

by Ipl1p triggers its dissociation from the microtubule and eventually causes the disassembly of spindle (Zimniak et al., 2009). Concurrently, Ipl1p also phosphorylates and activates She1p, which functions as a spindle destabilizer that promotes spindle disassembly (Woodruff et al., 2010).

In addition to Ipl1p, spindle disassembly is also regulated by the kinesin-8 motor protein, Kip3, which displays microtubule depolymerase activity (Gupta et al., 2006; Varga et al., 2006). Kip3p has been demonstrated to play a role in regulating the length of the astral microtubule and promoting microtubule depolymerization during spindle disassembly (Varga et al., 2006; Woodruff et al., 2010).

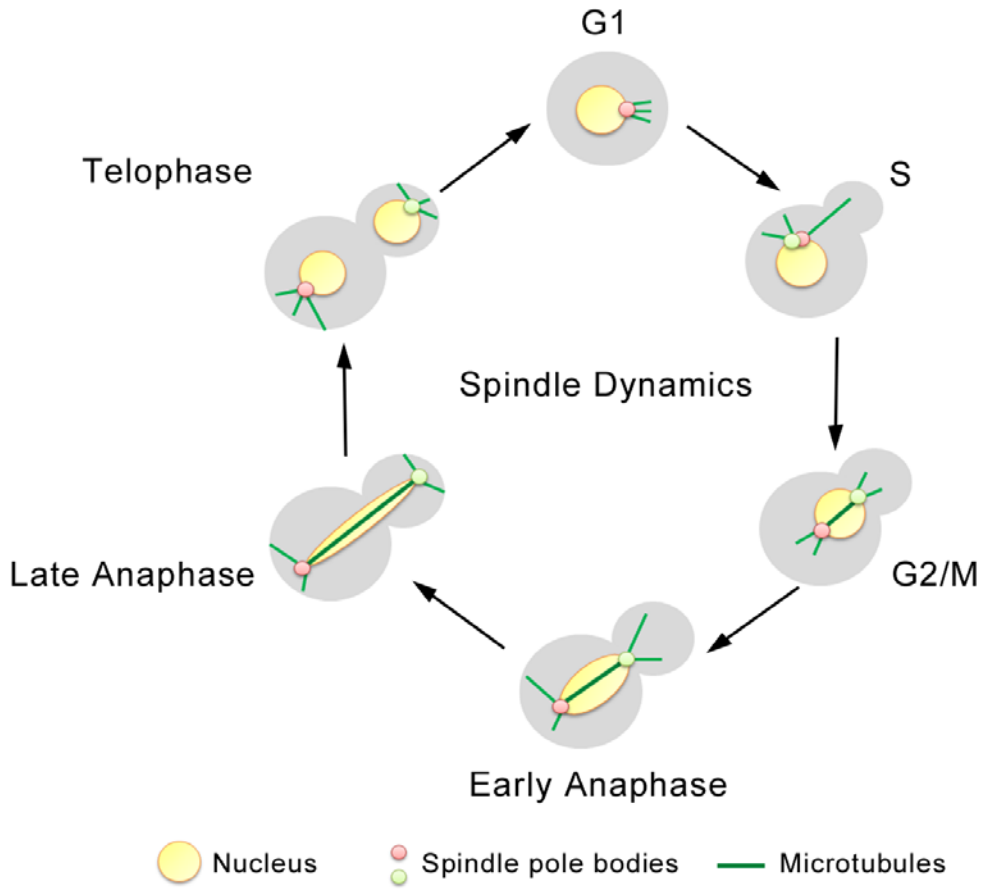

Figure 1.2 Mitotic spindle microtubules dynamics. The assembly of mitotic spindle begins during G1-S phase transition where duplication of spindle poles bodies (SPB) occurs. Once SPBs are duplicated, nuclear microtubules forms the bipolar mitotic spindle. At the onset of anaphase, dephosphorylation of microtubules-associated proteins promotes spindle elongation. During late anaphase, activation of MEN contributes to dismantle of mitotic spindle through different spindle disassembly pathways. After completion of cell separation, mother-daughter cells each contained a single SPB with a single set of genetic material.

1.2.6 Cytokinesis and cell separation

Cytokinesis is a process in which a mother-daughter cell undergoes physical separation after the segregation of genetic materials to yield two progeny cells. In budding yeast, cytokinesis is achieved by coordination between acto-myosin ring (AMR) constriction, membrane deposition and septum formation (Balasubramanian et al., 2004).

The core components of AMR in budding yeast include filamentous actin, Myo1 (Type II myosin heavy chain), Mlc1/2 (myosin light chains), and Iqg1 (IQ-motif containing GTPase-activating protein). Unlike fission yeast and mammalian cells, AMR assembly in budding yeast begins at the G1 phase when Myo1p localizes to the bud neck. (Bi et al., 1998; Lippincott and Li, 1998). This process is regulated by septins, which are GTP-binding proteins that are conserved from yeast to mammalian cells, but they are absent in plant cells and many protozoans. In budding yeast, the septins that are involved in cytokinesis during vegetative growth are encoded by five different genes namely, *CDC3*, *CDC10*, *CDC11*, *CDC12* and *SHS1* (Douglas et al., 2005). These proteins form the septin ring that functions as a scaffold for the assembly of AMR [reviewed in(Bi and Park, 2012b)].

At the onset of late anaphase, the activation of MEN component, Tem1p triggers the splitting of septin hourglass (Lippincott et al., 2001). However, the mechanism that promotes the splitting to septin hourglass is rather controversial. In a recent study, Meitinger and co-workers demonstrated that septin hourglass splitting is dependent on Dbf2p-Dbf20p activity. Defective septin ring splitting in *dbf2-2 dbf20*Δ cells can be rescued by ectopic expression of Sic1p suggesting that the activation of Dbf2p together with

mitotic kinase reduction triggers the septin hourglass splitting at late anaphase (Meitinger et al., 2010).

The split septin rings sandwich the AMR, Spa2p (component of polarisome), Sec3p (subunit of exocyst complex), Chs2p (chitin synthase II) and other factors at the cytokinetic site. It has been proposed that the split septin hourglass serves as a diffusion barrier to confine the cytokinetic proteins at the division site that is crucial in maintaining AMR function and membrane abscission (Dobbelaere and Barral, 2004). However, a recent report from Wloka and co-workers demonstrated that the septin diffusion barrier is not essential for faithful execution of cytokinesis (Wloka et al., 2011). The authors found that *cdc10*Δ cells that failed to form two discrete septin rings executed key processes in cytokinesis (AMR assembly, AMR constriction, primary and secondary septum formation) efficiently suggesting that septin diffusion barrier is dispensable for cytokinesis (Wloka et al., 2011).

In late anaphase, recruitment of yeast IQGAP protein, Iqg1 to the AMR triggers actin-cytoskeleton reorganization that leads to the realignment of actin cables to the division site (Epp and Chant, 1997). The realignment of actin cables targets the exocytosis of cytokinetic enzyme, Chs2p to the restricted membrane domain that is created by the splitting of septin hourglass (Dobbelaere and Barral, 2004). Arrival of Chs2p at the division site stabilizes the AMR, and subsequently triggers the constriction of AMR through deposition of chitin rich primary septum that promotes the ingression of plasma membrane (Schmidt et al., 2002; VerPlank and Li, 2005). Next, the AMR disassembles, the membranes of the mother-daughter cell pinches off, and the cells now are physically separated by a primary septum. Finally, the

cytokinesis process is completed. After primary septum formation, Fks1p (catalytic subunit of β-1,3-glucan synthase) together with Chs3p (chitin synthase III) synthesizes the glucan-mannan rich secondary septum at both side of the primary septum [reviewed in (Cabib et al., 2001; Lesage and Bussey, 2006)]. Once the tri-laminar septum is completed, the physical separation between the mother-daughter cells is achieved through secretion of digestive enzymes to the septum. Cell wall digestive enzymes such as chitinase, Cts1p together with a group of endoglucanases/ glucanosyltransferases (Dse2p, Dse4p, Egt2p, and Scw11p) digest the primary septum connecting the mother-daughter cells resulting in cells separation [(Baladron et al., 2002; Kuranda MJ, 1991) reviewed in (Adams, 2004; Weiss, 2012; Yeong, 2005)].

1.2.6.1 Septation

Septation is a process by which mother-daughter cells partition their cytoplasm through the synthesis of the cell wall known as septa. In budding yeast, the cytoplasm partition of cells is achieved by formation of primary and secondary septum during mitotic exit. The septa synthesis is tightly controlled by mitotic kinase destruction, Cdk1p inactivation and MEN. This mechanism ensures that the physical separation between the mother-daughter cells is strictly prohibited prior to chromosome segregation.

1.2.6.2 Primary septum formation

The primary septum is composed of chitin, a linear polysaccharide of 1-4 linked N-acetyl-β-glucosamine units (Bacon et al., 1966; Cabib and Bowers, 1971). Chitin in the primary septum is synthesized by the transmembrane

protein, Chs2p (chitin synthase 2). Consistent with its role in synthesizing the primary septum during cytokinesis, Chs2p transcription peaks at early G2/M phase (Cho et al., 1998; Pammer et al., 1992; Spellman et al., 1998). During metaphase, Clb2p-Cdk1p dependent phosphorylation of the N-terminal serine clusters of Chs2p leads to its retention in the rough endoplasmic reticulum (RER) (Martinez-Rucobo et al., 2009; Teh et al., 2009). Upon chromosome segregation, mitotic cyclins destruction and Cdk1p inactivation contributes to the decline in mitotic kinase activity. Concurrently, Chs2p is rapidly exported from the ER and transported to the mother-daughter neck via the COPII secretory pathway to deposit the primary septum (Chuang and Schekman, 1996; Meitinger et al., 2010; VerPlank and Li, 2005; Zhang et al., 2006).

Intriguingly, it has been previously shown that *in-vitro* Chs2p chitin synthase activity is relatively low without protease treatment (Silverman et al., 1988). This suggests that protease treatment on Chs2p might induce conformational changes that activate the enzyme. Hence, the Chs2p that is delivered to the division site might be inactive, and additional factors are required for the activation of Chs2p chitin synthase II activity. Indeed, a recent study identified Inn1p (required for Ingression) as a novel binding partner of Chs2p during mitotic exit (Devrekanli et al., 2012). *inn1*Δ cells display a phenotype that resembles *chs2*Δ cells where the plasma membrane fails to ingress, primary septum synthesis is inhibited, and the AMR is unstable and eventually collapses. This evidence indicates that Inn1p may be an activator for Chs2p. In addition to Inn1p, Cyk3p is also proposed to be a potential activator of Chs2p during cytokinesis as ectopic expression of Cyk3p rescues the cytokinesis defects in *inn1*Δ cells (Nishihama et al., 2009). Taken together, these data

suggest that Inn1p and Cyk3p serve as Chs2p activators which facilitate primary septum formation at the end of mitosis.

Upon arrival at the division site, Inn1p-Cyk3p activated Chs2p stabilizes the AMR, triggering the constriction of AMR that promotes the ingression of plasma membrane and deposits the chitinous primary septum (Schmidt et al., 2002; VerPlank and Li, 2005). At late stage of cytokinesis, Dbf2p phosphorylates Chs2p at serine-217 residue and promotes its dissociation from the AMR (Oh et al., 2012). Subsequently, Chs2p is rapidly internalized from the division site in a Sla2p dependent manner (Chuang and Schekman, 1996).

1.2.6.3 Secondary septum formation

Once the primary septum is formed, a glucan-mannan rich secondary septum is deposited on either side of the chitin disk.

In budding yeast, β-glucan of the cell wall is synthesized by the enzymatic complex β-1,3-Glucan Synthase (β-1,3-GS) which is comprised of Fks1p (catalytic subunit), Fks2p/Gsc2p (catalytic subunit), and Rho1p (regulatory subunit). The two catalytic subunits of β-1,3-GS, *FKS1* and *FKS2* are essential redundant paralogs that showed differential expression pattern. Fks1p is the major catalytic subunit of β-1,3-GS and mainly functions during vegetative growth whereas Fks2p is activated when cells are nutrient deprived (Mazur et al., 1995). At late mitosis, polarized secretion targets Fks1p translocation to the division site to synthesize the glucan-mannan rich secondary septum at either side of primary septum. Likewise, polarized secretion also delivers Chs3p (chitin synthase III) to the division site during mitotic exit. Concurrent with Fks1p, Chs3p synthesizes the chitin that provides structural

reinforcement to the glucan-mannan layer that is synthesized by β-1,3-GS (Cabib et al., 2001; Cabib and Schmidt, 2003; Schmidt et al., 2002; Ziman et al., 1998).

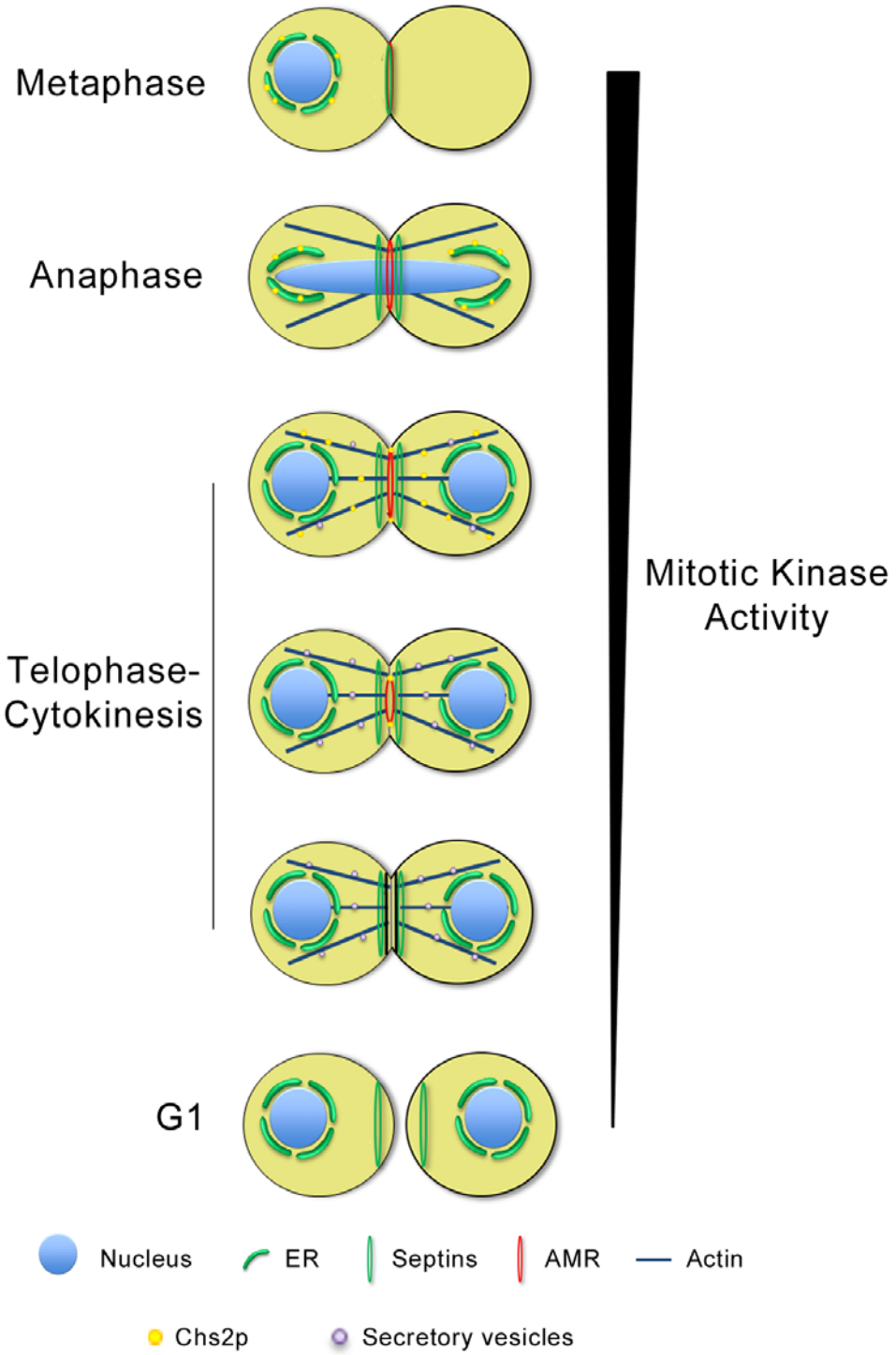

Figure 1.3 Cytokinesis in budding yeast. At metaphase when mitotic kinase activity is high, Chs2p is retained in the ER. During anaphase-telophase transition, inactivation of mitotic kinase activity (mitotic exit) contributes to the splitting of septins and actin-cytoskeleton repolarization towards the division site. This lead to the transport of Chs2p and other cytokinetic proteins contained secretory vesicles to the neck which in turn triggers the constriction of the AMR, septation and cell separation (see text for details).

1.3 Protein trafficking in *Saccharomyces cerevisiae.*

1.3.1 Secretory pathway

The secretory pathway is an evolutionarily conserved pathway in eukaryotic cells that utilizes specialized coated vesicles to deliver proteins from the endoplasmic reticulum to Golgi apparatus and finally to plasma membrane (Schekman, 2010). In budding yeast, the secretory pathway begins with the assembly of COPII coat that mediates the delivery of ER proteins to the Golgi apparatus. The secretory pathway begins with COPII coat assembly at ER exit sites (ERES- specialized, long lived sub-domains of ER) where the soluble and transmembrane cargoes are concentrated (Bannykh et al., 1996; Hammond and Glick, 2000). The COPII coat is comprised of Sar1p (a small GTPase), Sec12p (a Guanine nucleotide Exchange Factor, GEF), Sec23p/24p complex (COPII inner coat) and the Sec13p/31p complex (COPII outer coat).

Assembly of COPII coat is initiated with the recruitment of Sar1p (Bi et al., 2002). Upon activation by Sec12p, which resides in the ER membrane, the GTP-bound Sar1p then simultaneously induces the initial curvature of ER membrane and recruits the Sec23p/24p heterodimer that form the inner coat of COPII vesicle (Barlowe et al., 1993; Matsuoka et al., 1998). Sec23p serves as a GTPase Activating Protein (GAP) activating protein that upregulates the Sar1p GTPase activity (Yoshihisa et al., 1993). In parallel, Sec24p, which contains multiple independent cargo binding domains, captures the protein cargoes and packages the proteins into the COPII inner coat (Miller et al., 2002; Miller et al., 2003). Sar1p-Sec23p/23p complex forms the pre-budding complex and the Sec13p/31p hetero-tetramer is then recruited (Lederkremer et al., 2001). The Sec13p/31p complex further stimulates the Sar1p GTPase

activity and eventually unleashes COPII coated vesicles from the ER membrane.

Upon release from the ER, tethering and fusion of COPII vesicles with the Golgi apparatus is mediated through a group of tethering and fusion proteins such as Ypt1p (GTPase), Uso1p (tethering protein), TRAPPI (transport protein particle I) complex , Hrr25p (Casein kinase I) and Golgi SNAREs (Soluble NSF Attachment Protein Receptor) [reviewed in (Barlowe and Miller, 2013; Brandizzi and Barlowe, 2013)].

Once the vesicle fuses with the Golgi apparatus, the cargoes undergo modifications and are transported to the Trans-Golgi Network (TGN). After arrival at TGN, modified secretory cargo is sorted and packaged into post-Golgi vesicles which are eventually delivered to the destined organelles. The transport of post-Golgi vesicles to the plasma membrane requires actin cable and activity of type V Myosin, Myo2p (Pruyne et al., 1998). The tethering of secretory cargo to the plasma membrane is mediated by the evolutionarily conserved octameric complex termed as Exocyst which consist of Sec3p, Sec5p, Sec6p, Sec8p, Sec10p, Sec15p, Exo70p and Exo84p (Hsu et al., 1996; TerBush et al., 1996). The secretory vesicles then fuse with the plasma membrane and release their content into the extracellular matrix.

Previously, it has been assumed that the secretory cargoes are constitutively exported out from the ER throughout the cell cycle. For instance, the secretion of invertase and mating pheromone, alpha-factor was continuous even in mitosis (Makarow, 1988; Nevalainen et al., 1989). However, a study from Zhang and co-workers established a link between secretion and cell division

cycle. The authors demonstrated that the high mitotic kinase activity inhibited the ER export of cytokinetic enzyme, Chs2p to the division site during metaphase. During mitotic exit, destruction of mitotic kinase triggers the incorporation of Chs2p into the COPII vesicles which in turn translocated to the division site to lay down the primary septum (Zhang et al., 2006). This suggests that Chs2p is a secretory cargo and its secretion is controlled in a regulated manner.

1.3.2 Endocytic pathway

Endocytosis is a process by which cells internalize membrane proteins, extracellular particles and fluids, viruses and bacteria into the cell body. This process is highly conserved in all eukaryotic cells, and is involved in various cellular processes such as the turnover and degradation of proteins. Endocytosis is categorized into three main groups, namely; phagocytosis, pinocytosis, and receptor mediated endocytosis (clathrin or caveolin dependent) [reviewed in (Engqvist-Goldstein and Drubin, 2003)]. In this thesis, the literature review on endocytosis will mainly focus on clathrin-mediated endocytosis (CME) as the key interest in this study was to investigate the physiological significance of CME in regulating cytokinetic enzymes retrieval during mitotic exit.

1.3.2.1 Clathrin-mediated endocytosis in *Saccharomyces cerevisiae*

CME is the major route for protein cargo internalization from the plasma membrane in budding yeast. The endocytic proteins involved in the multi-stage CME were characterized from an elegant study using a combination of genetics and total internal reflection fluorescence (TIRF) microscopy (Kaksonen et al., 2003). In brief, CME is divided into 3 main phases:, early

immobile phase, intermediate/late immobile phase and WASP/ myosin/ actin/ slow mobile invagination phase [reviewed in (Boettner et al., 2011)]. During early immobile phase, arrival of clathrins- Chc1p and Clc1p, Eps15 homology (EH) domain protein Ede1p and the F-Bar protein Syp1p (FCHo1/SGIP1) at the endocytic initiation site establishes the endocytosis pits for protein internalization.

Next, intermediate/late immobile phase modules Sla2p and Pan1 complex (Sla1p-End3p-Pan1p) localizes to the site. Concurrently, yeast WASP- Las17p is recruited, followed by the departure of Ede1p and Syp1p from the endocytic site. Pan1p, Las17p, together with recruitment of other endocytic nucleation promoting factors (Myo3p/5p, Abp1p), endocytic factor- Vrp1p and actin trigger the WASP/Myosin/actin mobile invagination phase and promote a robust inward movement of the clathrin coat pit to form a tubular structure. Finally, the amphiphysins (Rvs161p/Rvs167p) and dynamin (Vps1p) drives the scission of the clathrin vesicle from the plasma membrane by narrowing the neck at the invagination tip.

After the scission of the clathrin vesicle from plasma membrane, the clathrin coat is rapidly removed by the synaptojanin and Ark1p/Prk1p kinases. Ark1p/Prk1p kinases phosphorylate several key endocytic components including Scd5p (targeting subunit of Protein Phosphatase 1, PP1), PAN complex components, Sla1p and Pan1p [(Henry et al., 2003; Huang et al., 2003; Zeng et al., 2001). This phosphorylation disrupts the interaction between the endocytosis complexes and contributes to the uncoating of the clathrin vesicle. The Ark1p/Prk1p dependent phosphorylation of endocytosis components are later reversed by Scd5-Glc7-PP1 phosphatase complex

(Chang et al., 2002; Zeng et al., 2007). The reversal of phosphorylation on endocytosis components is vital for the recycling of the endocytosis coat proteins for a new round of endocytosis. Subsequent to clathrin coat disassembly, the actin network is disassembled via the activity of a group of proteins such as Cof1p (ADP/Cofilin), Aip1p, Srv2p and Crn1p (Coronin) that bind and sever actin filaments [reviewed in (Boettner et al., 2011)]. The vesicle then associates with actin cables and is transported to the endosome (Huckaba et al., 2004).

1.3.2.2 Role of Yeast casein kinase I in mediating constitutive and regulated endocytosis.

Casein kinase 1 is an evolutionarily conserved serine/threonine kinase that is involved in diverse biological processes such as morphogenesis, endocytosis and cytokinesis. In budding yeast, casein kinase 1 is encoded by two essential genes, *YCK1* and *YCK2* (Robinson et al., 1992; Wang et al., 1992). Ubiquitously expressed Yck1p and Yck2p share similar biological functions, and single *YCK1* or *YCK2* is sufficient to maintain the cell viability. At most stages in the cell cycle, Yck1/2p are anchored to plasma membrane. The plasma membrane association is regulated by the prenylation motif at both C-terminal ends of Yck1/2p (Vancura et al., 1994).

It has been previously shown in multiple studies that Yck1/2p plays a role in both constitutive and regulated endocytosis. For instance, Yck1/2p has been shown to phosphorylate yeast GPCRs (G Protein-Coupled Receptors), Ste2p at its six serine residues located at C-terminal region (Hicke et al., 1998; Toshima et al., 2009). This phosphorylation serves as a signal for ubiquitination by NEDD4 family of E3 ubiquitin ligase, Rsp5p, that eventually

contribute to the internalization of Ste3p from the plasma membrane into the cell. Interestingly, Ste2p can be internalized into the cell through constitutive or ligand regulated endocytosis. Under normal circumstances, Ste2p is constitutively internalized from the plasma membrane. However, upon treatment with Ste2p ligand, alpha-factor, the internalization of Ste2p is greatly increased due to the increase in ubiquitnation by Rsp5p (Hicke and Riezman, 1996; Jenness and Spatrick, 1986). Failure to phosphorylate Ste2p in *yck1*Δ *yck2-2* double mutant cells or ubiquitination by Rsp5p leads to the inhibition of Ste2p internalization and its degradation through endocytic pathway (Dunn and Hicke, 2001; Hicke et al., 1998). Besides Ste2p, Fur4p, a uracil permease (mediates uracil uptake) is also endocytosed at the plasma membrane, but in a regulated fashion. Fur4p is constitutively delivered to the plasma membrane through secretory pathway under normal conditions. When cells encounter nutrient starvation, Fur4p will be subjected to degradation through endocytic pathway to maintain the uracil level in the cells. Degradation of Fur4p is dependent on phosphorylation of Yck1/2p, followed by ubiquitination, endocytosis and degradation in the vacuole (Blondel et al., 2004).

1.4 Gaps in interaction between cell division cycle and protein trafficking

1.4.1 Links between cell division cycle, secretory pathway and cytokinesis

At the end of mitosis, polarized secretion targets cytokinetic enzymes such as Chs2p, Chs3p and Fks1p to the division site through secretory pathway [reviewed in (Pruyne and Bretscher, 2000)]. Disruption of the secretory

pathway using thermo-sensitive alleles of exocyst complex, *sec3-2* and *sec10-2* has been shown to contribute to the failure of AMR constriction during mitotic exit (Dobbelaere and Barral, 2004; VerPlank and Li, 2005). This suggests that delivery of cell wall materials through secretory pathway indeed plays a vital role in mediating cytokinesis.

It has been previously shown that the transmembrane cytokinetic enzymes, Chs2p, Chs3p and Fks1p are exported from the ER through the COPII secretory pathway. Among the cytokinetic enzymes, molecular factors that facilitate secretion of Chs3p are well studied [reviewed in (Lesage and Bussey, 2006; Orlean, 2012)]. Conversely, the underlying molecular mechanism that regulates secretion of Chs2p and Fks1p from the ER to the division site remains poorly characterized. It has been shown that Clb2p-Cdk1p phosphorylated Chs2p is retained in the ER during metaphase (Teh et al., 2009). However, it remains unclear how Chs2p phosphorylation prevents its incorporation into COPII vesicles when Cdk1p activity is high. A previous study has suggested that secretion of Fks1p from the ER is regulated in a Soo1p (for suppressor of osmo-sensitive) dependent manner. Lee and co-workers demonstrated that the β-1,3-glucan content in the cell wall and β-1,3-glucan synthase activity are lowered in the *soo1-1* thermo-sensitive mutant indicating that secretion of Fks1p from the ER to plasma membrane is compromised (Lee et al., 1999). To date, Soo1p is the only protein identified that is involved in Fks1p ER secretion.

1.4.2 Links between cell division cycle and endocytosis

In mammalian cells, endocytosis is restrained during mitosis (Fielding et al., 2012). The increase in membrane tension of mitotic cells promotes the engagement of actin machinery in formation of a rigid actin cortex. This leads to the unavailability of actin that is essential in facilitating CME (Kaur et al., 2014). As cell progress through mitosis, the CME process is quickly restored before telophase (Schweitzer et al., 2005). However, the concept that CME is inhibited during mitosis is rather controversial. A recent study from Kirchhausen group demonstrated that CME is unaffected during unperturbed mitosis. Authors suggested that the discrepancy observed was due to the different experimental conditions used in the studies. Long-term exposure to nocodazole, RO-3306 (Cdk inhibitor), and STLC (S-Trityl-L-Cysteine), or changes in culture conditions such as drastic temperature shift or serum starvation, compromised the CME during mitosis (Tacheva-Grigorova et al., 2013).

Unlike mammalian cells, endocytosis is constitutively active throughout the cell division cycle in budding yeast. The endocytosis of both fluid phase cargo, Lucifer yellow and receptor mediated cargo, radiolabeled alpha factor were similar throughout the cell division cycle (Nevalainen and Makarow, 1991).

1.4.3 Links between endocytosis and cytokinesis

It is well-established that endocytosis plays an important role in regulating cytokinesis in many eukaryotic cells. For instance, cytokinesis defects were observed in HeLa cells that overexpressed the dominant negative endocytosis mutant- GTPase defective ARF, highlighting the importance of endocytosis in cytokinesis (Schweitzer et al., 2005). Moreover, studies in zebrafish also

revealed the role of endocytosis in cytokinesis. Zebrafish blastomere failed to execute cytokinesis upon treatment with clathrin-mediated endocytosis inhibitor methyl-β-cyclodextrin or chlorpromazine (Feng et al., 2002). The evidence gathered from the above studies indicates that endocytosis indeed plays an essential role in regulating cytokinesis at the end of mitosis.

In budding yeast, Yck1/2p dependent phosphorylation of endocytic cargoes has been shown to be a prerequisite for constitutive and regulated endocytosis of the membranous proteins (Marchal et al., 2000; Toshima et al., 2009). A previous study demonstrated that cells deficient in Yck1/2p activity displayed defects in cytokinesis and abnormal chitin deposition at the division site (Robinson et al., 1999). In addition, it has been previously shown that cytokinetic enzymes, Chs2p and Chs3p are endocytosed from the division site in a Sla2p dependent manner (Chuang and Schekman, 1996). These results suggest that aberrant chitin deposition in *yck1*Δ *yck2-2* temperature sensitive mutants might be due to the failure to internalize cytokinetic enzymes such as Chs2p, Chs3p and Fks1p during cytokinesis. Although the role of endocytosis and cytokinesis respectively has been well studied, the interaction between these processes remains unexplored.

1.4.4 Links between protein trafficking of Chs2p, spindle disassembly and AMR constriction during mitotic exit.

It has been previously demonstrated that spindle disassembly invariably occurs before cytokinesis, suggesting that there might be an intimate connection between these two events (VerPlank and Li, 2005; Woodruff et al., 2010). Indeed, a recent study showed that dividing cells in which spindle

disassembly was delayed due to defective motor protein Kip3p, had mitotic spindles that were abnormally severed as a result of AMR constriction (Woodruff et al., 2010). More significantly, these cells produced progeny cells that failed to establish the bi-polar spindle in the subsequent round of cell division (Woodruff et al., 2012). This indicates that spindle disassembly and cytokinesis must be tightly coordinated during mitotic exit to maintain spindle integrity. However, during mitotic exit, Chs2p that triggers the AMR constriction localizes to the neck prior to mitotic spindle disassembly (VerPlank and Li, 2005). This raises the question as to how cells ensure that the spindles are not broken prematurely in a normal cell division when mitotic exit occurs.

1.5 Research objectives, significance and scope of the study

1.5.1 Research objectives

As reviewed in previous chapter, the mechanisms of cytokinesis in budding yeast are well characterized in many studies. However, the underlying mechanisms of cytokinetic enzymes trafficking at the end of mitosis remains poorly understood. Research gaps for the current discovery of cytokinetic enzymes trafficking during mitotic exit are summarized as follows:

- Although the role of Chs2p in facilitating cytokinesis is well described, the molecular switch that triggers the timely Chs2p ER export is not well understood.
- The localization of key CME components during interphase is well characterized. However, the spatio-temporal localization of CME components specifically in mitosis has not been explored.

- Previous reports demonstrated that the cytokinetic enzymes, Chs2p and Chs3p are endocytosed from the division site during mitotic exit. However, the molecular factor that triggers the timely internalization of cytokinetic enzymes remains unknown.

The main aim of this study was to examine the regulation and the significance of cell cycle regulated protein trafficking of cytokinetic enzymes at the division site. The specific aims of this study are shown as below:

- To determine the molecular mechanism that regulates the timely export of Chs2p from the ER to the division site during mitotic exit.
- To examine the spatio-temporal localization of CME components during mitotic exit.
- To examine the factors (eg. Post-translational Modifications) that control the retrieval of cytokinetic enzymes from the division site during mitotic exit.
- To understand the significance of coordination between cell cycle regulated protein trafficking with late mitotic events.

1.5.2 Significance

It has been suggested that defects in cytokinesis play a role in aneuploidy and chromosome instability [reviewed in (Pfau and Amon, 2012)]. Therefore, it is crucial to ensure that the execution of the cytokinesis is inhibited prior to chromosome segregation in order to maintain the genomic stability. The interplay between exocytosis and endocytosis of cytokinetic enzymes is vital in safeguarding the faithful execution of the cytokinesis events.

Budding yeast (*Saccharomyces cerevisiae*) has been extensively used as a study model in understanding cell division cycle regulation, proteins trafficking (endocytosis and exocytosis) and cytokinesis due to evolutionarily conserved genes in higher eukaryotes. The findings in this study may shed light on the dissection of the complicated cytokinesis mechanisms in higher eukaryotic cells.

Chapter 2 Materials and Methods

2.1 Materials

2.2.1 *Saccharomyces cerevisiae* strains

Yeast strains used in this study (listed in Table1) were derived from W303a

Table 1 Yeast strains used in this study.

Name	Genotype	Source
US1363	*MAT a leu2-3,112 trp1-1 ura3-1 can1-100 ade2-1 his3-11,15 bar1Δ*	Uttam Surana
US1318	*MAT a leu2 his3 trp1 ura3 cdc15-2*	Uttam Surana
JKY5	*MAT α his3-d leu2-d mef15-d lys2-d ura3-d cdc14-Δ::CDC14:LEU2*	HongTao Yu
JKY8	*MAT α his3-d leu2-d mef15-d lys2-d ura3-d cdc14-Δ:: cdc14_L359A, I360A,L362A::LEU2*	HongTao Yu
HCY115	*MAT a LEU2::GAL-HA-CDC14::LEU2*	Harry Charboneau
HCY116	*MAT a LEU2::GAL-HA-CDC14(C283S)::LEU2*	Harry Charboneau
YL1051	*cdc14-degron GAL-sic1NTΔ::URA*	Chun Liang
FM1997	*MAT a GAL-sic1NTΔ::URA CHS2-GFP::KAN*	This study
FM1999	*MAT a cdc14-3 GAL-sic1NTΔ::URA CHS2-GFP::KAN*	This study
FM1603	*MAT α his3-d leu2-d mef15-d lys2-d ura3-d cdc14-Δ::CDC14:LEU2 CHS2-YFP::HIS*	This study
FM1605	*MAT α his3-d leu2-d mef15-d lys2-d ura3-d cdc14-Δ:: cdc14_L359A, I360A,L362A::LEU2 CHS2-YFP::HIS*	This study
FM1779	*MAT a cdc14-NES::LEU2 CHS2-YFP::HIS GAL-CDC14-9MYC::URA*	This study
FM1709	*MAT a cdc14-NES::LEU2 GAL-CHS2-YFP::TRP SEC63-CFP::SpHIS*	This study
FM1710	*MAT a cdc14-NES::LEU2 GAL-CHS2(4S-to-4A)-YFP::TRP SEC63-CFP::SpHIS*	This study
FM1850	*MAT a GAL-CHS2-13MYC::TRP*	This study
FM1893	*MAT a GAL-CHS2(4S-to-4A)-13MYC::TRP*	This study
FM1866	*MAT a LEU2::GAL-HA-CDC14::LEU2 CHS2-3MYC::TRP*	This study
FM1867	*MAT a LEU2::GAL-HA-CDC14(C283S)::LEU2 CHS2-3MYC::TRP*	This study
FM1906	*MAT a LEU2::GAL-HA-CDC14::LEU2 pep4Δ::HYGRO*	This study
FM1909	*MAT a LEU2::GAL-HA-CDC14(C283S)::LEU2 pep4Δ::HYGRO*	This study
FM1846	*MAT a CHS2-3MYC::TRP*	This study

FM2017	*MAT a CHS2-GFP::KAN CDC14-mCHERRY::HYGRO cdc55::NAT*	This study
FM2003	*MAT a CHS2-GFP::KAN CDC14-mCHERRY::HYGRO bub2::NAT*	This study
FM1880	*MAT a cdc15-2 CHS2-3MYC::TRP*	This study
FM2120	*MAT a leu2 his3 trp1 ura3 bar- CHS2-YFP::SpHIS5 CDC14-ECFP::KAN*	This study
FM2133	*MAT a leu2 his3 trp1 ura3 ADE bar- CHS2-YFP::SpHIS5 GAL-SIC1(myc)::URA (4-copies) NET1-mCHERRY::HYGRO CDC14-ECFP::KAN*	This study
FM2138	*MAT a leu2 his3 trp1 ura3 CHS2-GFP::KAN sla2Δ::HYGRO*	This study
KR3212	*MATa SPC42-RFP-KanMX6 GFP-TUB1-URA3::TUB1 ura3-1 his3-11,15 leu2-3,112*	Orna Cohen-Fix
Y1125	*MAT a ade2 his3 lys2 trp1 ura3 fks1::HIS ade3::FKS1-GFP::TRP1 fks2::LYS*	Yu Jiang
FM2705	*MAT a MYO1-GFP::KAN GFP-TUB1::URA CHS2-mCHERRY::HPH1*	This Study
FM2412	*MAT a CHS2-GFP::KAN ABP1-mCHERRY::HPH1*	This Study
FM2442	*MAT a CHS2-GFP::KAN ABP1-mCHERRY::HPH1 ede1::NAT*	This Study
FM2713	*MAT a CHS2-GFP::KAN ABP1-mCHERRY::NAT sla2::HYGRO*	This Study
FM2515	*MAT a CHS2-GFP::KAN ABP1-mCHERRY::HPH1 end3::NAT*	This Study
FM3221	*MAT a CHS2-GFP::KAN ABP1-mCHERRY::HPH1 rvs167::NAT rvs161::HIS*	This Study
FM3369	*MAT a GFP-TUB1::URA MYO1-GFP::TRP NDC10-tdtomato::loxp-KAN-loxp*	This Study
FM3382	*MAT a GFP-TUB1::URA MYO1-GFP::TRP NDC10-tdtomato::loxp-KAN-loxp end3::NAT*	This Study
FM3106	*MAT a CHS2-GFP::KAN MYO1-REDSTAR::NAT*	This Study
FM3111	*MAT a CHS2-GFP::KAN MYO1-REDSTAR::NAT end3::HPH1*	This Study
FM2642	*MAT a MYO1-GFP::KAN GFP-TUB1::URA*	This Study
FM3046	*MAT a MYO1-GFP::KAN GFP-TUB1::URA ede1::NAT*	This Study
FM3260	*MAT a MYO1-GFP::KAN GFP-TUB1::URA sla2::NAT*	This Study
FM2665	*MAT a MYO1-GFP::KAN GFP-TUB1::URA end3::NAT*	This Study
FM3262	*MAT a MYO1-GFP::KAN GFP-TUB1::URA rvs161::HIS rvs167::NAT*	This Study
FM2873	*Mat α GFP-TUB1::URA MYO1-GFP::KAN chs3::KAN*	This Study
FM2889	*Mat α GFP-TUB1::URA MYO1-GFP::KAN chs3::KAN end3::NAT*	This Study

FM3191	*MAT a MYO1-GFP::KAN GFP-TUB1::URA fks1::HPH1*	This Study
FM3198	*MAT a MYO1-GFP::KAN GFP-TUB1::URA fks1::HPH1 end3::NAT*	This Study
FM3314	*MAT a MYO1-GFP::KAN GFP-TUB1::URA kip3::HPH1*	This Study
FM3340	*MAT a MYO1-GFP::KAN GFP-TUB1::URA kip3::HPH1 end3::NAT*	This Study
FM3471	*MAT a MYO1-GFP::KAN GFP-TUB1::URA slk19::NAT*	This Study
FM3487	*MAT a MYO1-GFP::KAN GFP-TUB1::URA slk19::NAT end3::HPH1*	This Study
FM3614	*MAT a GFP-TUB1::URA MYO1-tdTomato::KAN GAL-CHS2-13MYC::TRP chs2::HIS*	This Study
FM3626	*MAT a GFP-TUB1::URA MYO1-tdTomato::KAN GAL-CHS2-13MYC::TRP chs2::HIS end3::NAT*	This Study
FM2784	*MAT a MYO1-GFP::KAN GFP-TUB1::URA SPC29-RFP::HPH1*	This Study
FM2908	*MAT a MYO1-GFP::KAN GFP-TUB1::URA SPC29-RFP::HPH1 ede1::NAT*	This Study
FM2817	*MAT a MYO1-GFP::KAN GFP-TUB1::URA end3::NAT SPC29-RFP::HPH1*	This Study
FM3224	*MAT a MYO1-GFP::KAN GFP-TUB1::URA SPC29-RFP::HPH1 rvs167::NAT rvs161::HIS*	This Study
FM3349	*MAT a MYO1-GFP::KAN GFP-TUB1::URA SPC29-RFP::HPH1 GAL-CHS2-13MYC::TRP chs2::HIS*	This Study
FM3200	*MAT a MYO1-GFP::KAN GFP-TUB1::URA SPC29-RFP::HPH1 GAL-CHS2-13MYC::TRP chs2::HIS end3::NAT*	This Study
FM3285	*MAT a MYO1-GFP::KAN GFP-TUB1::URA SPC29-RFP::HPH1 fks1::LEU*	This Study
FM3296	*MAT a MYO1-GFP::KAN GFP-TUB1::URA SPC29-RFP::HPH1 fks1::LEU end3::NAT*	This Study
FM2933	*MAT a MYO1-GFP::KAN GFP-TUB1::URA ABP1-mCHERRY::HPH1*	This Study
FM119	*MAT a MYO1-CFP::CaURA3 CHS2-YFP(Citrine)::SpHIS5 bar1Δ*	This Study
FM3561	*MAT a CHS2-mCHERRY::HYGRO CHS3-3mGFP::KAN*	This Study
FM3246	*MAT a fks1::HIS ade3::FKS1-GFP::TRP1 CHS2-mCHERRY*	This Study
FM2658	*Mat a his3 leu2 ura3-52 yck1::URA GFP-YCK2 CHS2-mCHERRY::HPH1*	This Study
FM2937	*Mat a his3 leu2 ura3-52 yck1::URA yck2-2-ts CHS2-GFP::KAN ABP1-mCHERRY::HPH1*	This Study

FM2938	*Mat a his3 leu2 ura3-52 CHS2-GFP::KAN ABP1-mCHERRY::HPH1*	This Study
FM3554	*MAT a GAL-CHS2(yck 15S-to-15A)-YFP::LEU*	This Study
FM3585	*MAT a GAL-CHS2-YFP::LEU ABP1-mCHERRY::HPH1*	This Study

CaURA3 refers to *Candida albicans*

SpHIS5 refers to *Schizosaccharomyces pombe*

NAT refers to Nourseothricin

HYGRO refers to Hygromycin B

2.2.2 *Escherichia coli* strains

Table 2: *E.coli* strains used in this study.

Name	Genotype	Source
DH5α	*F- φ80lacZΔM15 Δ(lacZYA-argF) U169 recA1 endA1 hsdR17 (rk-, mk+) phoA supE44 λ- thi-1 gyrA96 relA1*	Invitrogen
DH10B	*F- mcrA Δ(mrr-hsdRMS-mcrBC) φ80lacZΔM15 ΔlacX74 recA1 endA1 araD139 Δ (ara, leu)7697 galU galK λ- rpsL nupG /pMON14272 / pMON7124*	Invitrogen
DH5α-T1^{R}	*F- φ80lacZΔM15 Δ(lacZYA-argF)U169 recA1 endA1 hsdR17(rk-, mk+) phoA supE44 λ-thi-1 gyrA96 relA1 tonA*	Invitrogen

2.2.3 Plasmids

Table 3: Plasmids constructed in this study

Name	Vector backbone	Insert	Construction Descriptions
pFM145	pFM75	*CDC14-9MYC*	*CDC14-9MYC* was amplified from FM410 genomic DNA. SphI-*CDC14*-HindIII DNA fragment was digested and sub-cloned into pFM75.
pFM160	pFM75	*3MYC-NTΔsic1*	*3MYC* was amplified from pYM27. *NTΔsic1* was amplified from US1363 genomic DNA. *3MYC* DNA fragment was digested with BamHI and SalI. *NTΔsic1* DNA fragment was digested with SalI and HindIII. Digested *3MYC* and *NTΔsic1* DNA fragment were sub-cloned into pFM75.
pFM161	pFM39	*chs2- (6S to 6A)*	*chs2* S86A and S133A mutation were introduced using PCR based site-directed mutagenesis.
pFM218	pFM76	*CHS2- YFP*	*CHS2-YFP* DNA fragment was extracted from pFM39 digested with BamHI and HindIII. The *CHS2-YFP* fragment was sub-cloned into pFM76 with BamHI and HindIII.
pFM228	pFM218	*chs2- (15S to 15A)*	*chs2* S11A, S14A, S21A, S24A, S40A, S43A, S112A, S115A, S150A, S153A, S158A, S161A, S167A, S180A and S183A mutations were introduced using GeneArt site-directed mutagenesis kit (Invitrogen).

Table 4: Plasmids used in this study

Name	Description	Source
YIPlac128	Yeast Integrative Plasmid with *LEU2* marker	(Gietz and Sugino, 1988)
YIPlac204	Yeast Integrative Plasmid with *TRP1* marker	(Gietz and Sugino, 1988)
YIPlac211	Yeast Integrative Plasmid with *URA3* marker	(Gietz and Sugino, 1988)
pFM39	*YIPlac204-GAL-CHS2-YFP*	YFM Lab (Teh et al., 2009)
pFM140	*YIPlac204-GAL-chs2 (4S to 4A)-YFP*	YFM Lab (Teh et al., 2009)
pFM141	*YIPlac204-GAL-chs2 (4S to 4E)-YFP*	YFM (Teh et al., 2009)
pFM74	*YIPlac204-GAL*	YFM Lab
pFM75	*YIPlac211-GAL*	YFM Lab
pFM76	*YIPlac128-GAL*	YFM Lab
pDZ264	*pKAN tdtomato cyc loxP KAN loxP* For amplification of C-terminal *loxP* sites flanked *tdtomato* tagging cassette with *HPH1* selectable marker	(Larson et al., 2011)

pBS35	For amplification of C-terminal *mCHERRY* tagging cassette with *HPH1* selectable marker	Yeast Resource Centre
pFA6-hphNT1	For amplification of deletion cassette with *HPHNT1* selectable marker	(Janke et al., 2004)
pFA6-natNT2	For amplification of deletion cassette with *NATNT2* selectable marker	(Janke et al., 2004)
pYM18	For amplification of C-terminal *9MYC* tagging cassette with *KANMX4* selectable marker	(Janke et al., 2004)
pYM23	For amplification of C-terminal *3MYC* tagging cassette with *TRP* selectable marker	(Janke et al., 2004)
pYM27	For amplification of C-terminal *EGFP* tagging cassette with *KANMX4* selectable marker	(Janke et al., 2004)
pYM30	For amplification of C-terminal *ECFP* tagging cassette with *KAN* selectable marker	(Janke et al., 2004)
pYM-N23	For amplification of N-terminal *GAL1* promoter cassette with *NATNT2* selectable marker	(Janke et al., 2004)
YDP-H	For amplification of deletion cassette with *HIS3* selectable marker	(Berben et al., 1991)
YDP-L	For amplification of deletion cassette with *LEU2* selectable marker	(Berben et al., 1991)

2.2.4 Oligonucleotides

Oligonucleotides were purchased from Integrated DNA Technologies (IDT) and Sigma-Aldrich.

Table 5: Oligonucleotides used in this study

Name	Primer Sequence (5'-3')
Abp1-S2	AAGTATTTTTTTACGTAAGAATAATATAATAGCATGACGCTGACGTGTGATTCTAATCGATGAATTCG AGCTCG
Abp1-S3	AGAGAAAGACGGCTCAAAAGGTCTCTTCCCCAGCAATTATGTGTCTTTGGGCAACCGTACGCTGCAG GTCGAC
Abp1-Chk-F	AGA AGC TCT GCA GCT CCT
Abp1-Chk-R	TCG AGG TTT TGA CAA CGC
BamHI-3myc-For	CGCGGATCCATGTCTAGAGGTGAACAAAAGTTGATT
SalI-3myc-Rev	TAATGGCGCATTTTTAAAAGAGTCGACTCTAGATGATCCGTTCAA
Bub2-S1	AACGACGTAAAGGTAAAAGAAACAACAGACTTTTAAACTTGTTAACTTTTGCATGCGTACGCTGCAG GTCGAC
Bub2-S2	ACATATAAACGTTGTAGAATTAAACGATAAAATATAATATTTCTTCACATAGTTTAATCGATGAATTC GAGCTCG

Bub2-Del-Chk-F	AATTCAGTAAACGCCGTGCG
Bub2-Chk-R	AGGTGAAGGATATGCGTACG
Cdc14-S2	ACTATTGCCGGTATACATATGACTCTTTCGAAAAGACAGCGAGAAGGGACACTGGATCGATGAATTCGAGCTCG
Cdc14-S3	AAGGACTACAAGCGCCGCCGGTGGTATAAGAAAAATAAGTGGCTCCATCAAGAAACGTACGCTGCAGGTCGAC
Cdc14-Chk-F	CAGGATACCAACGGCACAAG
Cdc14-Chk-R	GCAGGACAGCAAGGAAGTTG
Cdc55-Del-Chk-F	CCCTTTTTTCGTCCTGTTTCGAT
Cdc5-Chk-R	AAAACACGCTTGAAGTAGAATAA
Chs2-S1	CAGAGGAAGTTACATATAGACCCAAATAAAAACCAAAGAACCACATATAGAAATGCGTACGCTGCAGGTCGAC
Chs2-S2	CAGAATGAGAAAAAAGAGGGAATGACGAGAAATTAGCTGAAAAATACTGGCATTAATCGATGAATTCGAGCTCG
Chs2-S3	CGGCTCATGGGAAGTCTCTAAATTAGACTTACCAAATGTTTTCCACAAAAAGGGCCGTACGCTGCAGGTCGAC
Chs2-S4	ACGAGAAACCCGTTTATGGTGGAACCTTCGAATGGCTCTCCTAATAGACGTGGTGCATCGATGAATTCTCTGTCG
Chs2-Chk-F	AGCTGCCTTTAGGGTGGTTG

Chs2-Chk-R	AACAGTGCGCTCTCTACCCA
Chs2-N-Chk-R	TTGAGTTCTATGGCGACG
Chs2-S86A-F	GATAGTGCCCATAACGCTCCAGTTGCTCCGAACAGG
Chs2-S86A-R	CCTGTTCGGAGCAACTGGAGCGTTATGGGCACTATC
Chs2-S133A-F	GACCCCTACCATCTAGCACCCCAGGAACAGCCCAGT
Chs2-S133A-R	ACTGGGCTGTTGCTGGGGTGCTAGATGGTAGGGGTC
Chs3-3mGFP-S3	ATTTGAAAGGGAAGATATTCTCAATCGGAAGGAGGAAAGTGACTCCTTCGTTGCAGATCCACCGGTCGCCACC
Chs3-S1	TCCCATTTTCTTCAAAGGTCCTGTTTAGACTATCCGCAGGAAAGAAATTAGAATGCGTACGCTGCAGGTCGAC
Chs3-S2	CACAACCATATATCAACTTGTAAGTATCACAGTAAAAATATTTTCATACTGTCTAATCGATGAATTCGAGCTCG
Chs3-Chk-F	AGGGAAGATATTCTCAATCG
Chs3-Chk-R	CGTGGCTAAGGCAATTACAG
Chs3-Del-Chk-F	AAA ACG CGT TAT TGG CGC
Chs2-Mut_31_FW	TTTATGGTGGAACCTGCTAATGGCGCTCCTAATAGACGTG

Chs2-Mut_31_RV	CACGTCTATTAGGAGCGCCATTAGCAGGTTCCACCATAAA
Chs2-Mut_61_FW	AATAGACGTGGTGCTGCAAACCTCGCCAAATTTTACGCAA
Chs2-Mut_61_RV	TTGCGTAAAATTTGGCGAGGTTTGCAGCACCACGTCTATT
Chs2-Mut_334_FW	GCTGTCATACATCTAGCTGAGGGGGCTAACCTTTACCCCCG
Chs2-Mut_334_RV	CGGGGGTAAAGGTTAGCCCCCTCAGCTAGATGTATGACAGC
Chs2-Mut_448_FW	AGTGGCAGATTGTATGCTCAAAGCTCGAAAT
Chs2-Mut_448_RV	ATTTCGAGCTTTGAGCATACAATCTGCCACT
Chs2-Mut_457_FW	TTGTATGCTCAAAGCGCTAAATACACGATGGCT
Chs2-Mut_457_RV	AGCCATCGTGTATTTAGCGCTTTGAGCATACAA
Chs2-Mut_547_FW	CTCACTGCTACTACTGCCTATGATGATCAGT
Chs2-Mut_547_RV	ACTGATCATCATAGGCAGTAGTAGCAGTGAG
Chs2-Mut_1236_FW	TTTTTGTCTAAAAGAAGAAAATAAGAAAAAGATCAATTCCCATCGTT
Chs2-Mut_1236_RV	AACGATGGGAATTGATCTTTTTCTTATTTTCTTCTTTTAGACAAAAA

Chs2-Mut_2536_FW	AAGTTTTTGGAAATAAAAAGTCGTTTGAAAG
Chs2-Mut_2536_RV	CTTTCAAACGACTTTTTATTTCCAAAAACTT
Ede1-S1	TTTTTCCTGTTTTTATCTGTGTGTTTTCAATAGGATTCGAACGATATAGGCCATGCGTACGCTGCAGGTCGAC
Ede1-S2	ATTCAGCTTCGAGGAAGAAGTACAAAAAGAAGACGAAATGGTCCATTACAGACTAATCGATGAATTCGAGCTCG
Ede1-Del-Chk-F	AATCATTACCCGTCGGCG
Ede1-Chk-R	TCCCATGTTGTAATACGC
End3-S1	AGAGTTAGTGGGTATTGGAAAGGCCGGTAAAGATAACAGGGATCTCTGAAAAATGCGTACGCTGCAGGTCGAC
End3-S2	ATAACAAACAGTAAATATTACACATTCATGTACATAAAATTAATTATCGGTGTCAATCGATGAATTCGAGCTCG
End3-Del-Chk-F	AGCAGCATTTAGACCGTC
End3-Chk-R	TCAGAGGGTTCAAGTACC
Fks1-S1	AATTAAAATAAGCAAGTAGCTGAAATCAAGTCTTTCATACAACGGTCAGACCATGCGTACGCTGCAGGTCGAC
Fks1-S2	CTTTTGGATAGAATATCAGTAAAATCAAGCGTTCAAGCAAGTATTGATTGTATTAATCGATGAATTCGAGCTCG
Fks1-YDp-S1	AATTAAAATAAGCAAGTAGCTGAAATCAAGTCTTTCATACAACGGTCAGACCATGGAATTCCCGGGGATCCGG

Fks1-YDp-S2	CTTTTGGATAGAATATCAGTAAAATCAAGCGTTCAAGCAAGTATTGATTGTATTACTTTATGCTTCCG GCTCG
Fks1-Del-Chk-F	CTCGAACACTAGCCTTCA
Fks1-Chk-R	AGGCCGATACTGGTGAAA
GAL-CDC14-SphI-F	AAGGCATGCATGCGTAGGAGTGTATACCTC
GAL-CDC14-HindIII-R	GCGAAGCTTTTAGCTAGTGGATCCGTTCAA
Inn1-S2	CTTAATTCTATTTAAATATTAGTATTACAATAACAGCATGTTTCTCTTGTCATTAATCGATGAATTCGA GCTCG
Inn1-S3	TTCGAGGAAGAATTCGATGTCTCCTACAAGAAAAAGACCACCTCCAAGGCTCAGCCGTACGCTGCAG GTCGAC
Inn1-Chk-F	CCGACCAGAGATGATATG
Inn1-Chk-R	AAATGAAGAGGCCGCCTT
Myo1-S2	CTCGTGTCGTCTTTTTCTGTTAATAATGCATATTCTCATTCTGTATATACAAAACATCGATGAATTCGA GCTCG
Myo1-S3	CATGATAGGCTCGAAAAATATTGATAGTAACAATGCACAGAGTAAAATTTTCAGTCGTACGCTGCAG GTCGAC
Myo1-tdtomato-S2	ATTTTTTTAAATAAAGGATATAAAGTCTTCCAAATTTTTAAAAAAAAGTTCGTTATAACCCTCACTAA AGGGA
Myo1-tdtomato-S3	CATGATAGGCTCGAAAAATATTGATAGTAACAATGCACAGAGTAAAATTTTCAGTGTGGATCCGGTC GCCACC

Myo1-Chk-F	AGAAGCGAATTTGAGGAAGC
Myo1-Chk-R	CTATCGAAGGATACGGGGTG
Ndc10-tdtomato-S2	AAACATACATGTCGGTATCCCTATACGAAACAGTTTAAACTTCGAAGCTCCCTCATAACCCTCACTAAAGGGA
Ndc10-tdtomato-S3	GTGGAGGCATGACCATCAAAATTCATTTGATGGTCTGTTAGTATATCTATCTAACGTGGATCCGGTCGCCACC
Ndc10-Chk-F	GTCGTGGAGAGCTAATTG
Ndc10-Chk-R	CTACCAACTCAGTCTTCC
Net1-S2	ATTTTTTTTTACTAGCTTTCTGTGACGTGTATTCTACTGAGACTTTCTGGTATCAATCGATGAATTCGAGCTCG
Net1-S3	GAAGAAGAAGCCAAGTGGTGGATTTGCATCATTAATAAAAGATTTCAAGAAAAAACGTACGCTGCAGGTCGAC
Net1-Chk-F	GCCCCTTCAAGTAGTGAT
Net1-Chk-R	AGTAACCAAGCTTTGATA
Pep4-S1	TAGTGACCTAGTATTTAATCCAAATAAAATTCAAACAAAAACCAAAACTAACATGCGTACGCTGCAGGTCGAC
Pep4-S2	AGCTCTCTAGATGGCAGAAAAGGATAGGGCGGAGAAGTAAGAAAAGTTTAGCTCAATCGATGAATTCGAGCTCG
Pep4-Del-Chk-F	AGAAGTTTGGGTAATTCGCTG

Pep4-Chk-R	AAACAAGGAAATTCTCGAGCC
Sla2-S1	TTAGTAATACAGCCATAGCAGTAGTAGTGATAGTACTAGCAGCTAGAACAGGATGCGTACGCTGCAGGTCGAC
Sla2-S2	AAATATATTTATATTAACGTTTATCTTTATATATAAAAAGTACAATTCATGATCAATCGATGAATTCGAGCTCG
Sla2-Del-Chk-F	CGTTTTGTACGACGACGC
Sla2-Chk-R	AGACTCCTACAGAGATGT
Sic1-NTdel-SalI-For	TTGAACGGATCATCTAGAGTCGACTCTTTTAAAAATGCGCCATTA
Sic1-NTdel-HindIII-Rev	CGCAAGCTTTCAATGCTCTTGATCCCTAGATTG
Spc29-S2	TATTTTAGTTTTAGTTACGATTATGCTGGTATTATTTAGTTAAGTACTTAATTCAATCGATGAATTCGAGCTCG
Spc29-S3	TGAAAATGAAAGTACGGAGGATATACTAAAAATATTGTCTTCGTCTTTTCACAATCGTACGCTGCAGGTCGAC
Spc29-Chk-F	TTTGCCTCTCTCGAACACTC
Spc29-Chk-R	TGGACACTGGATGAGTCAAG
Rvs161-Del-pKT	TAGAAAACTATACAAATCCTATTATAAGAAGCCAGAAGAAAGCTGATACAAGATGGTTTAGCTTGCCTCGT
Rvs161-S1	TAGAAAACTATACAAATCCTATTATAAGAAGCCAGAAGAAAGCTGATACAAGATGCGTACGCTGCAGGTCGAC

Rvs161-S2	TAAATGAAAGAAACATAAATGACCGTAAAAAACTAAAGGCAAAAGCATTAATTTAATCGATGAATTCGAGCTCG
Rvs161-Del-Chk-F	ACGTTTCCTTTACGTCCC
Rvs161-Chk-R	TGCTAGACATTCTTACGT
Rvs167-S1	TGAGGCTCACCTGGTCATTTAACACCAAGAATCAAGGAGCCAATAAGTGCACATGCGTACGCTGCAGGTCGAC
Rvs167-S2	GTAACATCTCACAATAGAAGGTAATGAATACAGAGGGATGCAGGGGCCTCCTCTAATCGATGAATTCGAGCTCG
Rvs167-Del-Chk-F	CCTTCCAGTTGCTATGGT
Rvs167-Chk-R	ACCATATTGGGAAGGTGG

2.2.5 Chemicals

Table 6: Chemicals used in this study

Source	Name
Bio-rad	2-mercaptoethanol
	Dithiothreitol (DTT)
	SDS
Becton Dickson (BD)	Bacto Agar
	Bacto Pepton
	Bacto Tryptone
	Bacto Yeast Extract
Invitrogen	Geneticin (G418)
	Hygromycin B
1st Base	Agarose
	Glycerol
	Tris Base
	Sodium Chloride
Merck	Ammonium Sulfate
	Imidazole
	Paraformaldehyde
	Potassium chloride
	Sodium Hydroxide
Molecular Probes	FM4-64 dye
Roche	Nonidet P-40 (NP-40)
Sigma	Adenine
	Ampicillin sodium salt
	Bovine Serum Albumin (BSA)
	Caspofungin diacetate
	Dimethyl Sulfoxide (DMSO)
	Deoxyribonucleic acid, single stranded from salmon testes
	Ethylenediaminetetraacetic acid (EDTA)
	Fluorescent Brightener 28 (Calcofluor white)
	L-arginine
	L-aspartic acid
	L-glutamic acid
	L-histidine
	L-leucine
	L-lysine
	L-methionine
	L-phenylalanine
	L-serine

	L-threonine L-tryptophan L-tyrosine L-valine Latrunculin B from *Latruncula magnifica* Lithium Acetate Lyticase from *Arthrobacter luteus* Nikkomycin Z from *Streptomyces tendae* Phosphatase inhibitor cocktail Polyethyleneglycol (PEG 3350) Protease inhibitor cocktail Sodium orthovanadate Sorbitol Trichloroacetic acid Uracil
SCRS	D-(+)-Glucose
US Biologicals	D-(+)-Galactose, Low endotoxin, Low glucose D-(+)-Raffinose, Low glucose Hydroxyurea Nocodazole Yeast Mating Factor Alpha, Acetate Salt Yeast Nitrogen Base-AA/AS
Wako	Phos-tag
Werner BioAgents	clonNAT

2.2.6 Culture media

2.1.6.1 Yeast culture media

Table 7: Yeast culture media used in this study

Name	Component
YPD (liquid)	1% (w/v) Bacto Yeast Extract 2% (w/v) Bacto Peptone 2% (w/v) D(+) Glucose 0.005% (w/v) Adenine
YPD Agar Plate	1% (w/v) Bacto Yeast Extract 2% (w/v) Bacto Peptone 2% (w/v) Bacto Agar 2% (w/v) D(+) Glucose 0.005% (w/v) Adenine

YPD Agar + Geneticin plate	YPD agar plate supplemented with 200µg/ml of Geneticin
YPD Agar + Hygromycin B plate	YPD agar plate supplemented with 300µg/ml of Hygromycin B
YP/Raff/Gal (liquid)	1% (w/v) Bacto Yeast Extract 2% (w/v) Bacto Peptone 2% (w/v) D(+) Glucose 0.005% (w/v) Adenine
YP/Raff/Gal plate	1% (w/v) Bacto Yeast Extract 2% (w/v) Bacto Peptone 2% (w/v) Bacto Agar 0.005% Adenine 2% (w/v) Raffinose 2% (w/v) Galactose
SC (liquid)	40µg/ml Adenine 20µg/ml L-arginine 100µg/ml L-aspartic acid 100µg/ml L-glutamic acid 20µg/ml L-histidine 60µg/ml L-leucine 30µg/ml L-lysine 20µg/ml L-methionine 50µg/ml L-phenylalanine 375µg/ml L-serine 200µg/ml L-threonine 40µg/ml L-tryptophan 30µg/ml L-tyrosine 150µg/ml L-valine 20µg/ml Uracil 2% (w/v) D(+) Glucose
Synthetic Defined Dropout plate	Contains all nutrients in SC medium but lacks a single nutrient 2% (w/v) Bacto Agar 2% (w/v) D(+) Glucose
Minimal plate	0.17% (w/v) Yeast Nitrogen Base –AA/AS 0.5% (w/v) $(NH_4)_2SO_4$ 2% (w/v) Bacto Agar 2% (w/v) D(+) Glucose
Sporulation plate	1% KCl 0.1% (w/v) Bacto Yeast Extract 2% (w/v) Bacto Agar 0.05% (w/v) D(+) Glucose

2.1.6.2 Bacterial culture media

Table 8: Bacterial culture media used in this study

Name	Component
LB (liquid)	1% (w/v) Bacto Tryptone 0.5% (w/v) Bacto Yeast Extract 0.5% (w/v) NaCl 1mM NaOH
LB-Ampicillin Plate	1% (w/v) Bacto Tryptone 0.5% (w/v) Bacto Yeast Extract 0.5% (w/v) NaCl 1mM NaOH 2% Bacto Agar 50µg/ml Ampicillin

2.2 Methods

2.2.1 Techniques of *E.coli* manipulations

6.2.1.1 *E.coli* transformation

E.coli transformation was performed according to (Hanahan, 1983). Chemically induced competent cells were frozen and stored at-80°C, and thawed on ice for transformation. 80µl of competent cells were added to either 1µl of plasmid (for plasmid propagation) or 20µl of ligation mixture (for plasmid construction). The suspension was then incubated on ice for 10min followed by heat shocked at 42°C for 2min. Cells were revived by addition of 200µl of S.O.C medium (2% tryptone, 0.5% yeast extract, 10mM NaCl, 2.5mM KCl, 10mM $MgCl_2$, 10mM $MgSO_4$, and 20mM glucose) and incubated at 37°C for 30min with shaking at 200rpm. Subsequently, cells were pelleted down by centrifugation at 13.2krpm for 10sec and spread on LB agar supplemented with the appropriate antibiotic. Plates were incubated at 37°C overnight. Colonies formed were isolated with the sharp end of a toothpick

and inoculated in 5ml of LB liquid medium containing 50μg/ml ampicillin. Cells were incubated at 37°C overnight with shaking at 200rpm.

6.2.1.2 *E.coli* plasmid extraction (Miniprep)

5ml of overnight culture were harvested by centrifugation at 13.2krpm for 3min. DNA plasmids were extracted with High Speed Plasmid Mini Kit (Geneaid). The concentration of plasmid DNA was determined using a NanoDrop spectrophotometer (Thermo Scientific). Plasmids were then subjected to restriction enzyme digestion followed by sequencing.

2.2.2 Cell culture and genetic manipulations in *Saccharomyces cerevisiae*

2.2.2.1 *Saccharomyces cerevisiae* culture condition

Yeast strains were routinely grown in YPD at 24^{o}C. For galactose promoter induction, cells were grown in YP supplemented with 2% raffinose (Raff), followed by addition of galactose (Gal) to a final concentration of 2% and 0.1% (Figure S2) respectively.

2.2.2.2 Cell synchronization

For cells synchronization, exponential-phase cells were diluted to 1x10^{7} cells/ml in growth medium at 24°C. To synchronize cells at G1 phase, alpha-factor was added to a final concentration of 0.4μg/ml for 3 hours. Cells were then released from G1 arrest by washing off alpha-factor through centrifugation and resuspended in growth medium as described in various sections. For a typical Noc arrest, cells were arrested with 7.5 μg/ml Noc for 2 hours, followed by addition of 7.5 μg/ml for another 2 hours at 24°C. For endocytosis deletion mutants, cells were shifted to 32°C for another 0.5h after 4 hours Noc arrest. The drug was washed off by centrifugation of the cells.

Cells were then released and sampled at intervals as described in the relevant sections. For S-phase arrest, cells were grown at 32^{o}C for 2 h, followed by addition of hydroxyurea to a final concentration of 0.2M. Cells were then incubated for another 5.5 h at 32^{o}C and harvested for fluorescent microscopy analysis.

2.2.2.3 Yeast mating

A sharp end of a toothpick full of mating type a (*MATa*) and alpha (*MATα*) were resuspended in 100µl of sterile dH_2O respectively. 10µl cells suspension of *MATa* and *MATα* strain were then spread on the opposite edge of YPD plate. Single *MATa* and *MATα* cell were put in close proximity at the centre of the YPD plate with automated dissection microscope, MSM400 (Singer Instrument, UK). The mated diploid cell was incubated at 24^{o}C for 3 days and the yeast colony formed was streaked on a fresh YPD.

2.2.2.4 Yeast sporulation and tetra dissection

To induce sporulation of diploid yeast cells, a blunt end toothpick full of yeast cells were transferred onto sporulation plate and incubated at 24^{o}C for 4-5 days. After conformation of ascus formation under microscope, a sharp end toothpick full of asci was suspended in 50U/ml lyticase solution (1µl of 5000U/ml lyticase in 99µl of sterile dH_2O). Cell suspensions were incubated at 30^{o}C for 20min to digest the ascus wall. 10µl of the lyticase digested cell suspension was streaked onto a YPD plate and asci were dissected using MSM400. Individual colony formed from the dissected tetrad was streaked on YPD plate and incubated at 24^{o}C for 2 days. The segregation of selectable markers was determined by replica plating on appropriate selective medium.

2.2.2.5 PCR based tagging and deletion of endogenous gene

PCR-based tagging and deletion of endogenous genes were performed as describes previously (Berben et al., 1991; Janke et al., 2004; Sheff and Thorn, 2004). The replacement of endogenous gene with selectable marker and N or C-terminal fusion of fluorescence or epitope-tag protein were achieved by homologous recombination using PCR product that is specific to target gene. The sequences for amplification of deletion cassette and N or C-terminal tagging were shown in table 9.

Table 9: Plasmids used in PCR based Tagging and Deletion of Endogenous Gene

Plasmids Series	Description	Primer	Sequence (5'to 3')
pDZ264 (Larson et al., 2011)	C-terminal tagging	S3	55 bases before the stop codon (excluding stop codon) - CGTACGCTGCAGGTCGAC
		S2	reverse complement of 55 bases downstream of stop codon (including stop codon) - ATCGATGAATTCGAGCTCG
pKT (Sheff and Thorn, 2004)	C-terminal tagging	F5	55 bases before the stop codon (excluding stop codon) - GGTGACGGTGCTGGTTTA
		R3	reverse complement of 55 bases downstream of stop codon (including stop codon) - TCGATGAATTCGAGCTCG
pYM (Janke et al., 2004)	Deletion	S1	55 bases before the start codon (including start codon) – CGTACGCTGCAGGTCGAC
		S2	reverse complement of 55 bases downstream of stop codon (including stop codon) - ATCGATGAATTCGAGCTCG
	C-terminal tagging	S3	55 bases before the stop codon (excluding stop codon) - CGTACGCTGCAGGTCGAC
		S2	reverse complement of 55 bases downstream of stop codon (including stop codon) - ATCGATGAATTCGAGCTCG
YDp (Berben et al., 1991)	Deletion	S1	55 bases before the start codon (including start codon) - CGTACGCTGCAGGTCGAC
		S2	reverse complement of 55 bases downstream of stop codon (including stop codon) - ATCGATGAATTCGAGCTCG

2.2.2.6 Yeast transformation

Freeze-thaw yeast transformation (for genes conferring antibiotic resistance markers)

Yeast transformation was performed according to previous report (Taxis and Knop, 2006). Yeast cells were grown overnight in YPD till saturation (OD_{600}>1) at 24 ^{o}C. 3 OD_{600} cells were harvested by centrifugation at 3500rpm for 30s, washed once with sterile dH_2O and washed once with sterile SORB solution [100mM lithium acetate, 10mM Tris-HCl pH8.0, 1mM EDTA-NaOH pH8.0, 1M sorbitol pH8.0 (adjusted with glacial acetic acid)]. Cells were then frozen at -80 ^{o}C. Before transformation, frozen yeast suspension was thawed and 50µl of cells suspension was used for each transformation. 10µl single stranded salmon sperm DNA (ssDNA) (10mg/ml) and 10µl of PCR products were added into the cells suspension. 6 volumes of polyethylene glycol solution (PEG) [40% PEG 3350, 100mM lithium acetate, 10mM Tris-HCl pH8.0, 1mM EDTA-NaOH pH8.0] were added into the transformation mixtures. The mixture was incubated on a rotating platform at 24^{o}C for 30min. Transformation reaction was then incubated at 42 ^{o}C for 20min and harvested by centrifugation at 3.5krpm for 3min. The cells were resuspended in 1ml of YPD and incubated on a rotating platform at 24^{o}C for 4 hours. Transformants were spread on YPD plate supplemented with appropriate antibiotic. Transformation plate was incubated at 24^{o}C until the appearance of yeast colonies (2-3 days). High background of transiently transformed cells was removed by replica plated onto the same antibiotic containing YPD plate.

High efficiency yeast transformation (for genes conferring auxotrophic marker)

High efficiency yeast transformation was performed as described previously (Gietz and Woods, 2006). In brief, yeast cells were grown overnight in YPD till saturation (OD_{600}>1) at 24^{o}C. 25x10^{7} cells were harvested, resuspended in 2xYPD and incubated at 30^{o}C until the cells OD_{600} reached 1x 10^{9} cells. Cells were then harvested and washed once with sterile dH_2O by centrifugation. Cells pellet was resupended in sterile dH_2O to final volume of 1ml. Aliquot of 100µl cells suspension was used for each transformation. Supernatant was removed by centrifugation at 3.5krpm for 30s. 335µl of transformation mixture [240µl 50% (w/v) PEG 3350, 36µl 1M lithium acetate, 25µl single stranded ssDNA (10mg/ml) and 34µl (PCR product or linearized yeast integrative plasmid) was added to the cell pellet and mix thoroughly by vortexing. Transformation reaction was incubated at 42 ^{o}C for 20min. Cells were then pellet down and washed once with sterile dH_2O by centrifugation at 3.5krpm for 3min. Transformants was resuspended in remaining dH_2O and plated on appropriate SC selection agar medium. Transformation plate was incubated at 24^{o}C until the appearance of yeast colonies (3-4 days).

2.2.2.7 Verification of yeast transformants

Yeast colonies were isolated from the selection plate and streaked onto the identical selection medium. Colony PCR was performed to verify the integration of deletion cassette and epitope-tagged genes at endogenous locus. For genes tagged with fluorescent-proteins, cells were directly examined under fluorescence microscope. Positive clones were further validated with colony PCR.

2.2.3 Molecular techniques

2.2.3.1 DNA restriction enzyme digestion, gel extraction, ligation and sequencing.

All restriction enzymes were purchased from Fermentas (Thermo Scientific) and New England Biolabs (NEB). DNA restriction digestion was performed according to manufacturer protocol. Restriction digested DNA fragment was extracted from agarose gel and purified using QIAquick Gel Extraction Kit (Qiagen). For DNA ligation, T4 DNA ligase was purchased from NEB and used according to manufacturer recommendation. DNA sequencing was performed by 1st Base (Singapore). Sequences obtained were analysed using Bioedit (Ibis Biosciences) and Serial Cloner.

2.2.3.2 Generation of C-terminal tagging and deletion PCR cassette for yeast genetic manipulation

PCR products were generated using Long PCR Enzyme Mix (Fermentas). A standard PCR reaction mixture (Table 10) and cycling parameters (Table11) were shown as follows:

Table 10: PCR reaction mix used in PCR based tagging and deletion of endogenous gene

Component	Volume (µl)	Final Concentration
10x Long PCR Buffer	5	1x
dNTP Mix (2mM)	5	0.2mM
$MgCl_2$ (25mM)	4	2mM
Forward Primer (100µM)	0.3	0.3µM
Reverse Primer (100µM)	0.3	0.3µM
DNA plasmid template	1	-
DMSO	1	2%
Long PCR Enzyme Mix (5U/µl)	0.3	1.5U
dH_2O	Top-up to 50µl	-

Table 11: PCR cycling parameters

Step	Temperature (^oC)	Time	Number of Cycles
Initial Denaturation	95	4min	1x
Denaturation	95	30sec	10x
Annealing	54	30sec	
Extension	68	2min	
Denaturation	95	30sec	20x
Annealing	54	30sec	
Extension	68	2min*	
Final Extension	68	10min	1x
Hold	16	∞	1x

* Auto extension- 1sec per cycle

2.2.3.3 Yeast genomic DNA extraction

Yeast genomic DNA extraction was performed as described previously (Looke et al., 2011). A blunt toothpick full of yeast cells were suspended in 100µl LiOAc/SDS solution (200mM LiOAc, 1% SDS) and incubated at 70^{o}C for 15min. 300µl of 95% ethanol was added and mixed thoroughly to precipitate DNA. Precipitated DNA was collected by centrifugation at 13.2krpm for 3min. The DNA pellet was then air-dried at 24^{o}C for 5mins and dissolved in 100µl dH_2O. The suspension was centrifuged at 13.2krpm for 1min and 1µl of the supernatant was used for colony PCR reaction.

2.2.3.4 Yeast colony PCR

PCR reaction was performed according to manufacturer's recommendations. A standard PCR reaction mixture and cycling parameters were shown in table and table respectively.

Table 12: Yeast colony PCR reaction mix

Component	**Volume (µl)**	**Final Concentration**
10x Long PCR Buffer	2.5	1x
dNTP Mix (2mM)	2.5	0.2mM
$MgCl_2$ (25mM)	2	2mM
Forward Primer (100µM)	0.15	0.3µM
Reverse Primer (100µM)	0.15	0.3µM
Genomic DNA	1	-
Long PCR Enzyme Mix (5U/µl)	0.15	0.75U
dH_2O	Top-up to 20µl	-

2.2.4 Yeast protein extraction, interaction and analysis TCA protein precipitation

2.2.4.1 Yeast TCA protein precipitation

Samples were collected from the respective time points stated. Protein lysates were prepared using TCA precipitation method as described previously (Zhang et al., 2006). In brief, 3 OD_{600} of cells were harvested by centrifugation and resuspended in 1ml of ice-cold dH_2O. 150µl of Yeast extract buffer (YEX) (1.85M NaOH, 7.5% β-mercaptoethanol) was added to the suspension, vortex followed by incubation on ice for 10min. 150µl of 50% TCA (w/v) was added into the suspension, vortex and incubated for another 10min on ice. Precipitated protein pellet was harvested by centrifugation at 13.2krpm for 3min. The protein pellet was then resuspended in 5 cell volumes of 1xSDS PAGE sample buffer (50mM Tris-HCl pH6.8, 2% SDS, 10% glycerol, 1% β-mercaptoethanol, 12.5mM EDTA, and 0.02% bromophenol blue) supplemented with 100mM Tris-HCl (pH8.0). Samples were boiled at 95^{o}C for 3min and protein lysate were cleared by centrifugation at 13.2krpm for 3min.

2.2.4.2 Yeast native protein extraction.

Samples harvested were resuspended in IP-lyse buffer (1% NP-40, 9% Glycerol, 18mM Tris-Cl pH8.0, and 121mM NaCl) supplemented with 1x protease inhibitor and 1x phosphatase inhibitor. Half liquid volume of Zirconia beads (Biospec) were added into the cells suspension. Cells were lysed by agitation with vortexer at maximum speed, 4^{o}C for 1min, followed by rest at 4^{o}C for another 1min. The lysis steps were repeated 8 times. Protein

extracts were then cleared by centrifugation at 13.2krpm, 4^{o}C for 10min. Concentration of the proteins extracted were quantified using Bicinchoninic acid (BCA) assay (Pierce, Thermo Scientific).

2.2.4.3 Co-immunoprecipitation (Co-IP)

25µl of α-HA-conjugated beads (Santa cruz, CA) were added into 2 mg of protein lysates in each IP. The mixtures incubated on a rotating platform at 4^{o}C for 2 hours. Beads with immuno-precipitated proteins were washed six times with IP wash buffer (10% glycerol, 20mM Tris-Cl pH8.0, 135mM NaCl). Immunoprecipitated proteins were eluted by boiling beads in 2xSDS PAGE sample buffer (100mM Tris-HCl pH6.8, 4% SDS, 20% glycerol, 2% β-mercaptoethanol, 25mM EDTA and 0.04% bromophenol blue) at 95^{o}C for 5min.

2.2.4.4 TCA lysates Immunoprecipitation

25µl of α-myc-conjugated beads (Santa cruz, CA) were added into 1:10 diluted TCA precipitated protein lysates (1 part of TCA lysates + 9 parts of IP wash buffer) in each IP. The mixtures incubated on a rotating platform at 4^{o}C for 2 hours. Beads with immuno-precipitated proteins were washed six times with IP wash buffer. Bound proteins were eluted by boiling beads in 2xSDS PAGE sample buffer at 95^{o}C for 5min.

2.2.4.5 Cdc14 in-vitro phosphatase assay

Chs2p-3myc was pulled-down from TCA lysates of cells arrested in Noc as described above with slight modification. After incubation on a rotating platform at 4^{o}C for 2 hours, the beads with precipitated Chs2p-3myc were washed six times with phosphatase buffer (50mM imidazole pH6.6, 1mM

EDTA, 1mM dithiothreitol, and 0.5mg/ml bovine serum albumin) (Traverso et al., 2001). Beads were then incubated with or without recombinant GST-6 His-Cdc14p (a gift from Dr. Yeong Foong May) for 1 hour at 30^{o}C. As control, 1mM sodium orthovanadate was used to inhibit the activity of GST-6 His-Cdc14p. For positive control, beads were treated with 400U of lambda phosphatase (NEB) for 1 hour at 30^{o}C. The supernatant was collected and subjected to western blot analysis. The beads were washed three times with IP lyse buffer, eluted with 2xSDS PAGE sample buffer and boiled at 95^{o}C for 5min. Eluted lysates were subjected to Phos-tag gel analysis (Kinoshita et al., 2009).

2.2.4.6 Western blot analysis

Protein lysates were subjected to SDS-PAGE analysis, transferred to nitrocellulose membrane (Thermo Scientific), and probed with respective primary antibodies followed by corresponding secondary antibodies (Table 2). The membrane was then incubated with Clarity enhanced chemi-luminescence kit (Bio-rad) and protein bands were developed with ChemiDoc MP System (Bio-rad). The protein band intensity was quantified with Image Lab Software (Bio-rad).

Table 13: Primary antibodies used in this study.

Primary Antibody	Company	Dilution Factor
α-Clb2p	Santa Cruz,CA	1:10000
α-Cdc14p	Santa Cruz,CA	1:5000
α-Cdc28p	Santa Cruz,CA	1:2500
α-HA	Santa Cruz,CA	1:1000
α-myc	Santa Cruz,CA	1:1000

α-C-myc	Bethyl Laboratories	1:10000
α-Pgk1p	Invitrogen	1:100000

Table 14: Secondary antibodies used in this study.

Secondary Antibody	Company	Dilution Factor
Goat-α-Rabbit-HRP	Thermo Scientific	1:10000
Goat-α-Mouse-HRP	Thermo Scientific	1:10000
Rabbit-α-Chicken-HRP	Thermo Scientific	1:10000

2.2.5 Fluorescence Microscopy

2.2.5.1 Calcofluor White and FM4-64 Staining.

3 OD_{600} of cells were harvested and fixed in 3.7% paraformaldehyde for 0.5h at room temperature. Cells were then resuspended in 1mg/ml calcofluor white solution (pH11.0) for 10min with gentle agitation. Excessive stain was washed off 3 times with pH11.0 dH_2O by centrifugation of the cells.

3 OD_{600} of cells were harvested for respective time-points. Cells were then and resuspended in YPD containing 0.02mg/ml of FM4-64 (Molecular probes) and incubated for 5min at room temperature with gentle agitation. Free dye was washed off 2 times with dH_2O by centrifugation of the cells.

Samples were then subjected to fluorescence microscopy analysis.

2.2.5.2 Wide-field time-point fluorescence microscopy and time-lapsed microscopy

Samples for fluorescence microscopy were taken at time points indicated in the relevant sections. Cells harbouring fluorescence protein fusions harvested by centrifugation and washed once with dH_2O. Samples were observed

directly without fixation using an IX81 wide-field fluorescence microscope (Olympus) with 60x NA 1.4 oil lens, and 1.5x optivar. Filter sets for fluorescence microscopy were purchased from Omega and Semrock, and images were capture using a SSD camera (CoolSnap HQ, Photometrics). Images acquisition was controlled by Metamorph software (Molecular Devices). Typically, the exposure time for the acquisition of the images was 0.25s for GFP, 1.8s for YFP, 0.6s for CFP, 0.03s for RFP and 0.1s for DAPI per plane. Nine-optical Z-sections at 0.5μm intervals were obtained for each time point. Images shown were either maximal projection of the Z-stacks or images taken at a single plane, as indicated in the relevant sections. For spindle collapsed analysis (Figure 4.12), 3D reconstruction of Z-stack captured was performed using Metamorph to ensure the monopolar spindles observed were not bi-polar spindles that positioned perpendicular to the slide. At least 50 cells were counted for each time-point from 3 independent experiments.

For time-lapsed microscopy, cells released from Noc arrest were resuspended in complete synthetic medium containing glucose and mounted onto agarose pad (5% agarose in SC/Glu medium) on slides. Time-lapsed images were captured as described in pervious section. Zero-drift compensation, ZDC (Olympus) was used for focal drift correction throughout the time-lapsed microscopy. For time-lapsed microscopy at 32^{o}C, stage top incubator was used to control the temperature. ImageJ (National Institutes of Health, Bethesda, MA) and Photoshop (Adobe, San Jose, CA) were used for the production of the montages and figures.

2.2.5.3 Spinning disk confocal time-lapsed microscopy

Cells were treated as described in the wide-field time-lapsed microscopy. Spinning disk images were captured using Olympus IX81-ZDC microscope, with a 60x NA 1.4 oil lens. Sapphire LP 488nm and 561nm solid-state lasers (Coherent) were used for the samples excitations. Filter sets for fluorescence microscopy were purchased from Omega and Semrock, and images were capture using the Photometrics 512EM-CCD attached behind the Yokogawa CSU22 connected to the microscope. GFP and RFP images were captured simultaneously using via a Dual-View image splitter (Optical Insights). Images acquisition was controlled by Metamorph software (Molecular Devices). Typically, the exposure time for the acquisition of the images was 0.2-0.35s per plane. 9-optical Z-sections at 0.5µm or 17-optical Z-sections at 0.25 µm intervals were obtained for each time point. Images shown were either maximal projection of the Z-stacks. For time-lapsed microscopy at 32^{o}C, stage top incubator was used to control the temperature. ImageJ (National Institutes of Health, Bethesda, MA) and Photoshop (Adobe, San Jose, CA) were used for the production of the montages and figures.

2.2.5.4 Chs2p signals classification parameters

Cells with visible Chs2p ER localization were counted as ‘ER’. Any cells with Chs2p neck signals were classified as ‘Neck’ count. Cells with bright fluorescence signals in the cell body and without visible ER or neck signals were refer as ‘vacuolar’ count.

Chapter 3 Results

It has been previously shown that Chs2p is retained in the ER when mitotic kinase activity is high during metaphase (Teh et al., 2009; Zhang et al., 2006). Chs2p retention at the ER during metaphase requires phosphorylation of its N-terminal serine cluster by mitotic kinase, Clb2p-Cdk1p complex. Upon mitotic exit, the destruction of mitotic cyclins causes rapid Chs2p ER export and localized to the division site (Teh et al., 2009). However, the molecular pathway that relieving the inhibitory action of Cdk1p on Chs2p that allows its ER export remains unknown. This section presents the evidence that elucidate the role of Cdc14p in triggering timely Chs2p ER export at the end of mitosis.

3.1 Cdc14p nucleolar release to the cytoplasm precedes Chs2p neck localization during mitotic exit.

A previous study demonstrated that a phospho-deficient mutant of Chs2p (Chs2p-4S-to-4A) is constitutively exported from the ER even in the presence of high mitotic kinase activity (Teh et al., 2009). We hypothesized that export of Chs2p from the ER at mitotic exit requires dephosphorylation of the N-terminal cluster of serine residues by an unknown phosphatase. Many of the proteins that are phosphorylated by Cdk1p appear to be potential substrate for Cdc14p (a dual specificity phosphatase) (Bloom et al., 2011). Besides, the N-terminal of Chs2p contains several consensus sequences for Cdc14p recognition (Gray et al., 2003). Hence, Cdc14p could be the key regulator that triggers Chs2p ER export at the end of mitosis. However, the dynamics of Cdc14p nucleolar release to the cytoplasm relative to Chs2p ER export is yet to be established. If Cdc14p is indeed the phosphatase that reverses the N-terminal serine clusters phosphorylation of Chs2p, the cytoplasm localization of Cdc14p must precedes Chs2p ER export during mitotic exit.

To test this idea, time-lapsed microscopy was conducted using cells harbouring *CDC14-ECFP CHS2-YFP* to examine the temporal localization of Cdc14p-ECFP relative to Chs2p-YFP following Noc release. At 0min, Cdc14p-ECFP was retained in the nucleolus. As cell progress from metaphase to early anaphase, FEAR triggers the Cdc14p-ECFP dispersal to the nucleoplasm as evident from the loss of distinct Cdc14p-ECFP nucleolar signal [Figure 3.1 (b) 6-9min]. Notably, Chs2p-YFP was retained in the ER. After nuclear division, Cdc14p-ECFP was resequestered back into the nucleolus. At the onset of late anaphase, MEN activation triggers the complete dispersal of Cdc14P-ECFP to the cytoplasm [Figure 3.1 (b) 27-33min]. Upon Cdc14p-ECFP cytoplasm dispersal, Chs2p-YFP was rapidly exported out from the ER and localized to the neck [Figure 3.1 (a) 30min]. The time interval between Cdc14p-ECFP cytoplasm dispersal of Chs2p-YFP neck localization was 7.06 ± 1.91min (n=48), with Cdc14p cytoplasm dispersal preceding Chs2p-YFP neck localization in all cells examined. Cdc14p-ECP was then resusquestered back into the nucleolus as evident from the re-appearance of two distinct nucleolus signals.

Taken together, the data showed that Cdc14p cytoplasm localization precedes Chs2p ER export. The complete dispersal of Cdc14p to the cytoplasm might be required for the reversal of Chs2p phosphorylation and permits its localization to the neck.

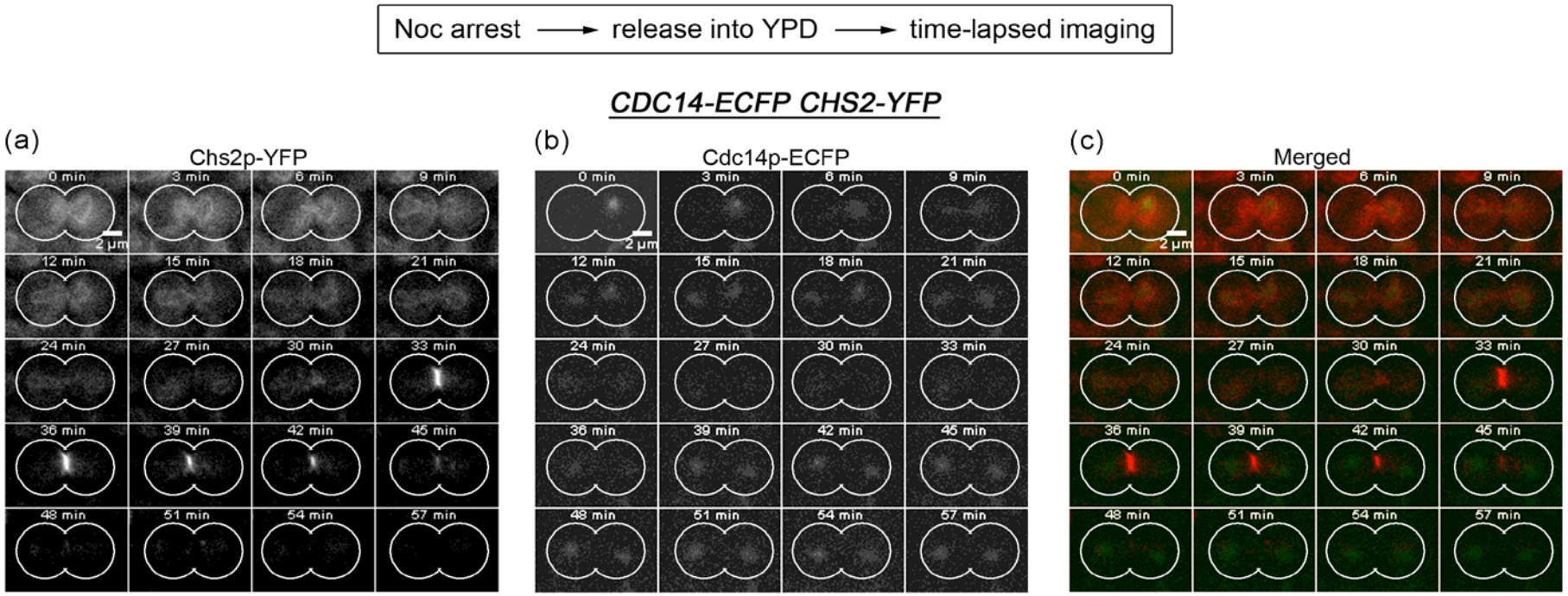

Figure 3.1 Cdc14p nucleolar release to the cytoplasm precedes Chs2p neck localization during mitotic exit. Cells harbouring *CDC14-ECFP CHS2-YFP* were arrested in YPD/Noc at 24^{o}C for 4 hours. Cells were then released from metaphase block and mounted on SC/Glu agar pad for time-lapsed microscopy. Images were taken at 3min intervals, with (a) single plane for Chs2p-YFP and (b) 9x0.5µm z-planes for Cdc14p-ECFP (Image shown was maximum projection of all 9 z-planes). (c) Merged images of Chs2p-YFP (labelled with red pseudo-colour) and Cdc14p-ECFP (labelled with green pseudo-colour).

3.2 Chs2p ER release is triggered by premature activation of MEN but not FEAR pathway in Noc arrested cells.

The results from the time-lapsed microscopy of the dynamics of Cdc14p-ECFP and Chs2p-YFP during Noc release suggest that Chs2p ER export may be mediated by the MEN dependent release of Cdc14p at the end of mitosis

To further demonstrate that MEN, but not FEAR triggers Chs2p ER export to the neck, yeast strains harbouring *CHS2-YFP CDC14-mCHERRY* with *bub2*Δ and *cdc55*Δ were generated. It has been previously established that deletion of Protein Phosphatase 2A regulatory B-subunit, *CDC55*, triggers the premature activation of FEAR pathway in metaphase that eventually contributes to Cdc14p release into nucleoplasm (Wang and Ng, 2006; Yellman and Burke, 2006). Hyperactivation of MEN in metaphase can be achieved through inactivation of the GAP Bfa1p-Bub2p complex (Wang et al., 2000; Wang and Ng, 2006). Cells were synchronized to G1 phase using alpha-factor and released into Noc containing medium. Upon arrest in metaphase (as evident from large budded cells), cells were harvested at 30min intervals and examined by fluorescence microscopy. In wild type cells, most of the Chs2p-GFP was retained in the ER with distinct Cdc14p-mCherry nucleolar signals [Figure 3.2 (a)]. In contrast, in *cdc55*Δ cells, Cdc14p-mCherry was release from the nucleolus to the nucleoplasm as evident from the diffusion of Cdc14p-mCherry signal to the perinuclear region, which is surrounded by Chs2p-GFP ER signals. However, the percentage of Chs2p-GFP neck signals was relatively low suggesting that premature FEAR activation was not capable to trigger Chs2p-GFP ER export [Figure 3.2 (b)]. Intriguingly, in *bub2*Δ cells, Chs2p-GFP ER export percentage as indicated by the loss of Chs2p-GFP ER

signals was gradually increased. The Chs2p-GFP ER release was associated with the diffusion of Cdc14p-mCherry to the cytoplasm [Figure 3.2 (c)]. Cdc14p-mCherry was later re-sequestered back into the nucleolus. This could be due to the lack of full MEN activity in Noc arrested cells (Mohl et al., 2009; Stegmeier and Amon, 2004). This suggests that the diffusion of Cdc14p-mCherry to the cytoplasm alleviates the Chs2p-GFP N-terminal phosphorylation and triggers its ER export.

Taken together, the data obtained further corroborates the results of the Cdc14p and Chs2p time-lapsed microscopy during Noc release, indicating that Chs2p ER export during late mitosis is likely facilitates by MEN dependent cytoplasm release of Cdc14p.

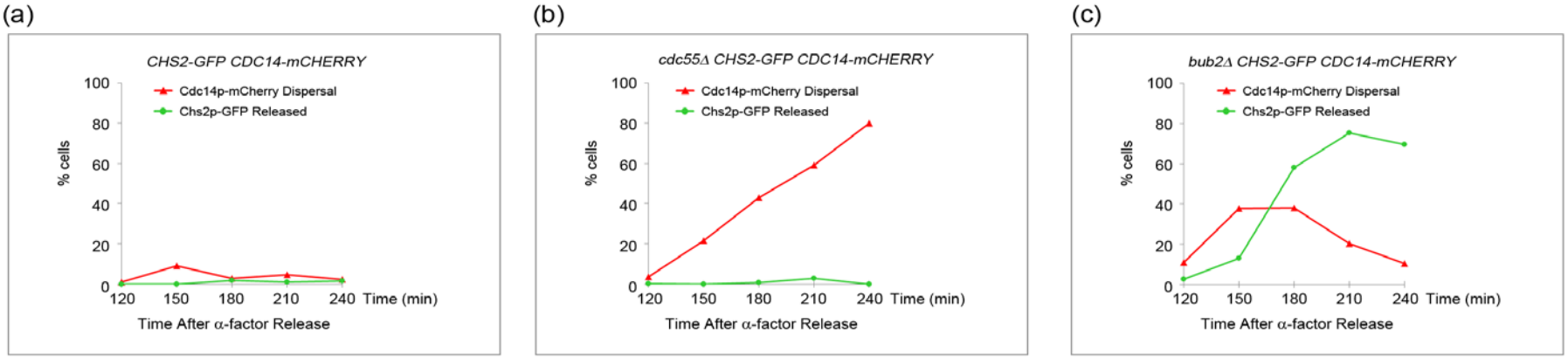

Figure 3.2 Chs2p ER release is triggered by premature activation of MEN but not FEAR pathway in Noc arrested cells. Cells harbouring (a) *CHS2-GFP CDC14-mCHERRY*, (b) *cdc55*Δ *CHS2-GFP CDC14-CHERRY*, and (c) *bub2*Δ *CHS2-GFP CDC14-CHERRY* were arrested in YPD/alpha-factor at 24^{o}C for 2 hours. Cells were then released into YPD medium containing Noc. Upon arrest in metaphase (as indicated by large budded cells), cells were harvested at 30min intervals and subjected to fluorescence microscopy analysis. Images were taken with single plane for Chs2p-GFP and 9x0.5µm z-planes for Cdc14p-mCherry. Graph plots showing the percentage of cells with Chs2p-GFP release and Cdc14p-mCherry dispersal.

3.3 Ectopic expression of Cdk1 inhibitor, Sic1p, triggers the premature Cdc14p nucleolar release and Chs2p ER export at metaphase.

A previous study demonstrated that ectopic expression of Cdk1p inhibitor, Sic1p triggers Chs2p ER export to the neck during metaphase (Zhang et al., 2006). This raises the question if overexpression of *SIC1* during metaphase contributes to the Cdc14p nucleolar release to the cytoplasm and facilitates the Chs2p ER export via the reversal of Chs2p N-terminal phosphorylation.

To ascertain if *SIC1* overexpression triggers Cdc14p nucleolar release and Chs2p ER export, cells harbouring *CDC14-ECFP CHS2-YFP NET1-mCHERRY GAL-SIC1-MYC (4-copies)* were employed. The localization of Cdc14p-ECFP and Chs2p-YFP was examined in cells arrested in Noc with or without Gal induction of Sic1p using time-lapsed microscopy. Net1p-mCherry, a core component of the RENT (for REgulator of Nucleolar silencing and Telophase) complex that sequesters Cdc14p in the nucleolus was used as a nucleolar marker (Shou et al., 1999). In glucose grown cells (no Sic1p induction), almost 95% of the Cdc14-ECFP was sequestered in the nucleolus with Chs2p-YFP retained in the ER. Approximately 5% of cells showed Chs2p-YFP ER export with dispersal of Cdc14p-ECFP. Interestingly, as low as 1% of cells showed nucleolar signals of Cdc14p-ECFP with Chs2p-ER neck signals [(n=178) Figure 3.3 (b) and (d)].

In contrast, in galactose-grown cells (ectopic Sic1p expression), 25% of cells showed a transient but complete Cdc14p-ECFP nucleolar release [Figure 3.3 (a) 18-39min] and re-sequestered back into nucleolus. The Cdc14p-ECFP nucleolar release was associated with Chs2p-YFP ER export as evident from

the loss of Chs2p ER signals and appearance of Chs2p-YFP neck signals [Figure 3.3 (a) 24min onward]. Net1p-mCherry signals were present throughout the duration of the time-lapsed microscopy indicating that the disappearance of Cdc14p-ECFP was indeed due to its nucleolar release [Figure 3.3 (a) 12-54min]. Intriguingly, about 22% of the cells showed Chs2p-YFP neck signals in the absence of visible Cdc14p-ECFP nucleolar release. In these cells, the Chs2p-YFP neck intensity was weaker and persisted longer at the neck. This suggests that the level of ectopic expression of *SIC1* in these cells was insufficient to trigger complete release of Cdc14p-ECFP to the cytoplasm. The partial release of Cdc14p-ECFP that is contributed by low levels of Sic1p might not be easily detected using the microscope, but sufficient to trigger Chs2p-YFP ER export in a sluggish manner.

Together, these data support the idea that ectopic expression of *SIC1* in metaphase triggers the Chs2p ER export via forced release of Cdc14p to the cytoplasm.

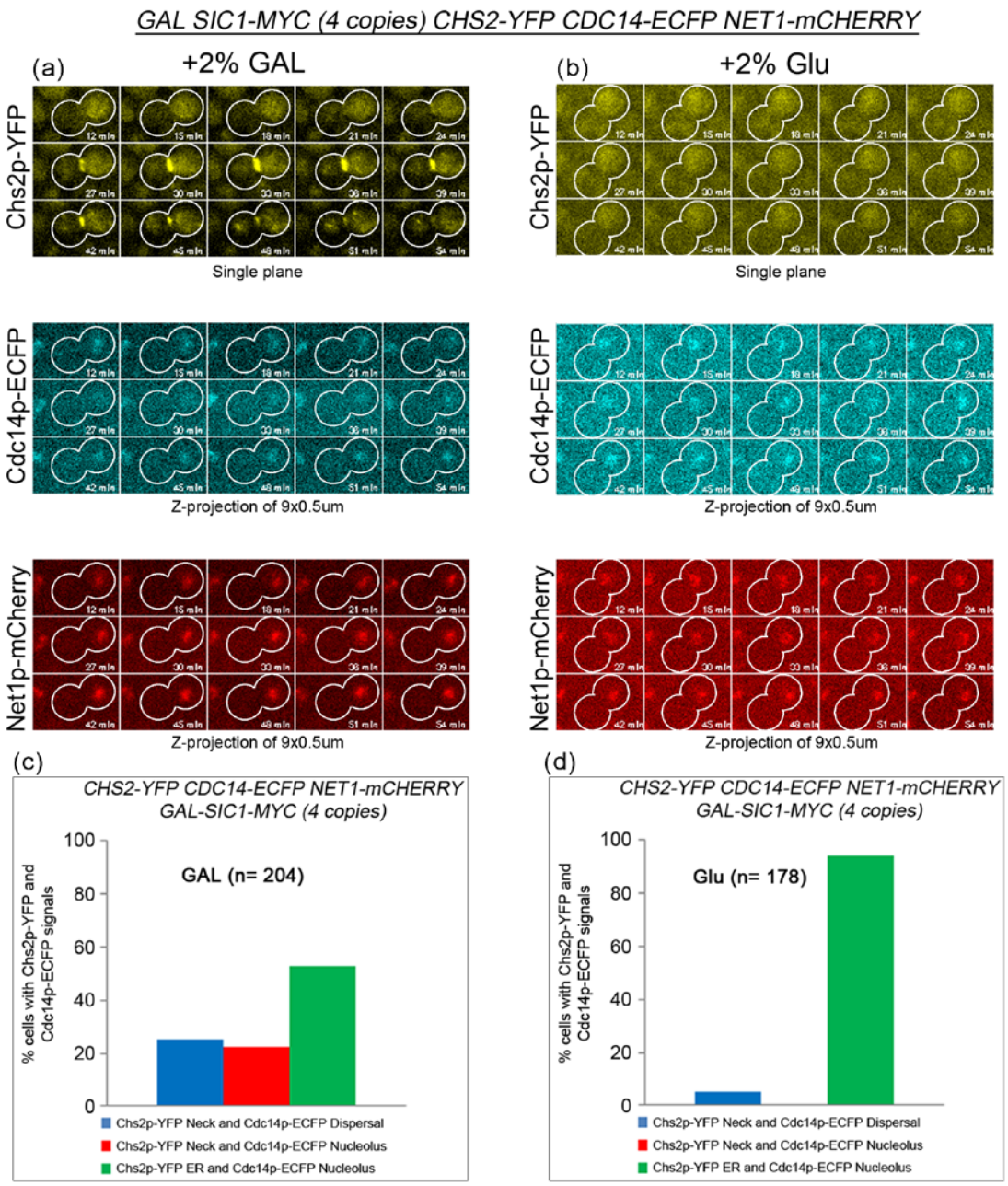

Figure 3.3 Ectopic expression of Cdk1 inhibitor, Sic1p, triggers the premature Cdc14p nucleolar release and Chs2p ER export at metaphase. Cells harbouring *GAL-SIC1-MYC (4-copies) CHS2-YFP CDC14-ECFP NET1-mCHERRY* were arrested in YP/Raff/Noc for 5 hours at 24^{o}C. (a) 2% Gal and (b) 2% Glu was added into the culture for 45min to induce the expression of Sic1p-myc. Cells were then mounted on SC/Glu agar pad containing Noc and subjected to time-lapsed microscopy. Images were taken at 3min intervals, with single plane for Chs2p-YFP and 9x0.5µm z-planes for Cdc14p-ECFP and Net1p-mCherry (Image shown was maximum projection of all 9 z-planes). [(c) and (d)] Graph plots showing percentage of cells with Chs2p-YFP and Cdc14p-ECFP nucleolar or dispersal.

3.4 Chs2p-GFP ER export is prohibited in the absence of Cdc14p activity.

Data above indicated that Chs2p ER export invariably occurs after Cdc14p cytoplasm localization. This led to the hypothesis that the cytoplasmic localization of Cdc14p is required for the reversal of Chs2p phosphorylation during mitotic exit.

To test this hypothesis, a temperature sensitive allele, *cdc14-3* (a mutant that displays loss of Cdc14p activity at non-permissive temperature, 37^{o}C) was employed. However, Cdc14p is the key factor that triggers mitotic exit via Cdh1p dephosphorylation which results in APC^{Cdh1p} activation. Besides, Cdc14p also regulates Cdk1p inhibition by dephosphorylating the mitotic kinase inhibitor, Sic1p transcription factor, Swi5p (Visintin et al., 1998). Loss of Cdc14p activity during mitotic exit will lead to the terminal arrest of cells at late anaphase (D'Amours and Amon, 2004). In order to substitute the function of Cdc14p in triggering mitotic exit, a strain harboring non-degradable form of Sic1p, *sic1-NT*Δ (Noton and Diffley, 2000) was constructed. The ectopic expression of sic1p-NTΔ under the control of inducible galactose promoter will force the mitotic exit of *cdc14-3* cells at 37^{o}C (Zhai et al., 2010).

To investigate if Cdc14p activity is required for timely Chs2p ER export during mitotic exit, the localization of Chs2p in cells harboring *CHS2-GFP GAL- sic1-NT*Δ with *CDC14* or *cdc14-3* were examined during nocodazole release at 37^{o}C. Consistent with previous study, Chs2p-GFP was retained in the ER during metaphase in both wild-type and *cdc14-3* mutant cells (Teh et al., 2009) [Figure 3.4 (a) and (c)]. Upon releasing into medium containing galactose, Chs2p-GFP neck localization signal can be seen in 14% of the wild-

type cells at 30min time-point. At 150min, only 1% of cells retained Chs2p-GFP ER localization [Figure 3.4 (b) and (e)]. The appearance of the Chs2p-GFP vacuolar structure indicated that Chs2p-GFP was exported out from the ER to the neck, endocytosed and finally delivered to the vacuole for degradation (Chuang and Schekman, 1996). Indeed, such vacuolar signals were absent in *sla2*Δ cells that were compromised in endocytosis process [Figure 3.5 (d) (40-100min) and (e)]. In contrast to wild-type cells, Chs2p-GFP was retained in the ER in 89% of *cdc14-3* cells, even after the cells exited from mitosis as evident from the emergence of new buds [Figure 3.4 (d) 150min, (f), and (g)]. The absence of the Chs2p-GFP vacuolar/endosome signals further corroborates the idea that Chs2p-GFP ER export in *cdc14-3* cells was defective. Taken together, these data suggest that Cdc14p activity is essential for timely Chs2p-GFP ER export at the end of mitosis.

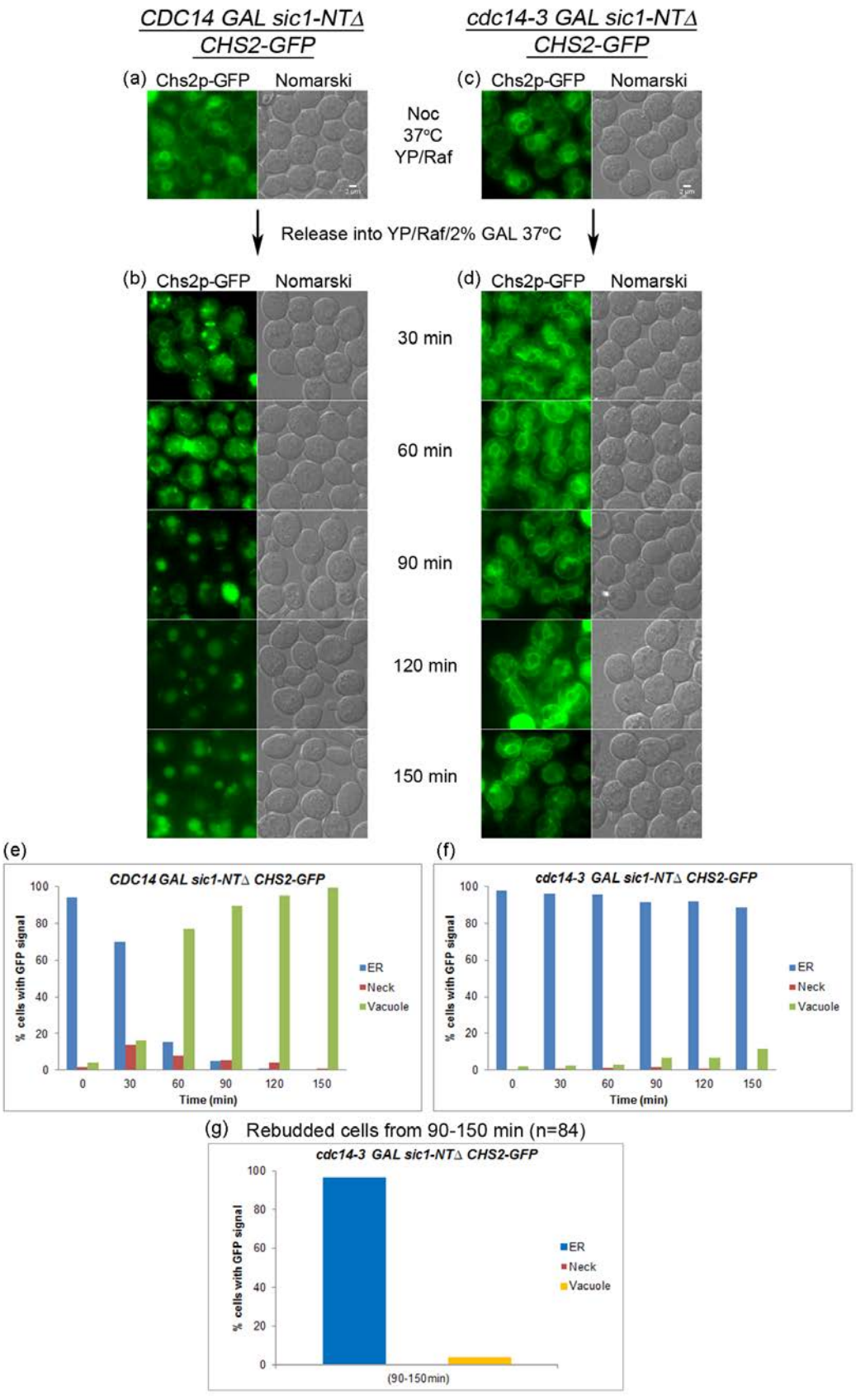
CDC14 GAL sic1-NTΔ CHS2-GFP
cdc14-3 GAL sic1-NTΔ CHS2-GFP
(a) Chs2p-GFP Nomarski
(c) Chs2p-GFP Nomarski
Noc
37°C
YP/Raf
Release into YP/Raf/2% GAL 37°C
(b) Chs2p-GFP Nomarski
(d) Chs2p-GFP Nomarski
30 min
60 min
90 min
120 min
150 min
(e)
CDC14 GAL sic1-NTΔ CHS2-GFP
% cells with GFP signal
Time (min)
ER
Neck
Vacuole
(f)
cdc14-3 GAL sic1-NTΔ CHS2-GFP
% cells with GFP signal
Time (min)
ER
Neck
Vacuole
(g) Rebudded cells from 90-150 min (n=84)
cdc14-3 GAL sic1-NTΔ CHS2-GFP
% cells with GFP signal
(90-150min)
ER
Neck
Vacuole

Figure 3.4 Chs2p-GFP ER export is prohibited in the absence of Cdc14p activity. (a) *CDC14* and (c) *cdc14-3* cells harbouring *CHS2-GFP GAL-sic1 NT*Δ respectively were arrested in YP/Raff/Noc for 4 hours and shifted up to 37^{o}C for another hour. [(b) and (d)] Cells were washed and released into YP/Raff/2% Gal at 37^{o}C. Samples were harvested at respective time-points shown and examined with fluorescence microscope. [(e) and (f)] Graph plots showing percentage of cells with Chs2p-GFP signals from 0-150 min time-points. (n>100 for each time-point) (g) Graph plots showing percentage of re-budded cells from 90-150 min time-points (n=84). Graph plots shown were typical representations of three independent experiments. Chs2p-GFP signals were classified as described in Material and Methods section.

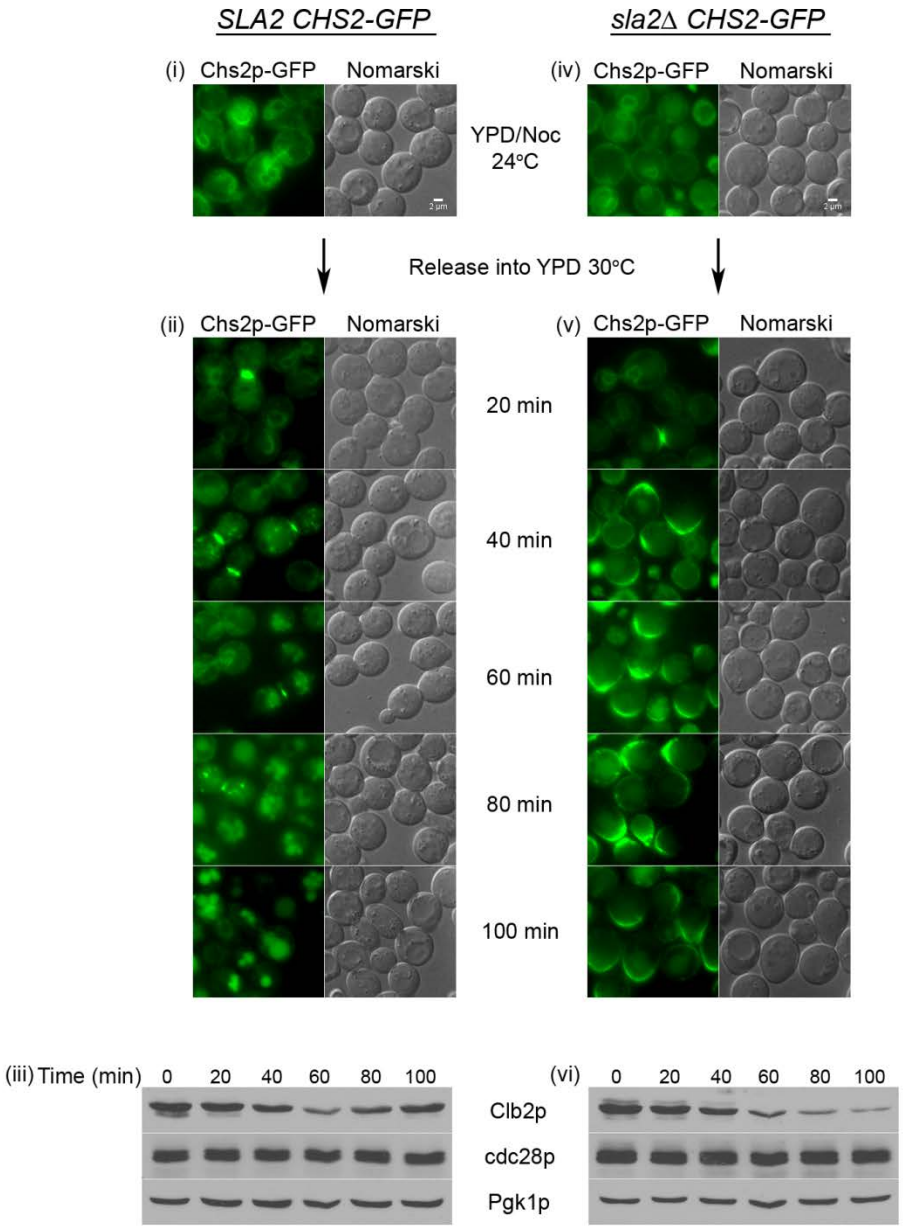

Figure 3.5 Chs2p-GFP failed to be internalized from the division site in *sla2*Δ mutant cells. (i) *SLA2* and (iii) *sla2*Δ cells harbouring *CHS2-GFP* respectively were arrested in YPD/Noc for 4.5 hours. [(ii) and (iv)] Cells were washed and released into fresh YPD Gal at 30^{o}C. Samples were harvested every 20min and subjected to fluorescence microscopy and western blot analysis.

3.5 Cdc14p nucleolar release to the cytoplasm triggers Chs2p-YFP ER export.

Previous studies demonstrated that the N-terminal of Chs2p is located in the cytoplasm while its C-terminal is embedded in the ER membrane (Martinez-Rucobo et al., 2009; Teh et al., 2009) during metaphase when Cdc14p is sequestered in the nucleolus (Visintin et al., 1999). At the onset of anaphase, MEN activation triggers the release of Cdc14p to the cytoplasm (Stegmeier and Amon, 2004). If Cdc14p is indeed the phosphatase that reverses the N-terminal serine clusters phosphorylation of Chs2p, inhibition of Cdc14p cytoplasm release should prevent the ER export of Chs2p during mitotic exit.

To test this idea, a temperature sensitive mutant, *cdc14*-Nuclear Export Sequence (*cdc14-NES*) that fails to localize to the cytoplasm at late anaphase but is capable of triggering mitotic exit was employed (Bembenek et al., 2005). Yeast strains harbouring *CHS2-YFP* with wild-type *CDC14* or *cdc14-NES* were constructed. Next, the Chs2p-YFP neck localization during metaphase release at 37^{o}C was examined. In wild-type cells, Chs2p-YFP was rapidly exported from the ER and localized to the division site at 20min (27%) and 40min (26%) respectively. Chs2p-YFP ER signals were diminished and vacuolar/endosome signals can be seen at 60mins onwards. This indicates that Chs2p-YFP was translocated from the ER to the neck. The neck localized Chs2p-YFP was then internalized and directed to vacuole for degradation [Figure 3.6 (a), (b) and (g)]. Surprisingly, Chs2p-YFP ER signals persisted throughout the duration of the metaphase release (20-100min) in *cdc14-NES* cells. However, a low percentage of Chs2p-YFP neck signals (14.6%) can be observed in *cdc14-NES* cells [Figure 3.6 (c), (d) and (h)]. In contrast to *cdc14-*

3 cells that displayed a strong inhibition of Cdc14p activity, the nucleolar release of *cdc14-NES* to the cytoplasm might be only partially suppressed at non-permissive temperature. This suggests that the small amount of Cdc14p that escaped to the cytoplasm allowed the partial release of Chs2p-YFP to the neck, but the amount is insufficient to trigger the full blown export of Chs2p-YFP from the ER. Nonetheless, the ER export of Chs2p-YFP was indeed severely affected as evident from Chs2p-YFP retention in 96.6% of *cdc14-NES* cells [100min, Figure 3.6 (h)]. In addition, the defective Chs2p-YFP ER export in *cdc14-NES* cells was not due to compromised mitotic exit, given that the degradation of mitotic cyclins, Clb2p was equivalent to wild-type cells during Noc release [Figure 3.6 (e) and (f)].

Collectively, these data further corroborate the hypothesis that Chs2p ER export is mediated by cytoplasmic localization of Cdc14p at the end of mitosis.

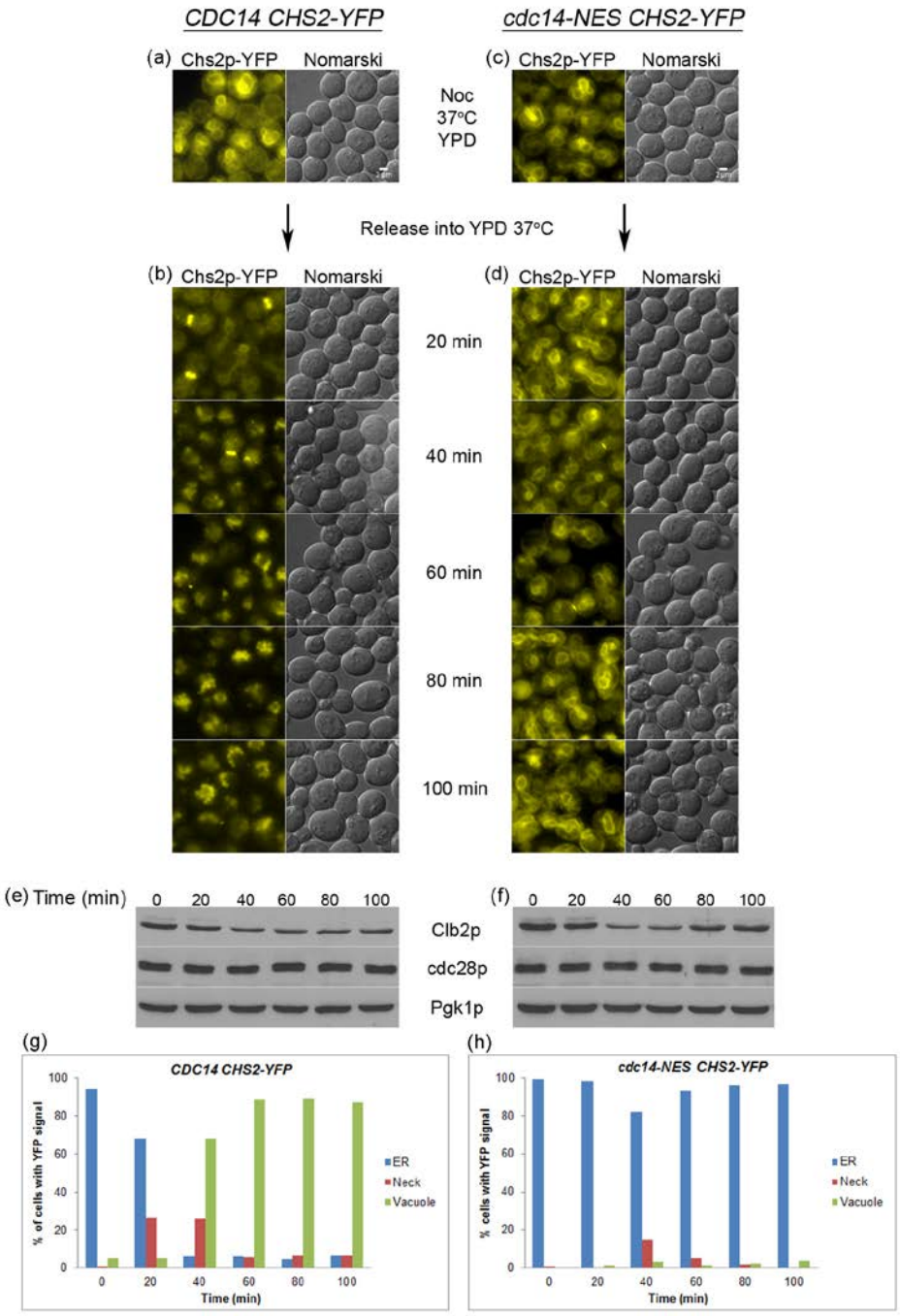

Figure 3.6 Cdc14p nucleolar release to the cytoplasm triggers Chs2p-YFP ER export. (a) *CDC14* and (c) *cdc14-NES* cells harbouring *CHS2-YFP* respectively were arrested in YPD/Noc for 4.75 hours and shifted up to 37^{o}C for 15min. [(b) and (d)] Cells were washed and released into fresh YPD at 37^{o}C. Samples were harvested every 20min and subjected to fluorescence microscopy and western blot analysis. [(e) and (f)] Western blot analysis of Clb2p, Cdc28p and Pgk1p to demonstrate equivalent mitotic exit in Noc released cells. [(g) and (h)] Graph plots showing percentage of cells with Chs2p-YFP signals from 0-100 min time-points (n>100 for each time-point). Graph plots shown were typical representations of three independent experiments. Chs2p-YFP signals were classified as described in Material and Methods section.

3.6 COPII secretory pathway is competent in *cdc14-NES* mutant.

Inhibition of COPII secretory pathway will lead to the retention of secretory cargoes in the ER (Novick et al., 1980). It has been established that the mutation of the N-terminal Cdk1 sites of *chs2* from four serine to alanine led to constitutive ER export even in the high mitotic kinase environment (Teh et al., 2009).

To determine if the secretory pathway is compromised in the *cdc14-NES* mutant, strains were constructed that harbored either the wild-type, *CHS2-YFP*, or the phospho-deficient *CHS2-(4S-to-4A)-YFP* under the control of a galactose-inducible promoter. The strain also contained *SEC63-CFP* cells to mark the ER. The localization of Chs2p-YFP during metaphase release was examined. Consistent with above observation [Figure 3.6 (d) and (h)], wild-type Chs2p-YFP failed to localize to the division site as indicated by the persistence of ER signals that colocalized with ER resident protein, Sec63p-CFP, and the low percentage of Chs2p-YFP vacuolar signals in *cdc14-NES* cells [30-120min, Figure 3.7 (b) and (e)]. As opposed to wild-type Chs2p-YFP, the phospho-deficient Chs2p-(4S-to-4A)-YFP was rapidly exported out from the ER [Figure 3.7 (d) and (f)]. As Chs2p-YFP endocytosis was rapid at 37^{o}C, latrunculin B, a F-actin inhibitor that disrupts endocytosis (Smythe and Ayscough, 2006) was added into the culture to enrich Chs2p-(4S-to-4A)-YFP neck signals. Chs2p-(4S-to-4A)-YFP neck signals percentage was gradually increased from 15.4% at 30min to 70.2% at 90min [Figure 3.7 (d) and (f)]. The sub-optimal concentration of latrunculin B (100µM) used in the experiment reduced the efficiency of endocytosis as Chs2p-(4S-to-4A)-YFP vacuolar signals can be seen at 150min [53.4%, Figure 3.7(f)].

Overall, these results demonstrate that the secretory pathway is competent in *cdc14-NES* mutant. The defect of Chs2p ER export may be primarily due to the absence of Cdc14p in the cytoplasm that is crucial for alleviation of Chs2p phosphorylation during mitotic exit.

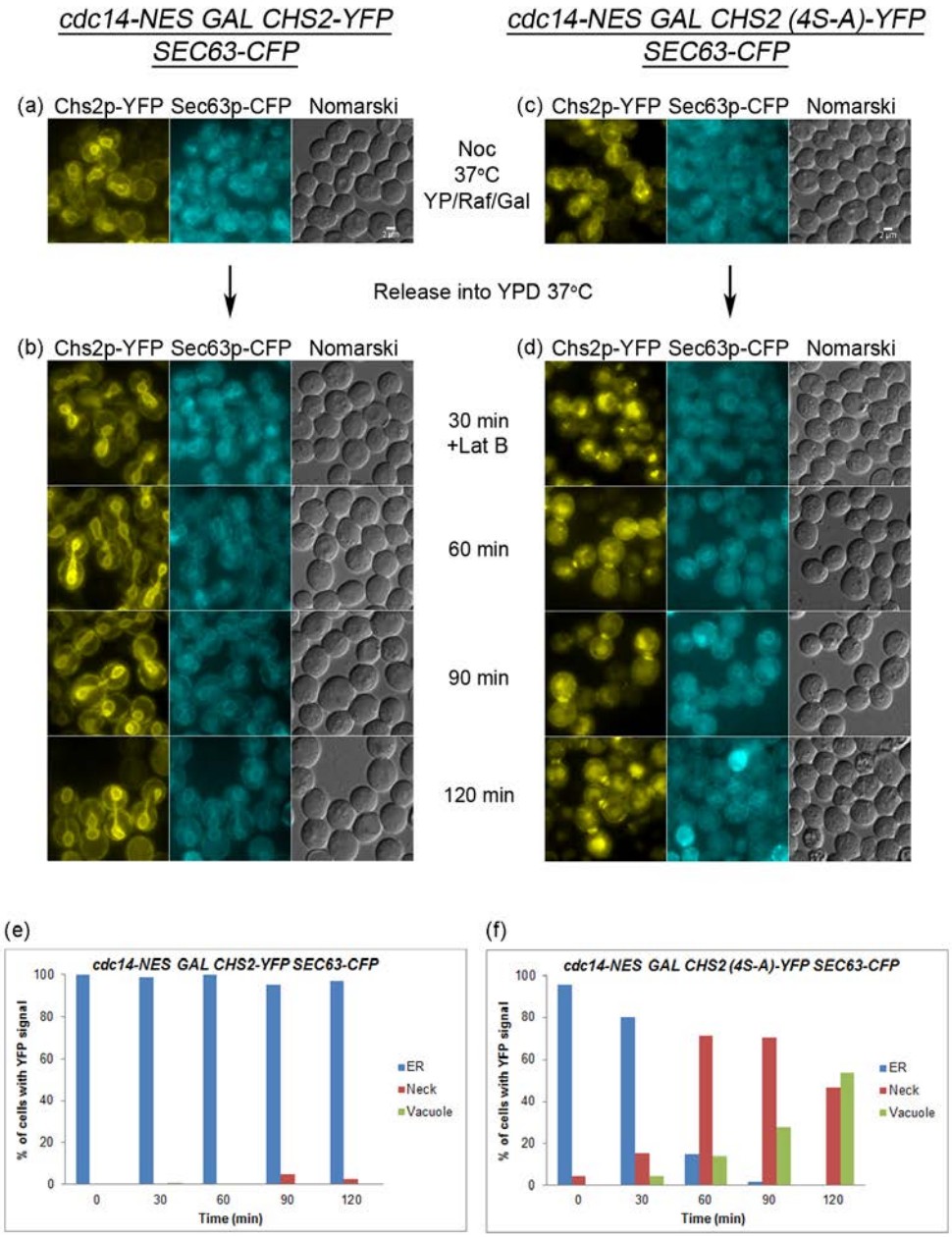

Figure 3.7 COPII secretory pathway is competent in *cdc14-NES* mutant. *cdc14-NES SEC63-CFP* cells harbouring (a) *GAL CHS2-YFP* and (c) *GAL CHS2(4S-A)-YFP* respectively were arrested in YP/Raff/Noc for 5 hours. 2% Gal was added for 45min to induce the expression of Chs2p-YFP. Cells were then shifted up to 37^{o}C for 15min. [(b) and (d)] Cells were washed and released into fresh YPD at 37^{o}C. LatB was added to final concentration of 100µM, 30min after release from Noc. Samples were harvested every 30min and examined with fluorescence microscopy. [(e) and (f)] Graph plots showing percentage of cells with Chs2p-YFP signals from 0-120 min time-points (n>100 for each time-point). Graph plots shown were typical representations of three independent experiments. Chs2p signals were classified as described in Material and Methods section.

3.7 Physical Interaction of Chs2p and Cdc14p

Live cell imaging and genetic data gathered in this study indicate that Chs2p ER exit during mitotic exit requires Cdc14p activity and cytoplasm localization. If Cdc14p is indeed the phosphatase that directly dephosphorylates Chs2p, it should be able to physically associates with Chs2p during mitotic exit.

To ascertain if Chs2p interacts with Cdc14p, a co-immunoprecipitation assay was conducted using cells harbouring *GAL-HA-CDC14 CHS2-13MYC* and *GAL-HA-CDC14 (C283S) CHS2-13MYC*. Due to the transient interaction between a substrate and a phosphatase, Cdc14p-(C283S) [a catalytic inactive mutant form of Cdc14p that forms stable complexes with the substrates (Hall et al., 2008)] was employed in this co-immunoprecipitation assay. Cells were arrested in Noc to enrich for phosphorylated Chs2p-13myc that is retained in the ER, followed by addition of galactose to induce the expression of wild-type HA-Cdc14p and the substrate trap mutant, HA-Cdc14p-(C283S). Interestingly, Chs2p-13myc was co-immunoprecipitated with both HA-Cdc14p and HA-Cdc14p-(C283S) [Figure 3.8 (a)]. Western blot analysis showed that the expression levels of Chs2p-13myc, HA-Cdc14p, HA-Cdc14-(C283S) were equivalent [Figure 3.8 (b)]. An analogous control experiment, which was conducted by substituting galactose with glucose, showed that the interaction between Cdc14p and Chs2p was indeed specific [Figure 3.8 (c) and (d)].

This evidence suggests that Cdc14p physical interacts with Chs2p during mitotic exit.

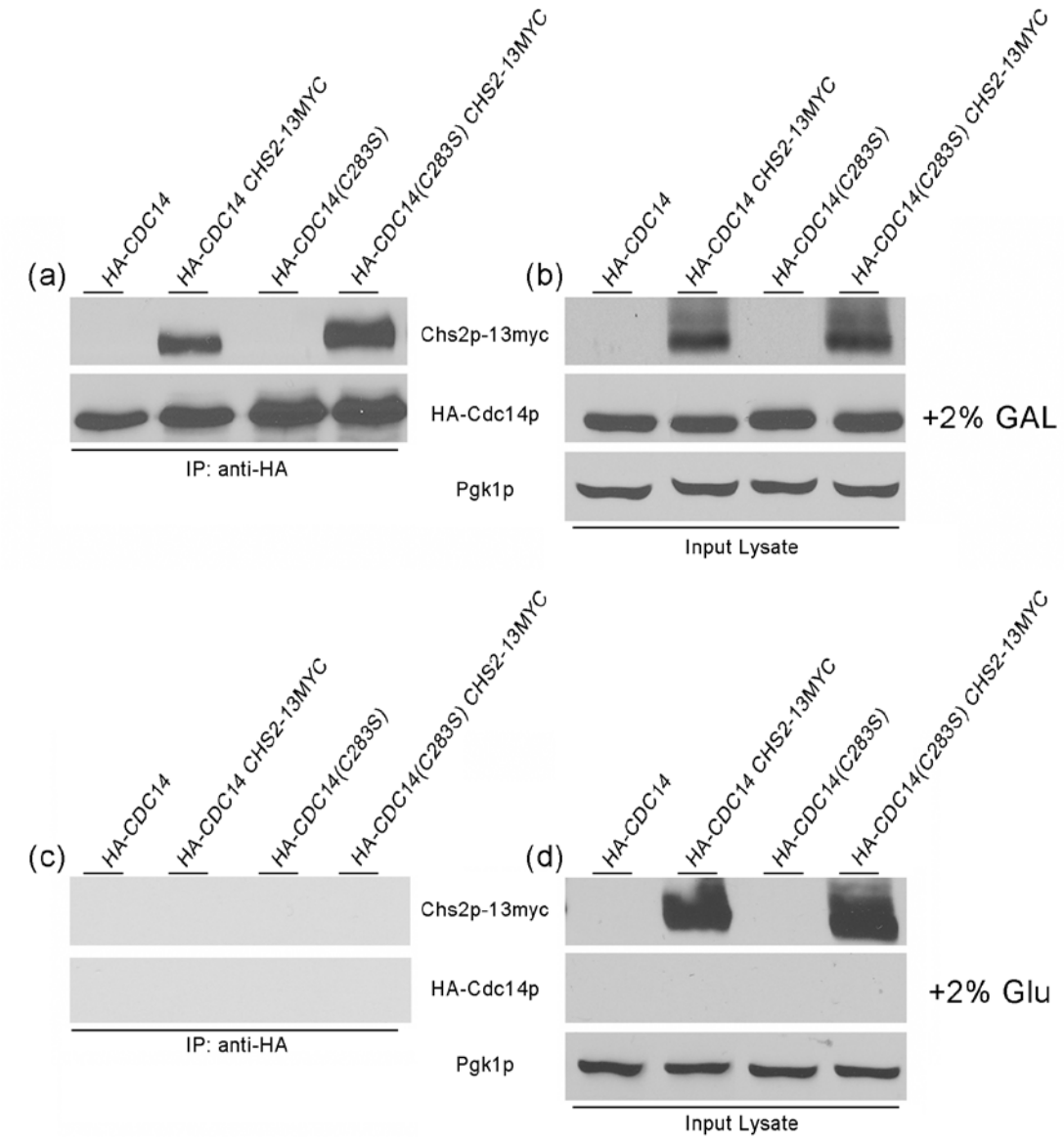

Figure 3.8 Physical interaction of Chs2p and Cdc14p. Cells harbouring *GAL-HA-CDC14*, *GAL-HA-CDC14 CHS2-13MYC*, *GAL-HA-CDC14 (C283S)* and *GAL-HA-CDC14-(C283S) CHS2-13MYC* were arrested in YP/Raff/Noc for 5 hours. (a) 2% Gal and (c) 2% Glu was added to the half of the culture for 45min respectively. Cells were then harvested, lysed and subjected to Co-immunoprecipitation (Co-IP) assay. [(b) and (d)] Western blot analysis of Chs2p-13myc, HA-Cdc14p and Pgk1p to show equivalent amount of protein lysate used in the Co-IP assay.

3.8 Chs2p is a substrate of Cdc14p in-vivo and in-vitro.

The Co-IP assay demonstrated that Chs2p physically interacts with Cdc14p. Mass spectrometry analysis of Chs2p-13myc isolated from *cdc15-2* cells at non-permissive temperature revealed that Chs2p was phosphorylated at six Cdk1 sites (S14, S69, S86, S100, S133 and S256) (shown by with Dr. Mark Hall group from Purdue University) (Chin et al., 2011). This observation raises the question of whether binding of Cdc14p to Chs2p facilitates the dephosphorylation of Chs2p at the end of mitosis.

To test this notion, an in-vivo phosphatase assay was performed using cells harbouring *GAL-HA-CDC14 CHS2-3MYC* and *GAL-HA-CDC14-(C283S) CHS2-3MYC*. Cells were synchronized in G1 phase using alpha-factor and released into medium containing YP/Raff/Noc. Upon metaphase arrest as evident from large budded cells, 2% Gal was added to induce the expression of HA-Cdc14p and the catalytic inactive mutant, HA-Cdc14p-(C283S). 100µM of LatB was added 15min after addition of Galactose to inhibit the endocytosis of Chs2p at the division site. Cells were then harvested at respective time-points and subjected to phostag-gel analysis (Kinoshita et al., 2009). In *GAL-HA-CDC14 CHS2-13MYC* cells, the phosphorylated Chs2p-13myc [Figure 3.9 (ai)-0min] was slowly converted to faster migrating band as gradual accumulation of HA-Cdc14p level [Figure 3.9 (ai)-60-120min and (aii)]. This indicates that Chs2p-13myc is efficiently dephosphoryalated by Cdc14p. Conversely, in *GAL-HA-CDC14 (C283S) CHS2-13MYC* cells, Chs2p-13myc phosphorylation persisted throughout the duration of the experiment [Figure 3.9 (ai)-60-120min and (aiii)]. The failure of Chs2p-13myc dephosphorylation in the catalytically inactive mutant strains, Cdc14p-

(C283S) suggests that the Cdc14p dephosphorylation on Chs2p was indeed specific. Taken together, the data indicates that ectopic expression of Cdc14p promotes dephosphorylation of Chs2p in metaphase.

To further demonstrate that Cdc14p directly dephosphorylates Chs2p, in-vitro phosphatase assay was conducted using bacterial expressed recombinant purified GST-6HIS-Cdc14p (a kind gift from Dr. Yeong Foong May). Phosphorylated Chs2p-3myc was immuno-precipitated from TCA extracts of cells arrested in Noc. Upon treatment with GST-6HIS-Cdc14p, Chs2p-3myc was dephosphorylated as evident from the faster migration of Chs2p band on phos-tag gel. Chs2p-3myc can be dephosphorylated by 10ng of GST-6HIS-Cdc14p. When treated with 25ng of GST-6HIS-Cdc14p, the extent of Chs2p-3myc dephosphorylation was comparable to generic lambda protein phosphatase [Figure 3.9 (b)]. To further determine the specificity of Cdc14p activity on Chs2p dephosphorylation, the activity of GST-6HIS-Cdc14p was inhibited by a potent protein tyrosine phosphatase family inhibitor, sodium orthovanadate. In the absence of Cdc14p activity, the Chs2p-3myc remained phosphorylated, supporting the specificity of Cdc14p activity [Figure 3.9 (b)].

Collectively, the evidence gathered in this study suggests that Cdc14p reverses the phosphorylation of Chs2p during mitosis. The results further supports the idea that Chs2p is a *bona fide* substrate of Cdc14p phosphatase and represents the first identified secretory cargo that is regulated in a Cdc14p dependent manner in eukaryotic cells.

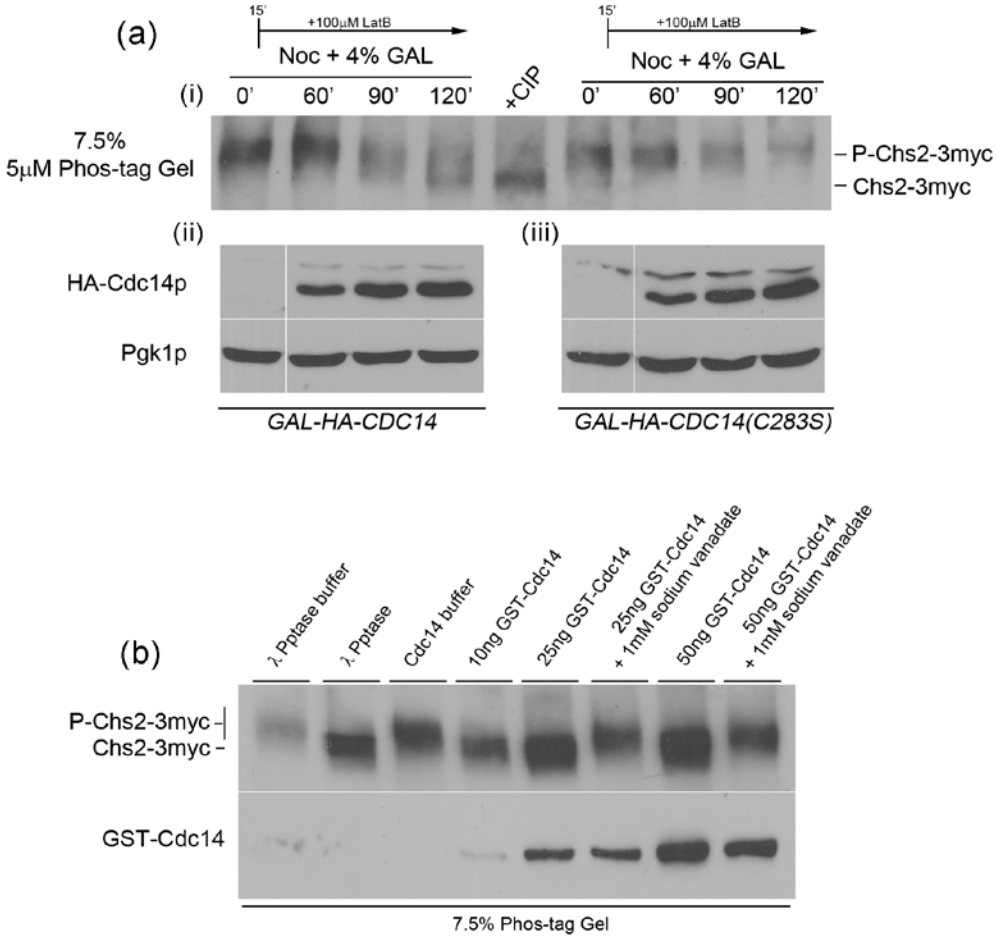

Figure 3.9 Chs2p is a substrate of Cdc14p in-vivo and in-vitro. (a) Cells harbouring *GAL-HA-CDC14 CHS2-3MYC* and *GAL-HA-CDC14-(C283S) CHS2-3MYC* were arrested in YP/Raff/alpha-factor for 3 hours. Cells were then released into fresh YP/Raff/Noc medium. (ai) Upon metaphase arrest, 4% Gal was added into the culture to induce expression of HA-Cdc14p and HA-Cdc14p-(C283S) respectively. After 15min of gal induction, 100μM of LatB was added into the culture. Cells were harvested at respective time-point, lysed and subjected to anti-myc immunoprecipitation. Immuno-precipitated Chs2p-3myc was resolved on 7.5% SDS-PAGE with 5μM Phos-tag. Anti-myc antibody was used to detect the Chs2p-3myc bands. [(aii) and (aiii) Western blot analysis of HA-Cdc14p, HA-Cdc14p-(C283S) and Pgk1p to show the galactose induction of HA-Cdc14p, HA-Cdc14p-(C283S). (b) Phosphorylated Chs2p was immunoprecipitated using anti-myc beads from Noc arrested TCA cell lysates. Chs2p-3myc bound beads were treated with phosphatase buffer or the indicated amount of recombinant purified GST-6HIS-Cdc14p at 30^{o}C for 30min. As a positive control, generic lambda protein phosphatase was used. As a negative control, sodium orthovanadate was used to inhibit the GST-6HIS-Cdc14p activity. Anti-Cdc14 antibody was used to detect the GST-6HIS-Cdc14p in the phosphatase reaction.

3.9 Chs2p ER export during late mitosis requires Cdc14p activity and inactivation of mitotic kinase.

The data gathered so far suggests that Chs2p ER export is triggered during late mitosis when Cdc14p is released into cytoplasm in parallel with mitotic kinase inactivation. This poses a question of how cells ensure that septum formation only occurs strictly after chromosome segregation as both events depend on Cdc14p activity.

To test this idea, the efficiency of Chs2p ER export and Sli15p dephoshorylation was examined in cells harbouring *GAL-SIC1-MYC (4 copies) CHS2-GFP SLI15-9MYC, GAL-HA-CDC14 CHS2-GFP SLI15-9MYC* and *GAL-HA-CDC14 (C283S) CHS2-GFP SLI15-9MYC* in metaphase. Sli15p is a component of chromosomal passenger complex that is phosphorylated by aurora B kinase, Ipl1 (Kang et al., 2001) and Cdk1p (Holt et al., 2009) during mitosis. At the onset of anaphase, FEAR dependent release of Cdc14p dephosphorylates Sli15p and triggers its translocation from the kinetochores to the mitotic spindle. As a result, spindle localized Sli15p recruits Slk19p to the midzone, which in turn promotes the spindle elongation (Pereira and Schiebel, 2003).

In cells with *SIC1* overexpression, Chs2p-GFP ER export was observed upon 60 min of galactose induction, as evident from the Chs2p-GFP neck localization and appearance of vacuolar signals [Figure 3.10 (b) and (j)]. In contrast, most of the Chs2p-GFP was retained in the ER, even after 120min of gal induction in *HA-CDC14* cells [Figure 3.10 (d) and (k), 30min onwards]. Interestingly, Sli15p-9myc dephosphorylation was observed in both *SIC1* and *HA-CDC14* overexpresssion cells, as indicated by the faster migrating band on

the SDS-PAGE [Figure 3.10 (g) and (h)]. Chs2p-ER export and Sli15-9myc dephosphorylation was not observed in catalytic inactive mutant, *HA-CDC14-(C283S)* cells [Figure 3.10 (f), (i) and (l)].

Collectively, these results suggest that Chs2p ER export requires Cdc14p activity in combination with mitotic kinase inactivation. Consistent with the results in this study, overexpression of *SIC1* in metaphase is able to trigger the release of Cdc14p from the nucleolus to the cytoplasm (Figure 3.3). Concurrently, Sic1p also acts as an inhibitor that reduces the mitotic kinase activity during metaphase. In contrast to Chs2p, Sli15p was efficiently dephosphorylated in both *SIC1* and *HA-CDC14* overexpresssion cells. This implies that Sli15p can be dephosphorylated by Cdc14p efficiently even in the presence of high mitotic kinase. This is consistent with previous findings showing Sli15p is dephosphorylated by Cdc14p when mitotic kinase is still high during early anaphase (Jin et al., 2008; Pereira and Schiebel, 2003).

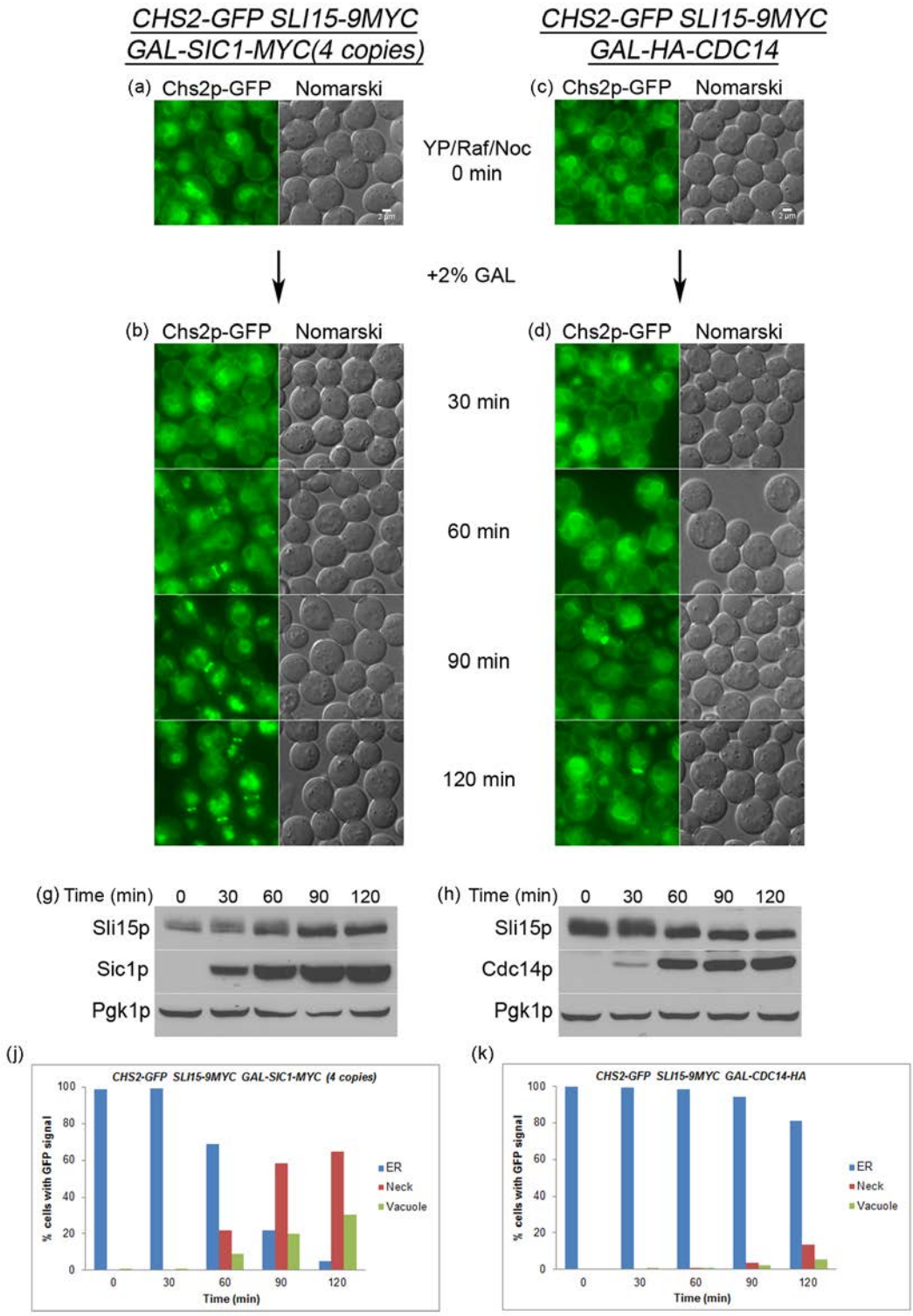
CHS2-GFP SLI15-9MYC
GAL-SIC1-MYC(4 copies)
CHS2-GFP SLI15-9MYC
GAL-HA-CDC14
(a) Chs2p-GFP Nomarski
(c) Chs2p-GFP Nomarski
YP/Raf/Noc
0 min
+2% GAL
(b) Chs2p-GFP Nomarski
(d) Chs2p-GFP Nomarski
30 min
60 min
90 min
120 min
(g) Time (min) 0 30 60 90 120
Sli15p
Sic1p
Pgk1p
(h) Time (min) 0 30 60 90 120
Sli15p
Cdc14p
Pgk1p
(j)
CHS2-GFP SLI15-9MYC GAL-SIC1-MYC (4 copies)
% cells with GFP signal
Time (min)
ER
Neck
Vacuole
(k)
CHS2-GFP SLI15-9MYC GAL-CDC14-HA
% cells with GFP signal
Time (min)
ER
Neck
Vacuole

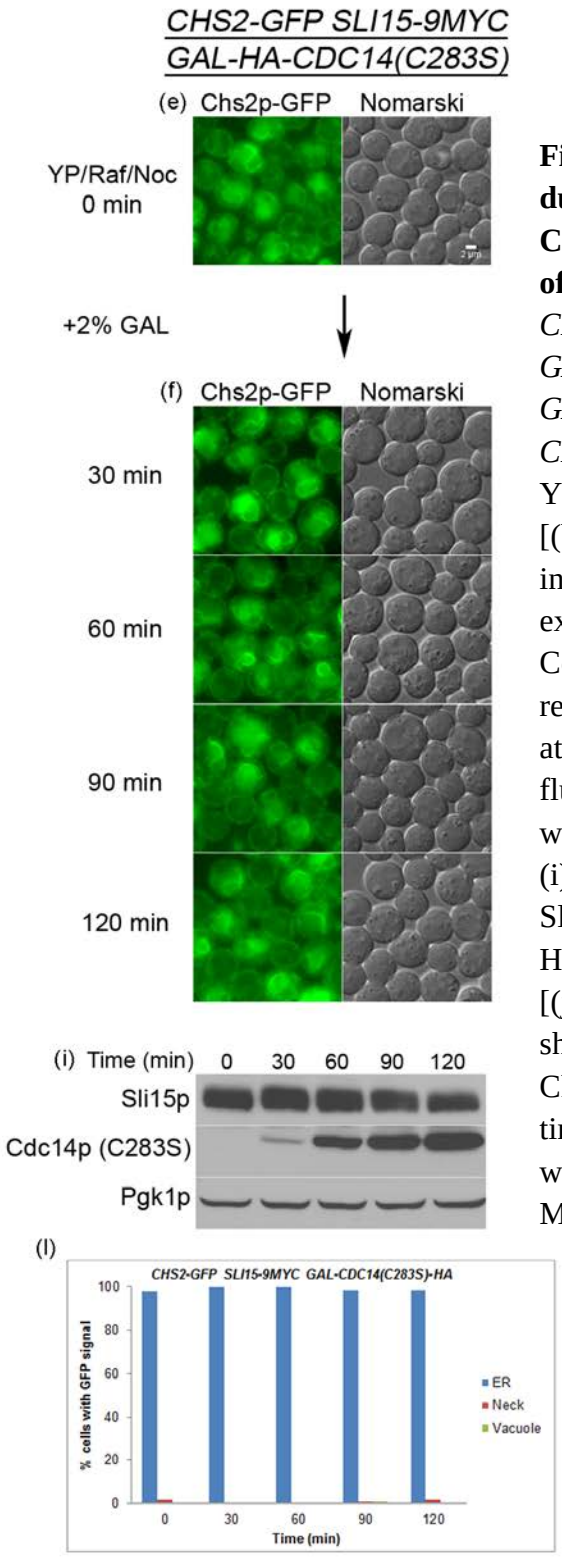

Figure 3.10 Chs2p ER export during late mitosis requires Cdc14p activity and inactivation of mitotic kinase. Cells harbouring *CHS2-GFP SLI15-9MYC* with (a) *GAL-SIC1-MYC (4-copies)* (c) *GAL-HA-CDC14* and *GAL-HA-CDC14-(C283S)* were arrested in YP/Raff/Noc for 5 hours at 24^{o}C. [(b), (d) and (e)] 2% Gal was added into the culture to induce the expression of Sic1p-myc, HA-Cdc14p and HA-Cdc14p-(C283S) respectively. Cells were harvested at 30min intervals, and subjected to fluorescence microscopy and western blot analysis. [(g),(h) and (i)] Western blot analysis of Sli15p, Sic1p-myc, HA-Cdc14p, HA-Cdc14p-(C283S) and Pgk1p. [(j),(k) and (l)] Graph plots showing percentage of cells with Chs2p-GFP signals (n>50 for each time point). Chs2p-GFP signals were classified as described in Material and Methods section.

Chapter 4 Results

In previous chapter, Cdc14p was identified as the key factor that triggers the trafficking of Chs2p from the ER to the neck during mitotic exit. Upon chromosome segregation and migration of the dSPB to the daughter cell triggers the activation of MEN, which in turn release Cdc14p from the nucleolus to the cytoplasm. The cytoplasmic localization of Cdc14p gained access to and reversed the phosphorylation of Chs2p N-terminal serine cluster that is exposed to the cytoplasm. Dephosphorylated Chs2p then translocated to the neck via secretory pathway. This spatio-temporal regulation of Cdc14p ensures that Chs2p neck delivery and septation occur strictly after chromosome segregation.

After arrival of Chs2p at the neck, it synthesizes the primary septum which in turn stabilizes and promotes the constriction of the AMR (VerPlank and Li, 2005). In parallel, Chs2p is also rapidly internalized at the neck in a Sla2p dependent manner (Chuang and Schekman, 1996). A study from the Rong Li group showed that Chs2p neck arrival precedes mitotic spindle disassembly (VerPlank and Li, 2005). This raises the question of how cells coordinate the spindle disassembly, retrieval of Chs2p at the neck, and AMR constriction to ensure cytokiensis invariably executes after spindle disassembly at the end of mitosis.

The results from subsequent section revealed the physiological significance of Chs2p retrieval from the neck during cytokinesis. Besides, the data gathered also provides some hints as to post-translational modification of Chs2p is required for Chs2p internalization upon arrival at the division site.

4.1 Dynamics of spindle disassembly relative to cytokinetic enzymes neck arrival and AMR constriction during late mitosis.

In budding yeast, late mitotic events are under tight regulation. For instance, cytokinesis requires the spatio-temporal coordination of membrane deposition and PS formation at the division site that drives AMR constriction (Bi, 2001; Bi and Park, 2012a). Moreover, a previous study demonstrated that the AMR constriction invariably occurs only after the mitotic spindle disassembly (Woodruff et al., 2010). However, it has been established that Chs2p neck localization precedes mitotic spindle disassembly during mitotic exit (VerPlank and Li, 2005). As AMR constriction is dependent on PS formation, this poses a question of how chitin deposition is regulated so as to prevent premature AMR constriction and spindle breakage.

It has also been noted that in the *chs2*Δ mutant cells in which the PS is absent, a remedial septum is laid by Chs3p. Also, in wild-type cells, shortly after primary septum is laid down, the secondary septum is deposited by Chs3p and Fks1p at either side of the primary septum. A study from the Pellman group demonstrated that Chs3p-GFP neck signal was observed in cells with intact mitotic spindle (labelled by GFP-Tub1p) using immunofluorescence imaging (Yoshida et al., 2009). However, the dynamics of mitotic spindle disassembly relative to these cytokinetic enzymes such as Chs3p and Fks1p has not been directly examined.

To understand how septation, AMR constriction and mitotic spindle disassembly is coordinated during late mitosis, the dynamics of neck localization of cytokinetic enzyme, Chs2p-mCherry relative to mitotic spindle disassembly (marked by α-tubulin, Tub1p-GFP) was characterized using time-

lapsed microscopy. Consistent with results from previous study (VerPlank and Li, 2005), Chs2p-mCherry arrived at the neck 2.06 ± 0.80min before spindle disassembly [Figure 4.1 (a) 2-4min]. The constriction of Myo1p-GFP was initiated 2.94 ± 0.68min after Chs2p-mCherry neck localization [Figure 4.1 (a) 2-5min] and completely constricted 6.05 ± 1.02min after Chs2p arrival. The mitotic spindle was dismantled 4.44 ± 0.88min prior to completion of AMR constriction (n=32) [Figure 4.1 (a) and (b)]. To determine the dynamics of mitotic spindle disassembly relative to other cytokinetic enzymes, the dynamics of Chs3p and Fks1p relative to Chs2p neck localization were examined. Chs2p-mCherry neck signals was colocalized with Chs3p-3mGFP (0.94 ± 0.85, n=34) [Figure 4.2 (a)] and GFP-Fks1p (1.48 ± 1.28, n=27) [Figure 4.2 (b)] neck signals respectively at the division site. These results suggest that cytokinetic enzymes, Chs3p and Fks1p together with Chs2p, localize to the neck prior to spindle disassembly. These observations further point out the issue of how cells maintain spindle integrity as the presence of cytokinetic enzymes at the division site could promote premature AMR constriction. Presumably, mitotic exit, a key event that triggers these processes is required. However, mitotic exit might not be sufficient to ensure proper coordination of these events to prevent untimely septation and constriction of the AMR in spite of the presence of cytokinetic enzyme, Chs2p at the neck while the spindles are still intact.

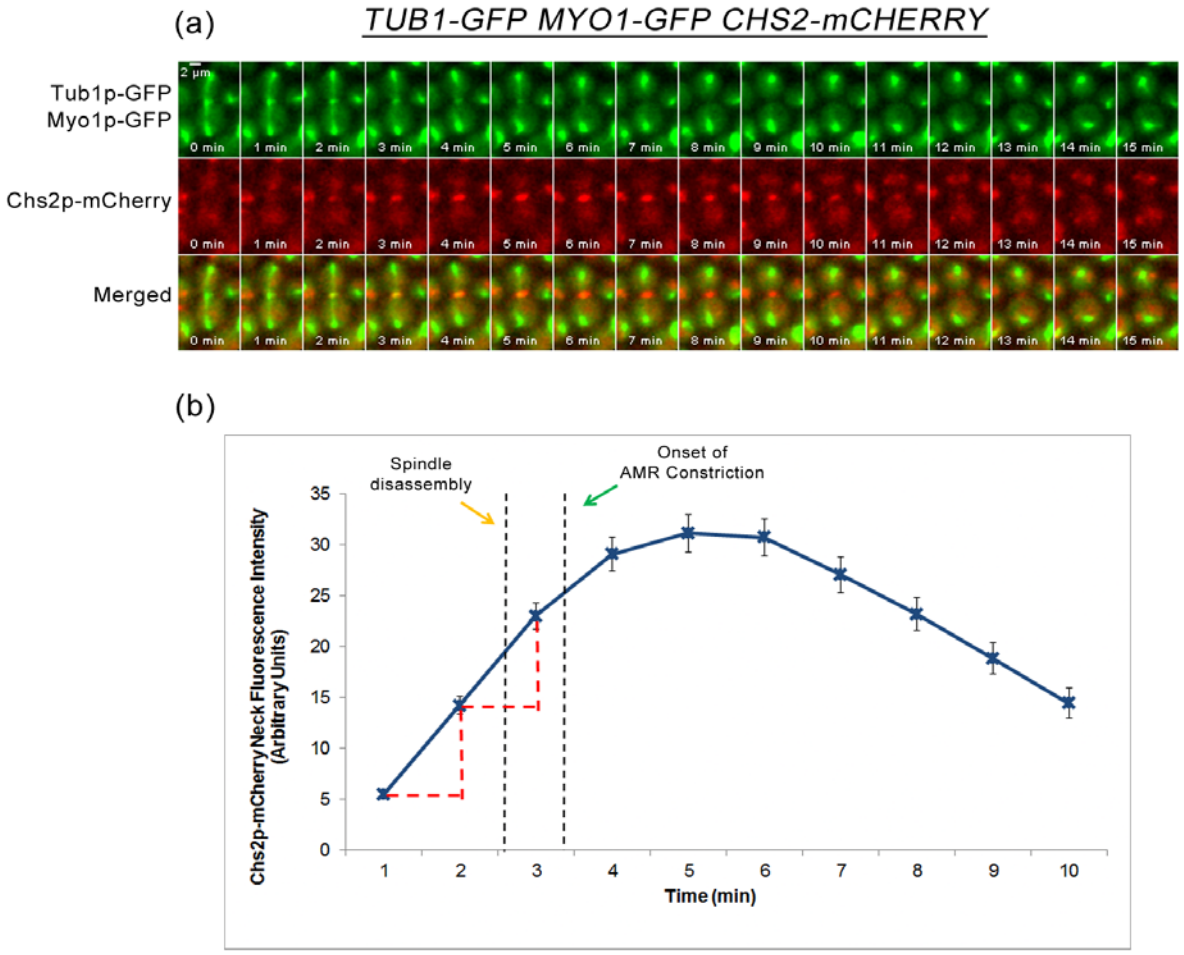

Figure 4.1 Dynamics of spindle disassembly relative to cytokinetic enzymes neck arrival and AMR constriction during late mitosis. (a) *TUB1-GFP MYO1-GFP CHS2-mCHERRY* cells were arrested in YPD/Noc at 24^{o}C. After 4 hours, cells were released from metaphase into fresh YPD for 30min. Cells were then mounted in SC/Glu agar pad and examined with time-lapsed microscopy (n=32). (b) Graph plot showing Chs2p-mCherry neck fluorescence intensity at the neck relative to mean time of spindle disassembly and mean time of AMR constriction.

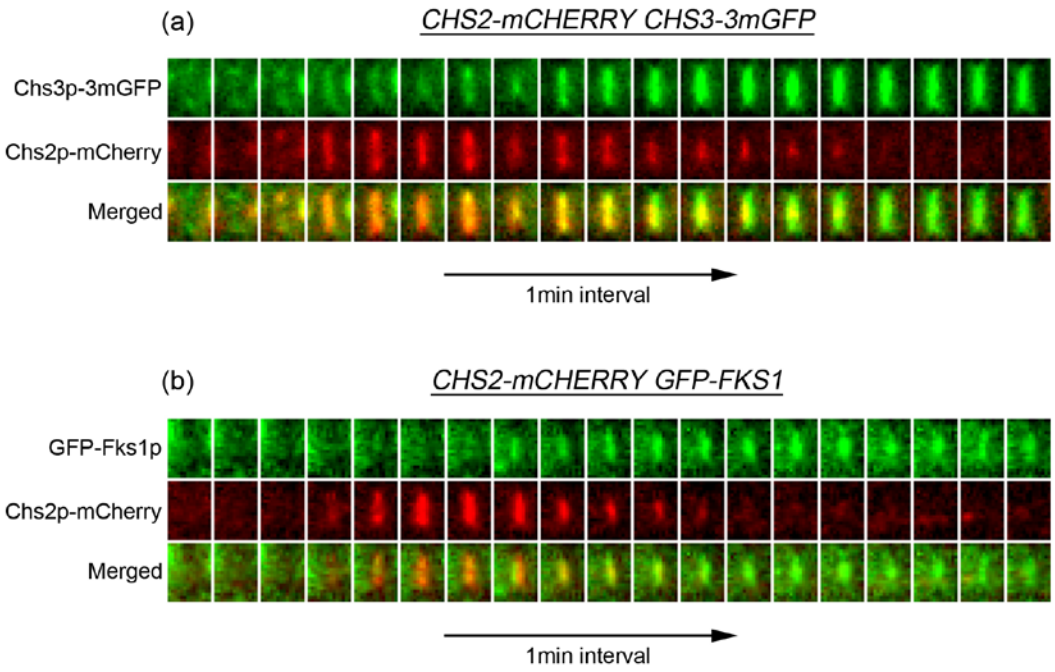

Figure 4.2 Chs2p-mCherry colocalizes with Chs3p-3mGFP and GFP-Fks1p at the neck during mitotic exit. (a) *CHS3-3mGFP CHS2-CHERRY* (n=34) and (b) *GFP-FKS1 CHS2-CHERRY* (n=27) cells were arrested in YPD/Noc for 4 hours at 24^{o}C. Upon arrested in metaphase, cells were washed and released into fresh YPD for 30min. Cells were then mounted on (a) SC/Glu and (b) 0.5xYPD agar pad and examined with time-lapsed microscopy. Images were captured at 1min interval.

4.2 Chs2p-GFP is endocytosed from the neck at the initial stage of mitotic exit.

A possible way to restrain septation and AMR constriction before spindle disassembly spindle disassemble is through the regulation of Chs2p at the neck (VerPlank and Li, 2005). The Chs2p concentration at the neck might be controlled through regulating the Chs2p RER export or removed via Sla2p dependent endocytosis.

To test how Chs2p might be regulated, the fluorescence intensity of Chs2p at the neck was measured in wild-type cells harbouring *TUB1-GFP MYO1-GFP CHS2-mCHERRY*. Chs2p-mCherry neck intensity increased gradually after its arrival at the neck [Fig. 4.1 (a) and (b)]. To determine the rate of Chs2p-mCherry forward trafficking, the fluorescence intensity over time was measured. The data shows that Chs2p-mCherry forward trafficking at the neck was constant for first 2min and decreased at 3min after its arrival at the neck (Chs2p-mCherry RER export rate, 1-2min =8.745 AU/min, 2-3min =8.749 min AU/min and 3-4min=6.092 AU/min). This suggests that the forward trafficking rate of Chs2p from RER to the neck remained constant prior to spindle disassembly.

Since forward trafficking rate of Chs2p from the ER to the division site was fairly constant, we wondered if Chs2p concentration at the neck could be regulated via clathrin-mediated endocytosis (CME) as Sla2p was reported to played a role in internalization of Chs2p (Chuang and Schekman, 1996). To test this idea, Chs2p neck internalization during mitotic exit was characterized by using key endocytosis mutants that are involved in different stages of CME (Boettner et al., 2011; Weinberg and Drubin, 2012). Time-lapsed microscopy

of *CHS2-GFP ABP1-mCHERRY* in *ede1*Δ, *sla2*Δ, *end3*Δ and *rvs161*Δ *rvs167*Δ deletion mutants respectively revealed that Chs2p-GFP internalization was compromised as evident from the Chs2p-GFP persistent neck signals [3 min onwards, Figure 4.3 (a) and (b)]. In wild-type cells, Chs2p-GFP is localized and efficiently internalized from the neck within 9.9 ±2.1 min (n=33). However, Chs2p-GFP was retained at the division site in the key endocytic component deletion mutants [Figure 4.3 (a)]. The signals were subsequently slowly diffused to the plasma membrane. To quantify the Chs2p retention at the division site, the fluorescence intensity of Chs2p-GFP was measured. In wild-type cells, the mean intensity of Chs2p-GFP neck signals gradually increased with time and started to decrease 4 mins after its arrival at the division site. The mean neck fluorescence intensity of Chs2p-GFP in cells with deletion of key endocytic component was higher and was retained longer than wild-type cells [Figure 4.3 (b)]. Intriguingly, in *sla2*Δ mutant cells, the mean fluorescence intensity of Chs2p-GFP was lower than wild-type cells at 1-2min (Figure 4.3). However, the mean fluorescence Chs2p-GFP intensity of *sla2*Δ mutant cells exceeded wild-type at 4min onwards [Figure 4.3]. The slow Chs2p-GFP fluorescence accumulation at the neck is due to partial defects of protein secretion in *sla2* mutant cells (Mulholland et al., 1997). Chs2p-GFP mean fluorescence intensity was stabilized as a result of severe endocytosis defects in *sla2*Δ mutant cells. These data suggest that Chs2p RER export was constant and its concentration at the neck was likely regulated by CME.

It has been previously shown that the temperature sensitive mutant *sla2-41* exhibits aberrant septum formation (Mulholland et al., 1997). However, the ultrastructure of septum in other key endocytosis deletion mutants has not

been documented. In agreement with the data in this study, endocytosis mutants displayed a thick chitin layer and abnormal septa structure were observed when stained with Calcoflour white (appendices-Figure S1) or when examined using transmission electron microscopy (in collaboration with Dr. Masayuki Onishi from Stanford University) (data not shown). These results suggest that the thickened septum observed in endocytosis mutants is perhaps due to the failure in retrieval of chitin synthases and glucan synthase at the division site. Taken together, endocytosis at the division site might be important to remove the excessive cytokinetic enzymes in order to prevent abnormal septation.

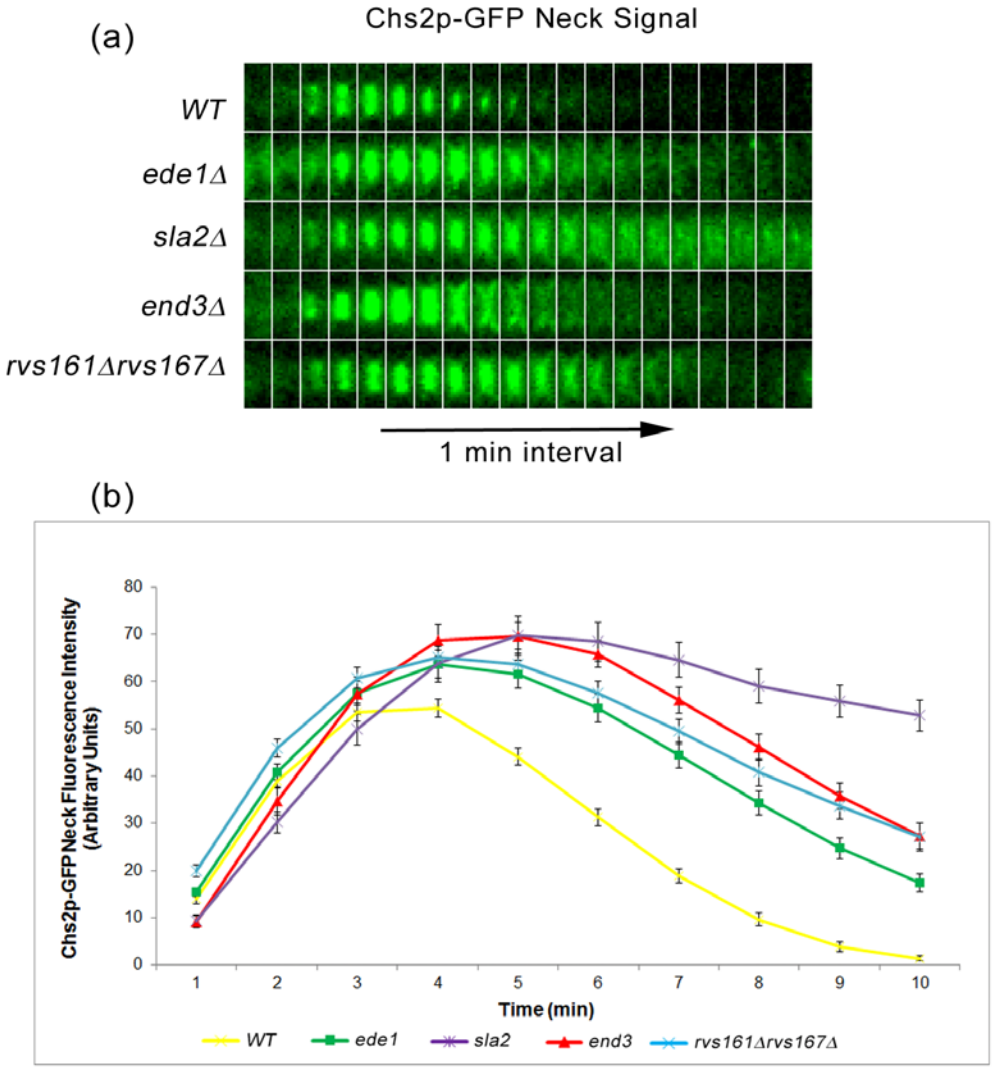

Figure 4.3 Chs2p-GFP is endocytosed from the neck at the initial stage of mitotic exit. (a) *CHS2-GFP ABP1-mCHERRY* cells harbouring deletion of respective key endocytic component were arrested in YPD/Noc at 24^{o}C and shifted to 32^{o}C for another 30min. Next, cells were released from metaphase into fresh YPD for 30min. Cells were then mounted in SC/Glu agar pad and examined with time-lapsed microscopy. (b) Graph plot showing Chs2p-GFP mean fluorescence intensity at the neck. Error bars represent standard error of the mean (S.E.M).

4.3 Endocytosis at the division site is highly active during mitotic exit.

Above data demonstrate that the concentration of Chs2p at the division site is regulated via CME throughout mitosis upon Chs2p delivery to the neck. To investigate the status of endocytic internalization at the division site during mitotic exit, an amphiphilic dye FM4-64 was employed as an exogenous cargo. An increased accumulation of FM4-64 at the neck was observed coinciding with Chs2p-YFP neck localization during mitotic exit. This result suggests that the endocytosis at the neck is highly active at the end of mitosis. This is consistent with previous report in fission yeast which demonstrated that the endocytosis uptake of FM4-64 is concentrated at the equator during cell separation (Gachet and Hyams, 2005). Interestingly, as evident from the Myo1p-CFP neck signal, the increase of endocytosis at the neck occurred upon arrival of Chs2p and before completion of cytokinesis [Figure 4.4 (a), (c), (d) and (e)]. However, the increase accumulation of FM4-64 at the neck region might be also due to the active membrane deposition at cleavage furrow during cytokinesis (Balasubramanian et al., 2004).

In budding yeast, the cortical actin patches are essential components for endocytosis (Kaksonen et al., 2003). The dynamics of the endocytosis marker, Abp1p-GFP (actin binding protein that localizes to actin patches) localization relative to Chs2p-mCherry neck localization was examined using live-cell imaging. Interestingly, a mass accumulation of Abp1p-GFP at the division site was observed during mitotic exit. Besides, Chs2p-mCherry neck localization precedes Abp1p-GFP neck accumulation (1.9 ± 1.25min, n=61) [Figure 4.5(e)]. Similarly, accumulation of others key CME components were also observed during mitotic exit. It has been established that the endocytic

components localize to the punctate cortical actin patches (Kaksonen et al., 2003). However, the accumulation of endocytic components at the division site at late mitosis has not been previously documented. Hence, the finding in study is the first to describe the neck accumulation of key endocytic components at the division site.

The Chs2p-mCherry neck localization precedes the neck accumulation of all key CME components examined [(Ede1p-GFP, 1.87 ± 0.87min, n=63), (Sla2p-GFP, 1.52 ± 1.04min, n=43), (Las17p-GFP, 1.80 ± 0.73min, n=44), (Sla1p-GFP, 1.33 ± 0.92min, n=30), and (Rvs167p-GFP, 2.21 ± 0.89min, n=52)] (Figure 4.5). This evidence implies that the rate of endocytosis at the neck was increased when cells exit from mitosis.

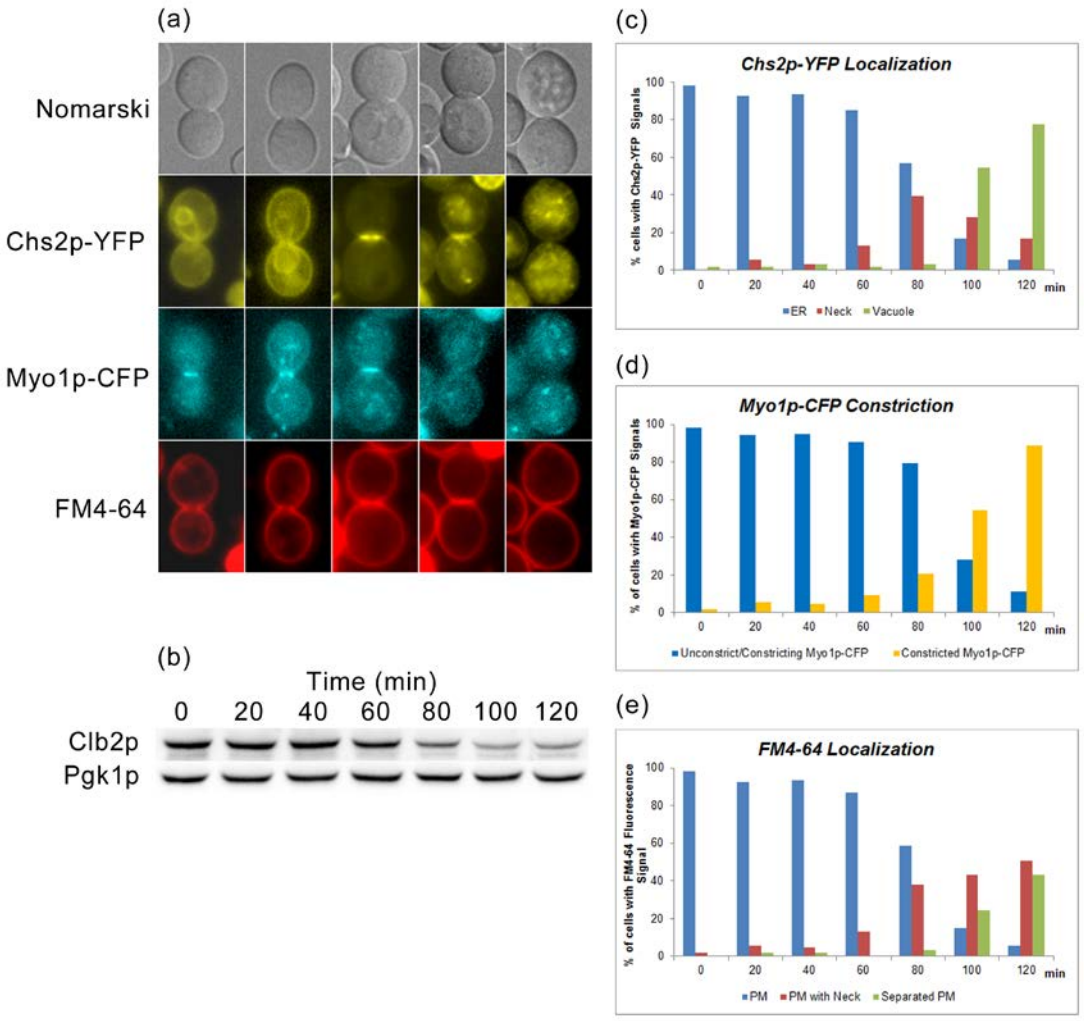

Figure 4.4 Endocytosis is highly active at the division site during mitotic exit. (a) *CHS2-YFP MYO1-CFP* cells were arrested in YPD/Noc at 24^{o}C. Cells were then released from metaphase into fresh YPD. Samples were harvested at 20min intervals, stained with FM4-64 dye, and subjected to fluorescence microscopy and western blot analysis. (b) Western blot analysis of Clb2p and Pgk1p to demonstrate mitotic exit in Noc released cells. Graph plots showing percentage of (c) Chs2p-YFP signals, (d) Myo1p-CFP constriction signals and (e) FM4-64 fluorescence signals. Graph plots shown were typical representations of three independent experiments. For FM4-64 signals classification, 'PM' refers to stained plasma membrane without neck signals,' PM with neck' refers to stained plasma membrane with distinct neck signal, and 'separated PM' refers to separated plasma membrane stained without neck signals'.

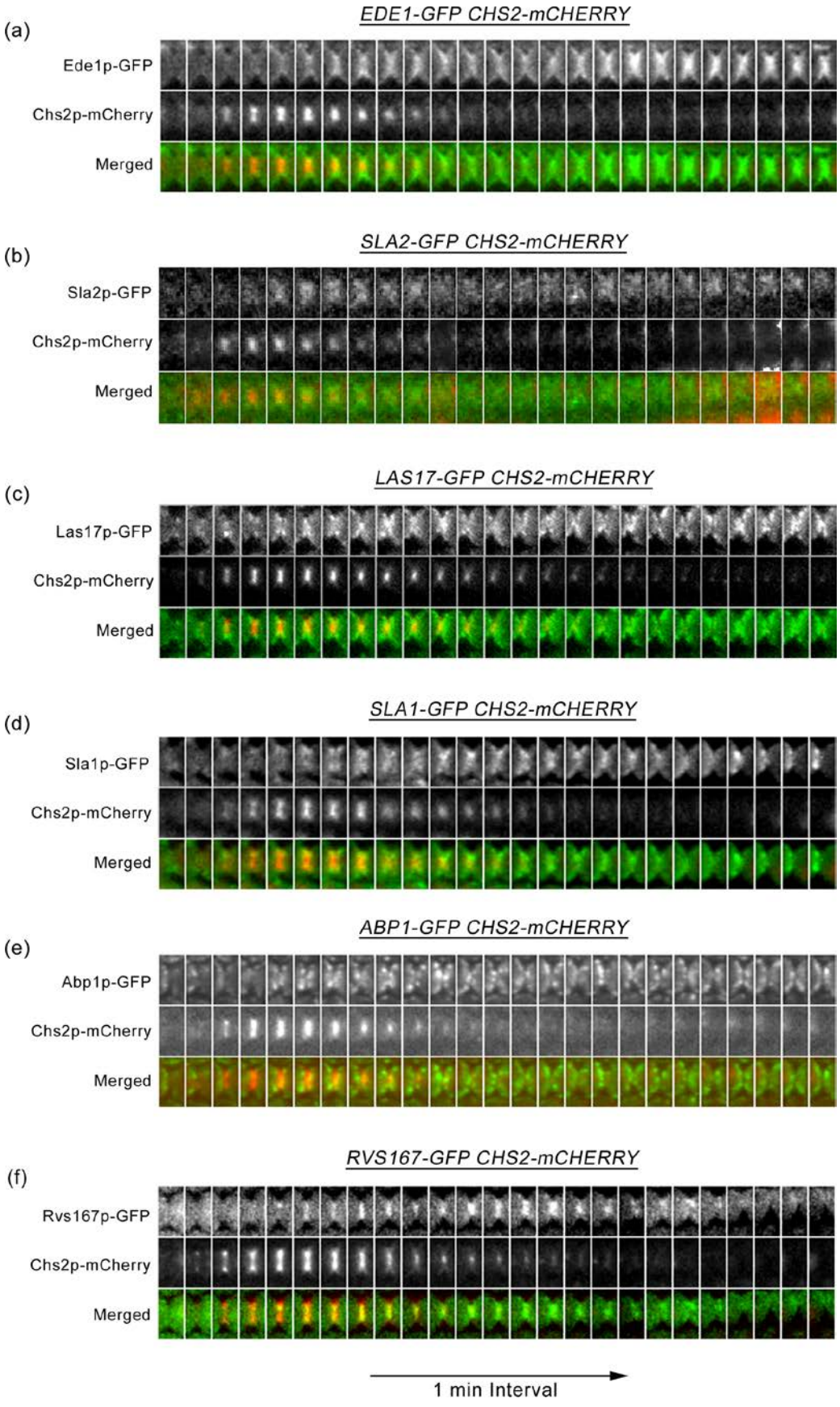
(a)
EDE1-GFP CHS2-mCHERRY
Ede1p-GFP
Chs2p-mCherry
Merged
(b)
SLA2-GFP CHS2-mCHERRY
Sla2p-GFP
Chs2p-mCherry
Merged
(c)
LAS17-GFP CHS2-mCHERRY
Las17p-GFP
Chs2p-mCherry
Merged
(d)
SLA1-GFP CHS2-mCHERRY
Sla1p-GFP
Chs2p-mCherry
Merged
(e)
ABP1-GFP CHS2-mCHERRY
Abp1p-GFP
Chs2p-mCherry
Merged
(f)
RVS167-GFP CHS2-mCHERRY
Rvs167p-GFP
Chs2p-mCherry
Merged
1 min Interval

Figure 4.5 Chs2p-mCherry neck localization precedes neck accumulation of key CME components-GFP. *CHS2-mCHERRY* (a) *EDE1-GFP* (n=63), (b) *SLA2-GFP* (n=43), (c) *LAS17-GFP* (n=44), (d) *SLA1-GFP* (n=30), (e) *ABP1-GFP* (n=61), (f) *RVS167-GFP* (n=52) cells were arrested in YPD/Noc at 24^{o}C. Upon metaphase arrest, cells were washed and released into fresh YPD for 30min. Cells were then mounted in SC/Glu agar pad and examined with time-lapsed microscopy.

4.4 Endocytosis mutant, *end3* exhibits spindle breakage and asymmetric midzone separation phenotype during Noc release.

Previous studies have shown that there is a close relationship between AMR constriction and primary septum formation (Schmidt et al., 2002; VerPlank and Li, 2005). During mitotic exit, arrival of Chs2p at the neck leads to the synthesis of primary septum that stabilizes the AMR to promote cytokinesis (VerPlank and Li, 2005). However, it has been shown that Chs2p neck localization precedes mitotic spindle disassembly. As PS formation is dependent on the level of Chs2p at the division site, this raises the question of how the cell coordinates PS formation and spindle disassembly during mitotic exit.

To test if defects in internalization of Chs2p during late mitosis could affect the integrity of the mitotic spindle, spindle dynamics in strain harboring *TUB1-GFP MYO1-GFP NDC10-tdTOMATO* and *TUB1-GFP MYO1-GFP NDC10-tdTOMATO end3*Δ were examined during Noc release. In wild type cells, the mitotic spindle was disassembled prior to constriction of Myo1p-GFP (98.7%, n=75) [Figure 4.6 (a) 12-20min onwards]. Strikingly, spindle breakage was observed in *end3*Δ cells as evident from AMR constriction preceding spindle disassembly (60.4%, n=53) [Figure 4.6 (b) 13min and (f)]. The breakage of mitotic spindle in *end3*Δ mutant resembled the *kip3Δ* (kinesin-8 motor protein) and *cdh1Δ* (activator of anaphase promoting complex, APC) mutant phenotype that exhibits a hyper-stable spindle (Woodruff et al., 2010).

A previous study from the Barnes group demonstrated that *cdh1*Δ, *doc1*Δ, and *dbf2*Δ mutant cells with spindle breakage exhibited an abnormal distribution

of midzone proteins, Ase1p and Cin8p between mother-daughter cells (Woodruff et al., 2010). To ascertain if the spindle breakage in *end3*Δ mutant cells was also associated with abnormal distribution of midzone proteins, the dynamics of spindle disassembly relative to Myo1p constriction was examined by using a midzone marker, Ndc10p. Ndc10p is an inner kinetochore protein that is associated with the midzone to promote the stability of the mitotic spindle during late anaphase (Bouck and Bloom, 2005). As anticipated, an abnormal separation of midzone (marked by Ndc10p-tdtomato) was observed in *end3*Δ mutants that exhibit spindle breakage. In wild-type cells, Ndc10p-tdtomato localized at the midzone during late anaphase. Upon spindle disassembly, Ndc10p-tomato can be seen at both the plus end of the retracting microtubules and it eventually migrates to the respective spindle pole bodies of the dividing cells. In the *end3*Δ mutant, the AMR constriction broke the spindle away from the midzone and led to asymmetric localization of Ndc10p-tdtomato in one of the dividing cell (56.6%, n=53) [Figure 4.6 (b) 13-16min]. After the spindle breakage by the contractile ring, Ndc10p-tdtomato migrated into one of the spindle pole bodies of the dividing cell. The broken spindle was then rapidly disassembled 2.19 ± 1.26min (n=53) after spindle breakage in *end3*Δ cells [Figure 4.6 (b)].

Next, Ndc10p-tdTomato was also employed as an independent marker to determine the dynamics of spindle elongation relative to AMR constriction. The time taken from midzone localization of Ndc10p-tdTomato to the completion of Myo1p-GFP constriction was measured. Also, the time taken from anaphase-B (spindle length >6µm) to the completion of Myo1p-GFP constriction was determined. Interestingly, the interval from anaphase-B to the

completion of Myo1p-GFP constriction was significantly shorter in *end3*Δ (13.4 ± 0.36 min, n=53) [Figure 4.6 (b) 2-13min and (d)] mutant as compared to wild-type cells (16.5 ± 0.32 min, n= 75, p-value<0.0001) [Figure 4.6 (a) 2-20min and (d)]. Consistently, a shorter interval between Ndc10p-tdtomato midzone loading and Myo1p-GFP complete constriction was also observed in *end3*Δ cells [Figure 4.6 (e)]. These results suggest that the AMR constricts prematurely in *end3*Δ cells.

To further demonstrate that AMR is indeed prematurely constricted in *end3*Δ mutant, the time taken for complete constriction of Myo1p-RedStar relative to Chs2p-GFP neck localization was examined in wild-type and *end3*Δ cells harbouring *CHS2-GFP MYO1-REDSTAR* respectively [Figure 4.8 (a) and (b)]. Consistent with above results, Myo1p-RedStar constriction was also significantly faster in *end3*Δ mutant (5.29 ± 0.17min, n=34) as compared to wild-type cells (6.96 ± 0.28min, n=51, p-value <0.0001) [Figure 4.8 (c)]. This suggests that failure in CME internalization of Chs2p might accelerate the AMR constriction during cytokinesis.

4.5 Mitotic spindle breakage in *end3*Δ mutant cells is not due to delay in spindle disassembly.

It has been previously proposed that localization of Ndc10p on the mitotic spindle serves as a signal to commence the disassembly of mitotic spindle (Montpetit et al., 2006). To exclude the possibility that the spindle breakage observed in *end3*Δ mutant cells was due to delay in Ndc10p-tdtomato midzone localization, the timing of the midzone localization of Ndc10p-tdtomato relative to anaphase-B was also measured. As expected, there was no significant difference between the timing of Ndc10p-tdtomato midzone

localization relative to anaphase-B in wild-type and *end3*Δ cells (p-value=0.4919) [Figure 4.6 (c)]. This is consistent with our western blot results showing that the mitotic exit in endocytosis defective cells is comparable to that in wild-type cells (Figure 4.7). These results suggest that spindle breakage in endocytosis mutant, *end3*Δ is caused by premature AMR constriction.

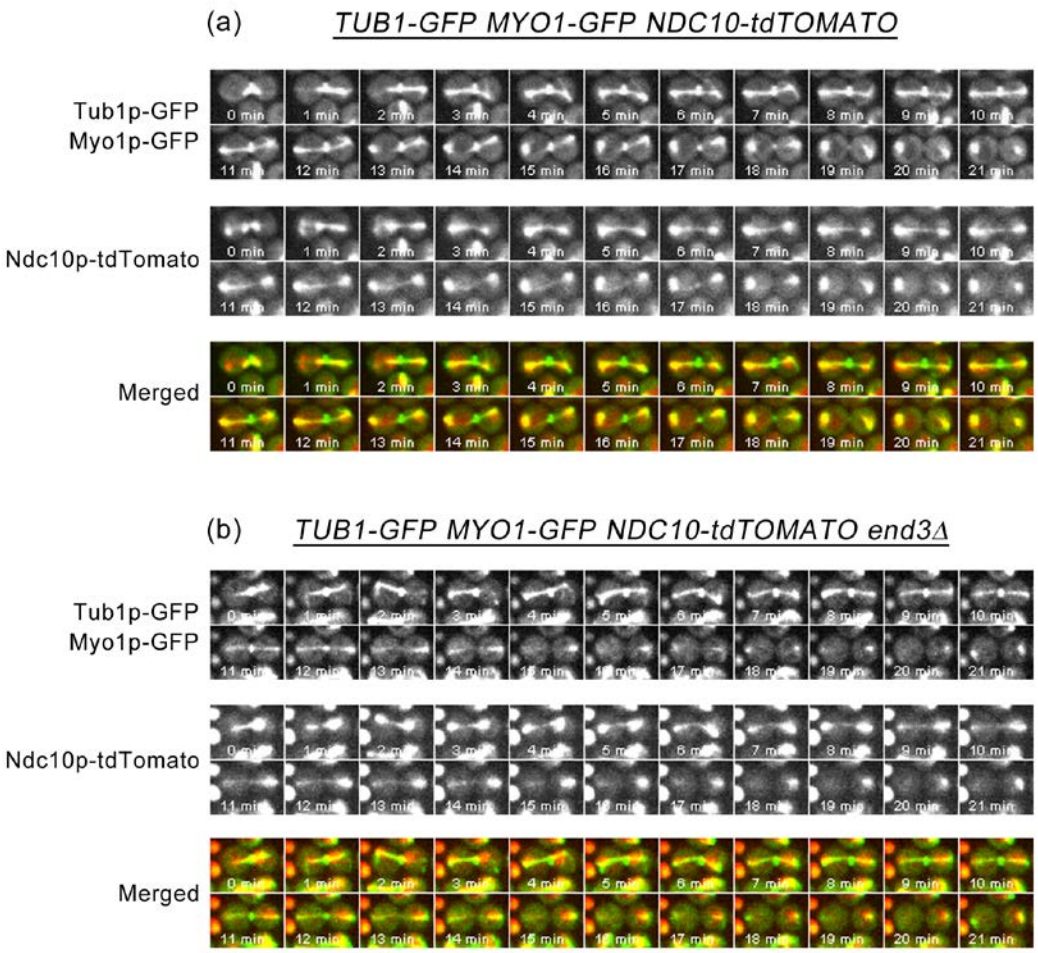
(a)
TUB1-GFP MYO1-GFP NDC10-tdTOMATO
Tub1p-GFP
Myo1p-GFP
Ndc10p-tdTomato
Merged
(b)
TUB1-GFP MYO1-GFP NDC10-tdTOMATO end3Δ
Tub1p-GFP
Myo1p-GFP
Ndc10p-tdTomato
Merged

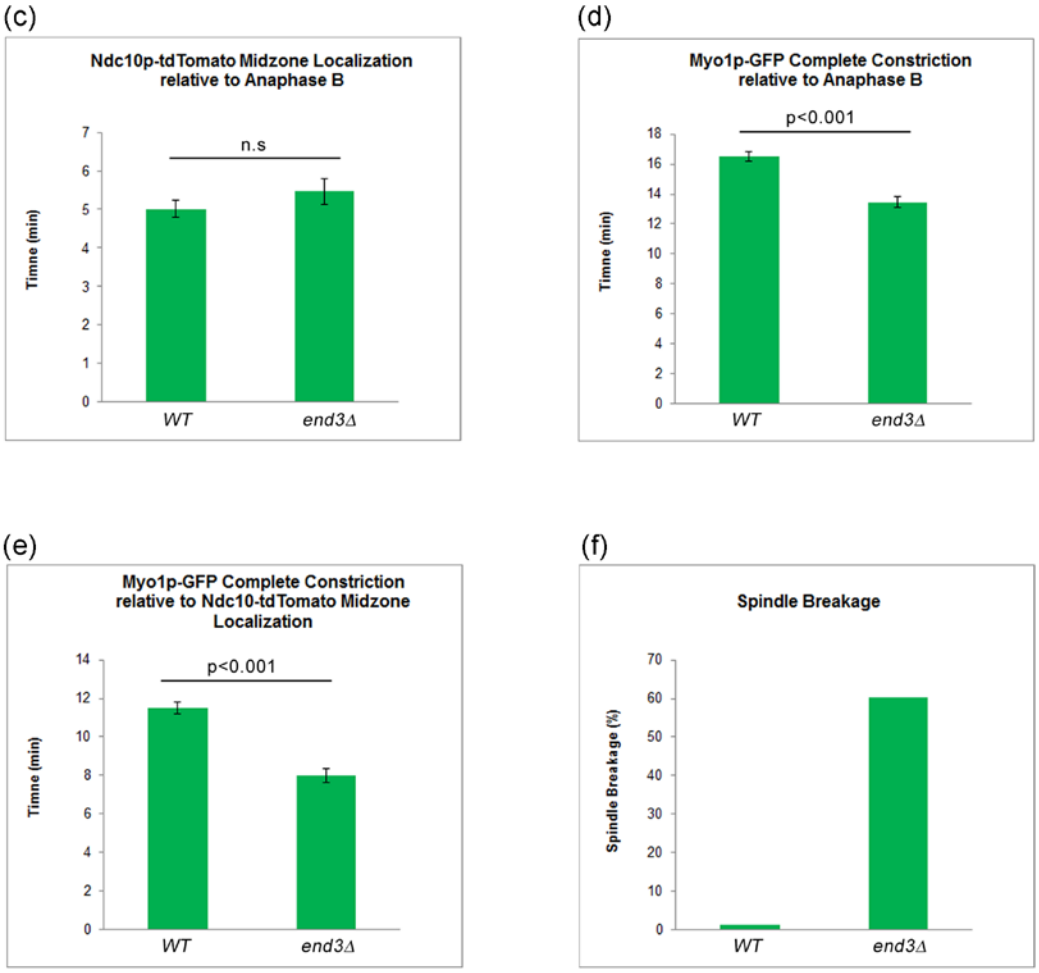

Figure 4.6 Endocytosis mutant, *end3* exhibits spindle breakage and asymmetric midzone separation phenotype during Noc release. (a) Wild Type and (b) *end3*Δ cells harbouring *TUB1-GFP MYO1-GFP NDC10-tdTOMATO* respectively were arrested in Noc. After 4 hours, cells were shifted to 32^{o}C for 30min. Cells were then released from metaphase and examined with time-lapsed microscopy. Graph shows (c) Time taken for Ndc10p-tdTomato midzone localization relative to anaphase (Mann-Whitney U test, p=0.4919), (d) Time taken for Myo1p-GFP Complete Constriction relative to anaphase B (Student t-test, p<0.001), (e) Time taken for Myo1p-GFP complete constriction relative to Ndc10p-tdTomato midzone localization (Student t-test, p<0.001), and (f) Percentage of spindle breakage in WT and *end3*Δ respectively (WT=75, *end3*Δ=53). The total number of cells analysed was taken from 3 independent experiments. The error bar represents SEM.

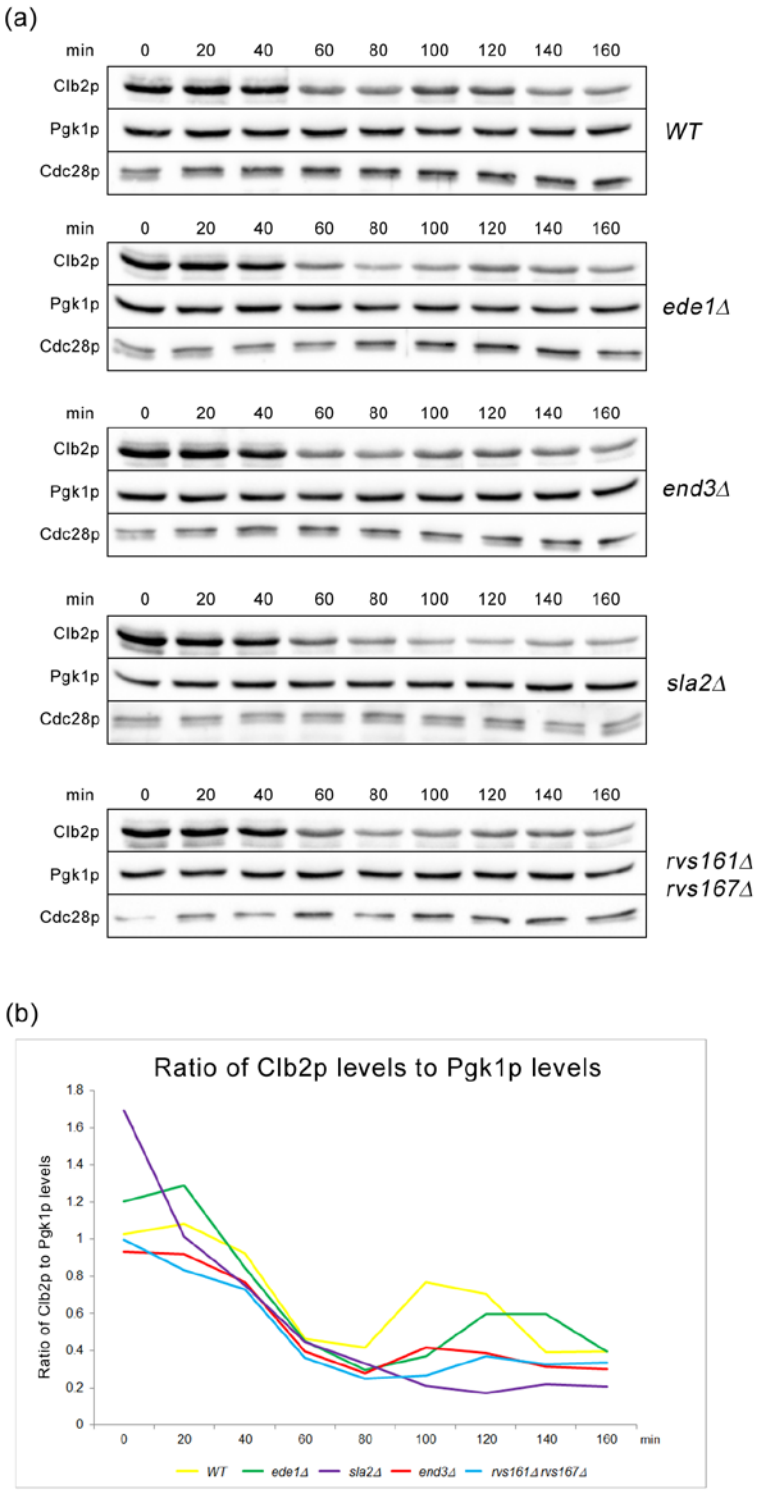

Figure 4.7 Key CME component deletion mutant does not display defect in mitotic exit. (A) Yeast strain harbouring the respective endocytic component deletion was arrested in YPD/Noc 24^{o}C. After 4 hours, cells were shifted to 32^{o}C for 30min. Cells were then released from metaphase into pre-warmed 32^{o}C YPD. Western blot analysis of Clb2p, Cdc28p and Pgk1p levels are shown to demonstrate equivalent mitotic exit during release from Noc. (B) Graph shows the Clb2p signals normalized against loading control Pgk1p.

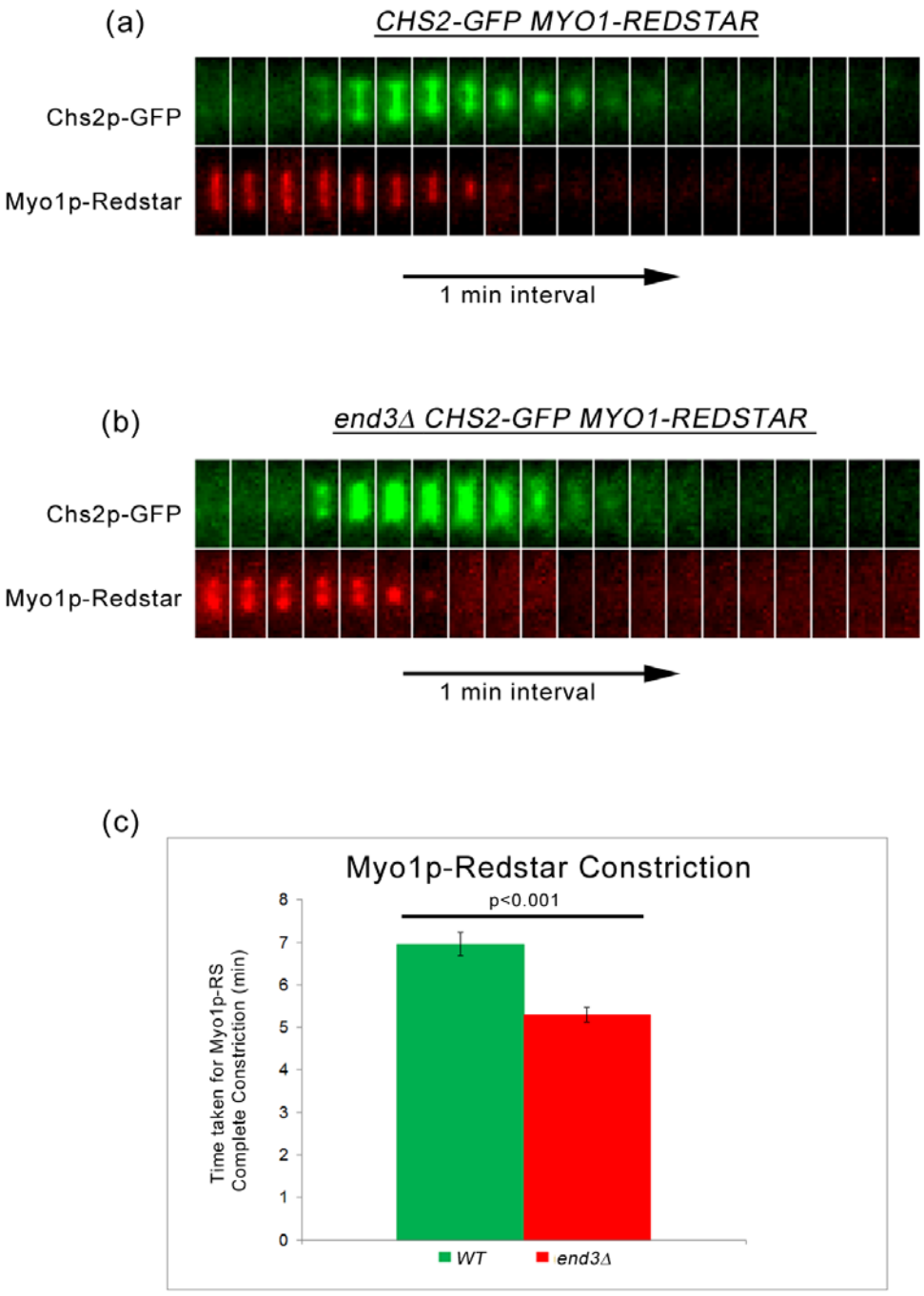

Figure 4.8 Accelerated AMR constriction in *end3*Δ mutant. (a) Wild type and (b) *end3*Δ cells harbouring *CHS2-GFP MYO1-REDSTAR* were arrested in Noc respectively. After 4 hours, cells were shifted to 32^{o}C for 30min. Cells were then released from metaphase and examined with time-lapsed microscopy. (c) Bar graph showing time taken for Myo1p-Redstar complete constriction. The total number of cells analysed was taken from 3 independent experiments. Statistical analysis was performed using Mann Whitney-U test. The error bar represents SEM.

4.6 Spindle Breakage Phenotype is not exclusive to *end3*Δ mutant and can be rescued by deletion of *chs3* and *fks1* or deletion of *slk19*.

To exclude the possibility that the spindle breakage observed is *end3*Δ specific, the dynamics of mitotic spindle disassembly in other key endocytosis mutants, *ede1*Δ, *sla2*Δ, and *rvs161*Δ *rvs167*Δ was examined. Indeed, the inhibition of endocytosis during mitotic exit in the other mutants also led to mitotic spindle breakage. In 38.8 ± 7.7% of *ede1*Δ (n=109), 35.6 ± 13.5% of *sla2*Δ (n=85), 72.2 ± 3.3% of *end3*Δ (n=114) and 55.1 ± 9.4% of *rvs161*Δ *rvs167*Δ (n=110) cells constricted their AMR before mitotic spindle disassembly [Figure 4.9 (c)].

Since the cytokinetic enzymes that synthesize primary and secondary septum were colocalized during mitotic exit, the question if the deletion of these genes could rescue the spindle breakage phenotype observed in *end3*Δ cells was raised. Interestingly, the spindle breakage can be rescued by deleting *chs3*Δ or *fks1*Δ in combination with *end3*Δ. The spindle breakage percentage of *chs3*Δ *end3*Δ and *fks1*Δ *end3*Δ was reduced to 42.2 ± 2.9% (n=38) and 46.1 ± 9.4% (n=91) respectively [Figure 4.9 (b) and (c)]. These data suggested that the spindle breakage in *end3*Δ mutant cells might be partially due to failure in endocytic turnover of Chs3p and Fks1p. Surprisingly, a significant increase of spindle breakage was also observed in *chs3*Δ mutant. It has been previously shown that Chs3p shuttles between plasma membrane and endosomes via endocytic pathway (Ziman et al., 1998). As the recruitment of endocytic components is dependent on the presence of substrates, the deletion of *chs3* might cause a general reduction in endocytosis dynamics as a result of the loss of endocytic cargo, Chs3p at the plasma membrane (Toshima et al., 2006).

This eventually causes slightly higher percentage of spindle breakage in *chs3*Δ mutant as compared to wild-type cells [Figure 4.9 (b) and (c)]. However, further experiment need to be performed in order to validate this possibility. The role of *chs2*Δ in rescuing the *end3*Δ spindle breakage phenotype was not assessed due to the compromised viability of *chs2*Δ strain in Noc. The retrieval of cytokinetic enzymes through CME is crucial in preventing premature AMR constriction prior to spindle disassembly.

Consistent with a previous report (Woodruff et al., 2010), 68.8 ± 0.2% of *kip3*Δ cells displayed a spindle breakage phenotype. Kip3p is a kinesin-8 motor protein that promotes microtubule depolymerization during spindle disassembly (Varga et al., 2006; Woodruff et al., 2010). Interestingly, the percentage of spindle breakage in *kip3*Δ mutant cells was increased with deletion of *end3*, a key endocytic component. In *kip3*Δ *end3*Δ double mutant cells, the spindle breakage is significantly increased to 93.7 ± 1.9% (n=54). Since *kip3*Δ *end3*Δ double mutant cells displayed an increase in percentage of spindle breakage as compared to *kip3*Δ mutant cells, it is speculated that premature spindle disassembly might suppress the spindle breakage phenotype. To test this, the mitotic spindle integrity in *slk19*Δ *end3*Δ double mutant was examined. Cells harbouring a deletion of *slk19* (microtubule stabilizing protein), have been reported to exhibit a short and destabilized spindle (Zeng et al., 1999). Indeed, *slk19*Δ in the *end3*Δ mutant greatly reduced the spindle breakage to 11.4 ± 4.4% (n=88) [Figure 4.9 (b) and (c)]. This result suggested that the spindle breakage observed in endocytosis mutants is likely a result of premature AMR constriction.

Together, the data shows that the timely turnover of cytokinetic enzymes at the neck in a continuous CME dependent manner is crucial in ensuring that spindle disassembly occurs prior to AMR constriction. These two events must be tightly coordinated as any delay in mitotic spindle disassembly or premature constriction of AMR disrupts the balance which eventually contributes to spindle breakage during mitotic exit.

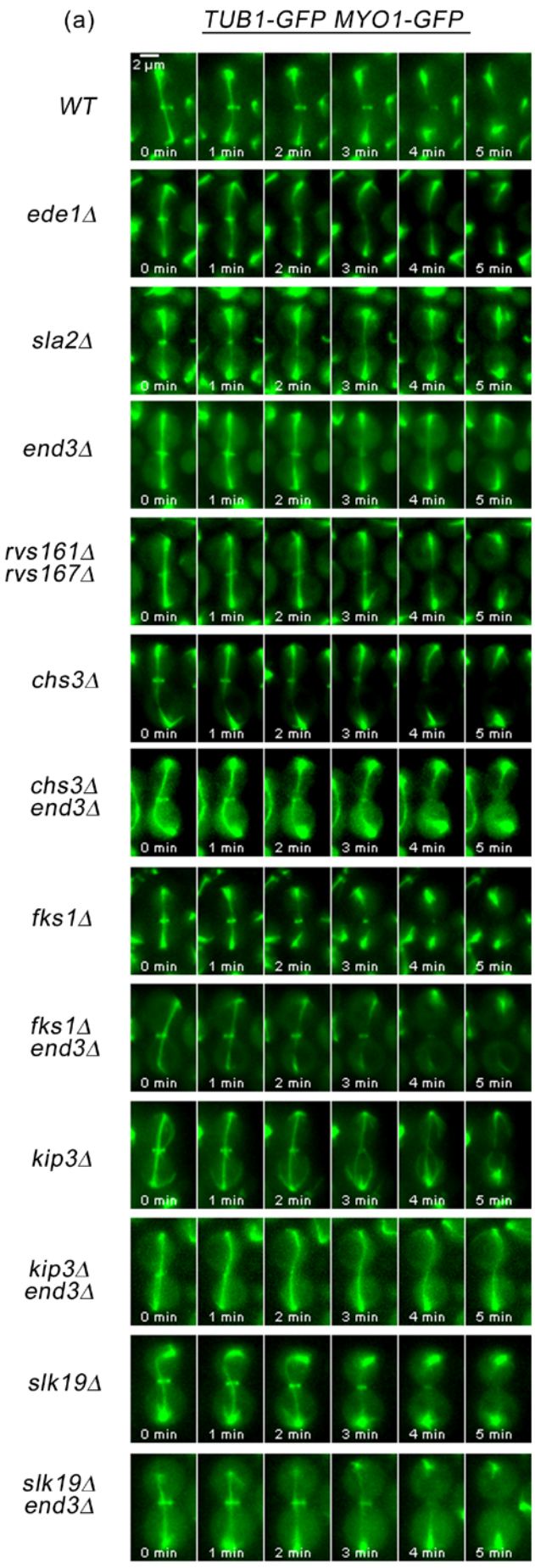
(a)
TUB1-GFP MYO1-GFP
2 μm
WT
ede1Δ
sla2Δ
end3Δ
rvs161Δ rvs167Δ
chs3Δ
chs3Δ end3Δ
fks1Δ
fks1Δ end3Δ
kip3Δ
kip3Δ end3Δ
slk19Δ
slk19Δ end3Δ
0 min
1 min
2 min
3 min
4 min
5 min

(b)

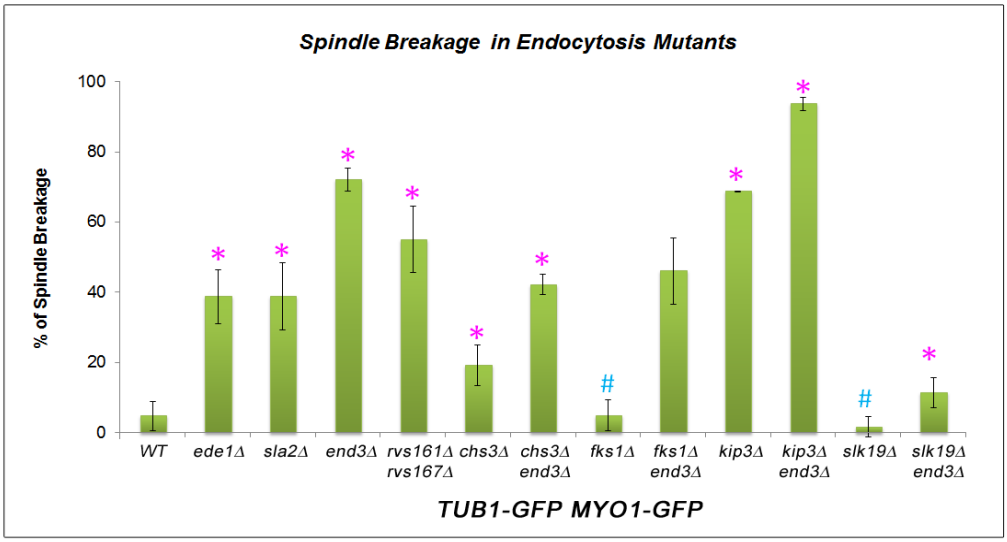

(c)

Genotype	Spindle Breakage (%)	n	p-value (compared to *WT*)	p-value (compared to *end3*Δ)
WT	4.8 ± 4.2	137	NA	-
*ede1*Δ	38.8 ± 7.7	109	0.006	-
*sla2*Δ	35.6 ± 13.5	85	0.014	-
*end3*Δ	72.2 ± 3.3	119	<0.001	NA
*rvs161*Δ *rvs167*Δ	55.1 ± 9.4	110	0.005	-
*chs3*Δ	19.3 ± 5.8	97	0.029	-
*chs3*Δ *end3*Δ	42.2 ± 5.9	38	<0.001	<0.001
*fks1*Δ	5.0 ± 4.4	73	0.953	-
*fks1*Δ *end3*Δ	46.1 ± 9.4	91	0.015	0.048
*kip3*Δ	68.8 ± 0.2	96	0.001	-
*kip3*Δ *end3*Δ	93.7 ± 1.9	79	<0.001	0.002
*slk19*Δ	1.7 ± 2.9	116	0.351	-
*slk19*Δ *end3*Δ	11.4 ± 4.4	88	0.132	<0.001

Figure 4.9 Spindle Breakage Phenotype is not exclusive to *end3*Δ mutant and can be rescued by deletion *chs3* and *fks1* or *slk19*. (a) *TUB1-GFP MYO1-GFP* cells harbouring deletion of respective key endocytic component were arrested in YPD/Noc at 24^{o}C for 4 hours and shifted to 32^{o}C for another 30min. Next, cells were released from metaphase into fresh YPD for 30min. Cells were then mounted in SC/Glu agar pad and examined with time-lapsed microscopy. (b) Graph plot showing percentage of spindle breakage in endocytosis mutants. Pink asterisk represents statistical significance as compared to wild-type cells. Blue hash represents no statistical significance as compared to wild-type cells. Error bars represent standard deviation. Student-t test was employed for the statistical analysis. (c) Table showing the percentage of spindle breakage and p-values for endocytosis mutants.

4.7 Suppression of cytokinetic enzymes activity rescues spindle breakage in *end3*Δ mutant.

The data gathered in this study suggests that continuous CME is vital in regulating the concentration of cytokinetic enzymes at the neck. This raises the question if the activity of cytokinetic enzymes was the main factor that triggers premature AMR constriction observed in endocytosis mutants. To ascertain if activity of the Chs3p or Fks1p is indeed required for the premature AMR constriction, the activity of Chs3p or Fks1p in *end3*Δ mutant was inhibited using nikkomycin-Z (chitin synthase III specific inhibitor) (Gaughran et al., 1994) and caspofungin [β(1-3)-D-glucan synthase inhibitor] (Kurtz and Douglas, 1997), respectively. Interestingly, drug treatment using nikkomycin-Z and caspofungin rescued the spindle breakage phenotype in *end3*Δ mutant cells. The incidences of spindle breakage of the caspofungin and nikkomycin-Z treated *end3*Δ mutant cells was decreased to 26.5 ± 5.3% (n=110) and 26.4 ± 1.2% (n=113) respectively [Figure 4.10 (a), (b) and (c)]. These results suggest that the spindle breakage in endocytosis mutant cells can be abrogated by inhibiting the Chs3p or Fks1p activity.

The reduction in spindle breakage incidence in *end3*Δ mutant cells treated with nikkomycin-Z and caspofungin led to the speculation that the rescue in spindle breakage is a result of altered AMR constriction dynamics. To test this idea, the AMR constriction time relative to Chs2p-GFP neck arrival was examined in cells harbouring *CHS2-GFP MYO1-REDSTAR* that were treated with caspofungin and nikkomycin-Z respectively. In *end3*Δ mutant cells, the time taken for complete Myo1p-Redstar constriction relative to Chs2p-GFP neck arrival was 5.07 ± 0.14 min [(n=92), Figure 4.11 (a), (b) and (c)].

Interestingly, the time taken for complete AMR constriction in *end3*Δ cells treated with caspofungin [5.66 ± 0.19min (n=61), p-value < 0.05] and nikkomycin-Z [6.07 ± 0.19min (n=55), p-value<0.001] was significantly longer as compared to untreated *end3*Δ cells [Figure 4.11 (a), (b) and (c)].

Taken together, the data in this study imply that spindle breakage in the *end3*Δ mutant cells might be due to excessive accumulation of chitin synthase III and glucan synthase at the division site during cytokinesis. Suppression of Chs3p or Fks1p activity rescued the spindle breakage phenotype observed in *end3*Δ cells through alteration in AMR constriction dynamics.

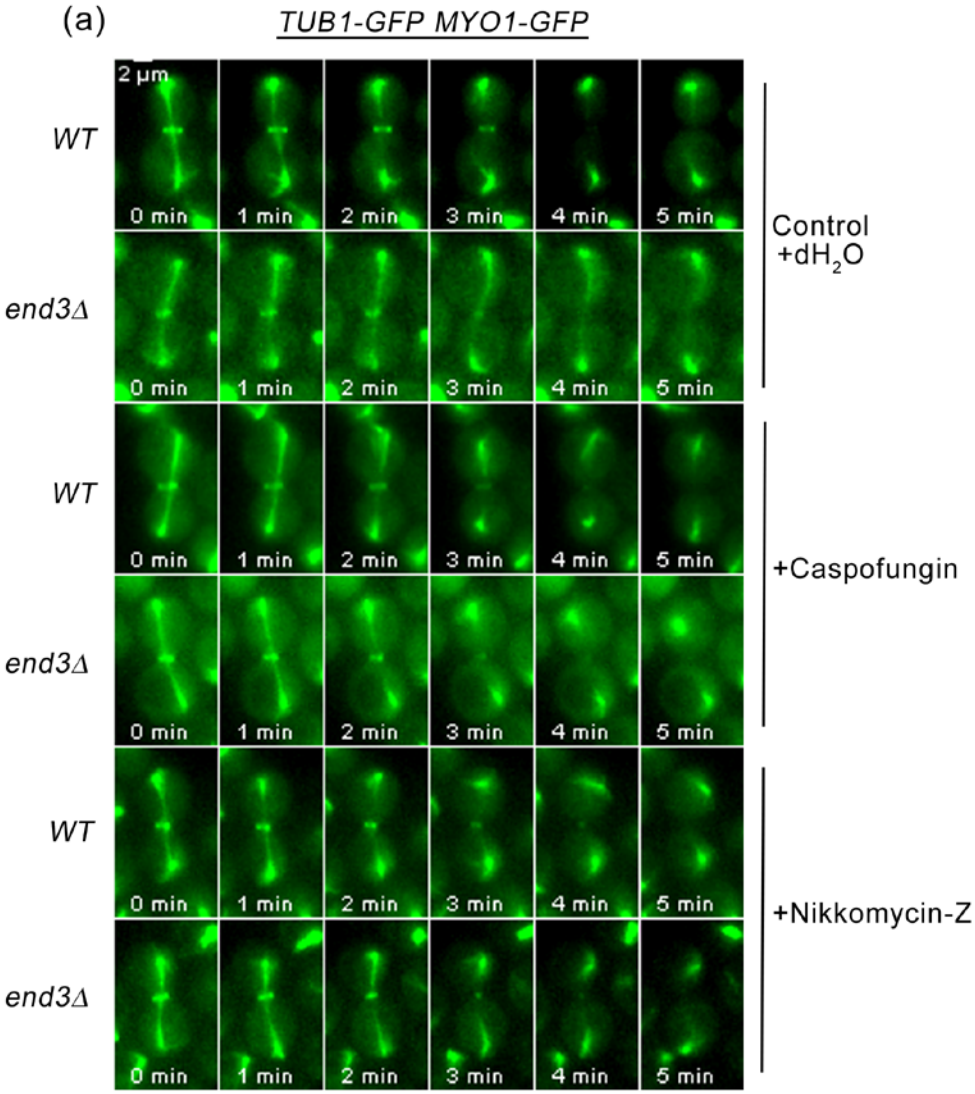
(a)
TUB1-GFP MYO1-GFP
2 μm
WT
end3Δ
WT
end3Δ
WT
end3Δ
0 min
1 min
2 min
3 min
4 min
5 min
Control
+dH2O
+Caspofungin
+Nikkomycin-Z

(b)

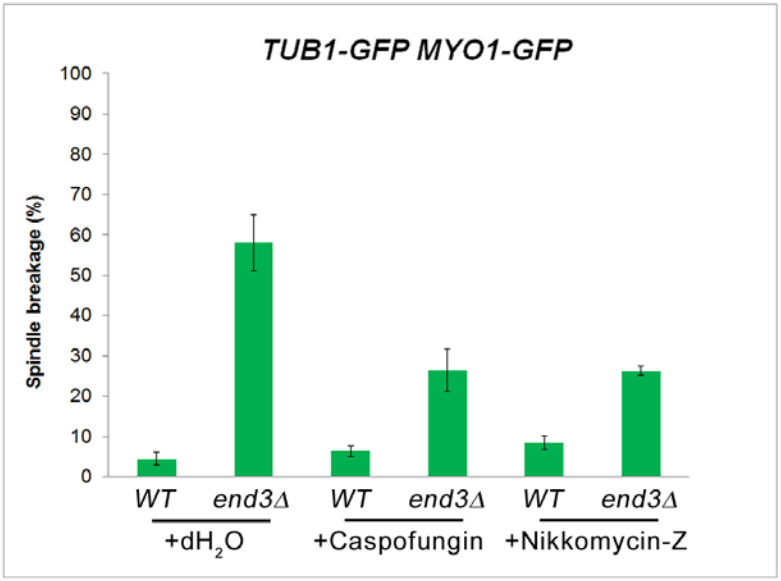

(c)

Genotype	Mean Spindle Breakage (%)	n	p-value (compared to *WT*)	p-value (compared to *end3*Δ)
WT Untreated	4.5 ± 1.6	158	NA	-
*end3*Δ Untreated	58.1 ± 7.0	141	0.004	NA
WT+Caspofungin	6.4 ± 1.4	87	0.214	-
*end3*Δ+Caspofungin	26.5 ± 5.3	110	0.013	0.004
WT+Nikkomycin-Z	8.5 ± 1.8	104	0.047	-
*end3*Δ+Nikkomycin-Z	26.4 ± 1.2	113	<0.001	0.014

Figure 4.10 Suppression of cytokinetic enzymes activity rescues spindle breakage in *end3*Δ mutant. (a) *TUB1-GFP MYO1-GFP* and *CHS2-GFP MYO1-GFP end3*Δ cells were arrested in YPD/Noc at 24°C for 2 hours. Cells were treated with 50ng/ml caspofungin and 1mM nikkomycin-Z respectively for another 2 hours in YPD/Noc. Upon arrested in metaphase, cells were shifted to 32°C for another 30min. Next, cells were released from metaphase into fresh YPD for 30min. Cells were then mounted in SC/Glu agar pad and examined with time-lapsed microscopy. (b) Graph plot showing the mean percentage of cells with spindle breakage. Error bars represent standard deviation. (c) Table showing the mean percentage of cells with spindle breakage and p-values of statistical analysis. Statistical analysis was performed using Student-t test.

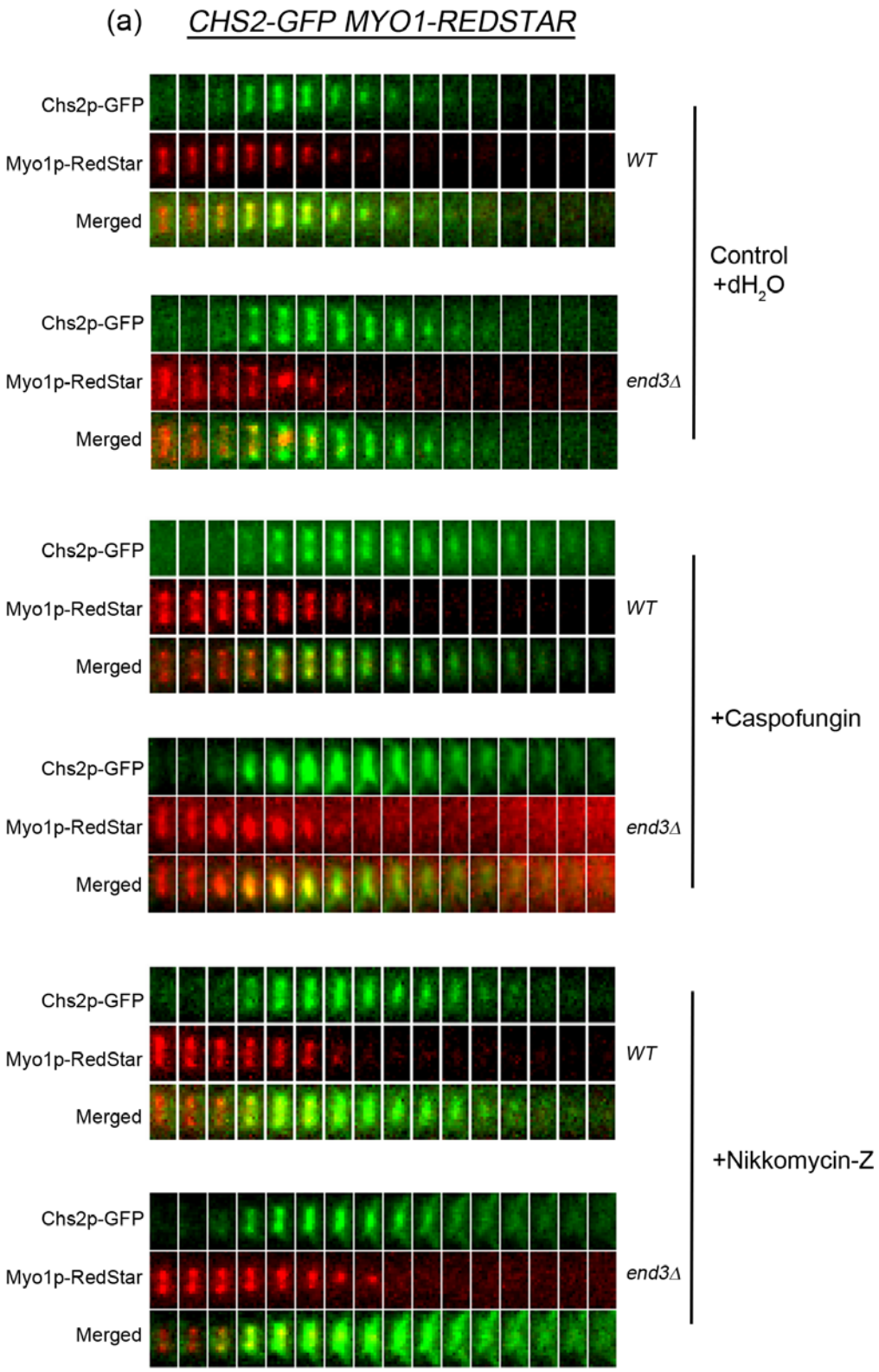
(a) CHS2-GFP MYO1-REDSTAR
Chs2p-GFP
Myo1p-RedStar
Merged
WT
end3Δ
Control
+dH2O
+Caspofungin
+Nikkomycin-Z

(b)

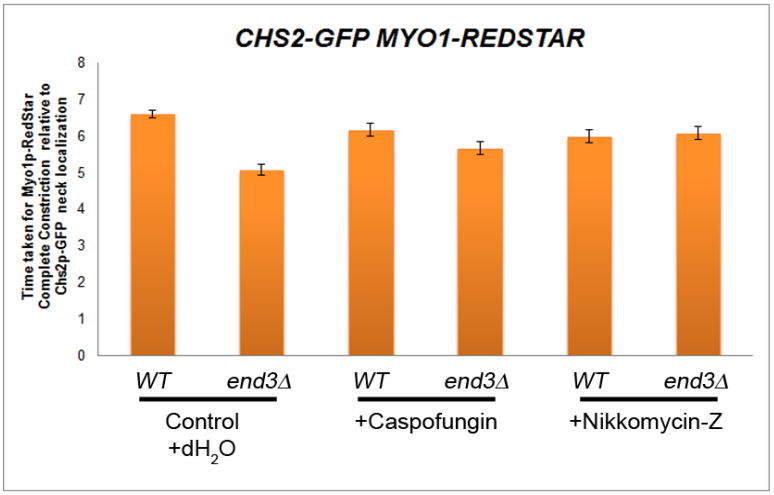

(c)

Genotype	Mean time taken for Myo1p-RS Complete Constriction Relative to Chs2p-GFP Neck Arrival ± SEM	n	p-value (compared to *WT*)	p-value (compared to *end3*Δ)
WT Untreated	6.15 ± 0.10	113	NA	-
*end3*Δ Untreated	5.07 ± 0.14	92	<0.001	NA
WT+Caspofungin	6.17 ± 0.19	82	0.5464	-
*end3*Δ+Caspofungin	5.66 ± 0.19	61	0.0028	0.0191
WT+Nikkomycin-Z	5.99 ± 0.17	65	0.2530	-
*end3*Δ+Nikkomycin-Z	6.07 ± 0.19	55	0.6132	<0.001

Figure 4.11 AMR constriction dynamics is altered in *end3*Δ cells treated with Caspofungin and Nikkomycin-Z. (a) *CHS2-GFP MYO1-REDSTAR* and *CHS2-GFP MYO1-REDSTAR end3*Δ cells were arrested in YPD/Noc at 24^{o}C for 2 hours. Cells were treated with 50ng/ml caspofungin and 1mM Nikkomycin-Z respectively for another 2 hours in YPD/Noc. Upon arrested in metaphase, cells were shifted to 32^{o}C for another 30min. Next, cells were released from metaphase into fresh YPD for 30min. Cells were then mounted in SC/Glu agar pad and examined with time-lapsed microscopy. (b) Graph plot showing time taken for complete AMR constriction relative to Chs2p-GFP neck localization. Error bars represent standard error of the mean. (c) Table showing the mean time taken for complete Myo1p-GFP constriction relative to Chs2p-GFP neck localization and p-values of statistical analysis. Statistical analysis was performed using Mann Whitney-U test.

4.8 Mitotic spindle breakage in endocytosis mutants contributes to failure in spindle re-establishment in progeny cells.

To ascertain if the spindle breakage observed in endocytosis mutants affects spindle morphology in the subsequent division cycle, the spindle morphology of *TUB1-GFP MYO1-GFP SPC29-RFP* cells arrested in hydroxyurea (HU) was assessed. It has been previously shown that hydroxyurea (HU) which reduces the rate of DNA synthesis via dNTP pools depletion arrests cells in S-phase with a short bi-polar spindle (Liu et al., 2008). Prior to HU arrest, cells were cycling at 32^{o}C for 2 hours to induce spindle breakage in endocytosis mutants. In wild type cells, 98.1 ± 0.05 % (n=203) displayed a short bipolar spindle phenotype [Figure 4.12 (a) and (b)]. In contrast, the endocytosis mutants, *end3*Δ and *rvs161*Δ *rvs167*Δ showed a significantly higher incidence of monopolar spindle formation as compared to wild-type cells [p-value<0.05, Figure 4.12 (a) and (c)]. The *end3*Δ mutant showed highest percentage of monopolar spindle (25.3 ± 9.3%, n=221), followed by *rvs161*Δ *rvs167*Δ (7.2 ± 2.1%, n=152) [Figure 4.12 (c)]. The breakage of the mitotic spindle by AMR has been previously shown to contribute to monopolar spindle formation due to an insufficient pool of tubulin for the re-establishment of spindle in progeny cells (Woodruff et al., 2012). This evidence suggests that monopolar spindle formation in endocytosis mutants might be attributed to the inadequate amount of tubulin due to spindle breakage. Alternatively, asymmetric division of the midzone that is caused by premature AMR constriction could also contribute to monopolar spindle formation. Surprisingly, there was no significant difference in monopolar spindle formation found between wild-type and *ede1*Δ mutant cells. The low percentage of monopolar spindle observed might

be due to the low incidence of spindle breakage in *ede1*Δ mutant cells [Figure 4.9 (a), (b) and (c)].

Next, the question if the monopolar spindle formation in *end3*Δ can be rescued by deletion of *chs2*Δ or *fks1*Δ was raised. However, *chs2*Δ is inviable in W303 genetic background yeast strain. To maintain the viability of *chs2*Δ cells, *CHS2* was controlled under inducible galactose promoter. *GAL-CHS2-13MYC chs2*Δ *TUB1-GFP MYO1-GFP SPC29-RFP* cells were grown overnight in YP/Raff/ medium containing 0.1% galactose (minimum concentration of galactose to support the cell growth) (appendices, Figure S2). Consistent with the results from the spindle breakage rescue, there is a significant decrease in the percentage of monopolar spindle formation in *chs2*Δ *end3*Δ (4.3 ± 4.4%, n=155, p-value <0.05) and *fks1*Δ *end3*Δ cells (4.6 ± 3.1%, n= 146, p-value <0.05) [Fig.4.12 (a) and (c)]. However, monopolar spindle formation in *sla2*Δ, *chs3*Δ and *chs3*Δ *end3*Δ cells was not examined due to the compromised viability of these mutants in HU (data not shown). Previous studies demonstrated that *chs3* is synthetic lethal with endocytic components, *rvs161*, *rvs167* and *vrp1* (Friesen et al., 2006; Lesage et al., 2005). Hence, the compromised viability of *end3*Δ *chs3*Δ double mutant cells was likely due to prolonged arrest in HU at 32^{o}C.

Taken together, the evidence gathered indicates that spindle breakage in the endocytosis mutants leads to failure in re-establishment of spindle in G1-S phase transition. The monopolar spindle formation can be rescued by deletion of *chs2*Δ and *fks1*Δ.

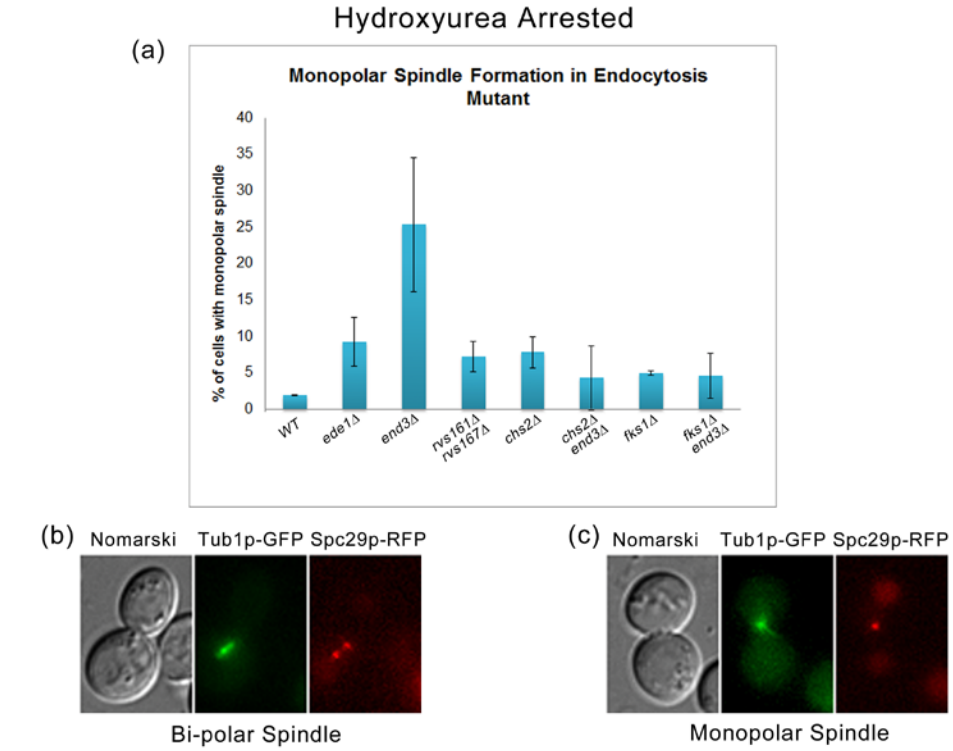

(c)

Genotype	Monopolar Spindle (%)	n	p-value (compared to WT)	p-value (compared to *end3*Δ)
WT	1.9 ± 0	207	NA	-
*ede1*Δ	9.3 ± 3.4	162	0.065	-
*end3*Δ	25.3 ± 9.3	221	0.015	NA
*rvs161*Δ *rvs167*Δ	7.2 ± 2.1	152	0.048	-
*chs2*Δ	7.8 ± 2.1	110	0.040	-
*chs2*Δ *end3*Δ	4.3 ± 4.4	162	0.461	0.014
*fks1*Δ	5.0 ± 0.3	181	0.003	-
*fks1*Δ *end3*Δ	4.6 ± 3.1	153	0.273	0.016

Figure 4.12 Mitotic spindle breakage in endocytosis mutants contributes to failure in spindle re-establishment in progeny cells. *TUB1-GFP MYO1-GFP SPC29-RFP* cells harbouring deletion of respective key endocytic component were cultured in YPD for 2 hours at 32°C. Hydroxyurea was added to final concentration of 0.2M. Cells were arrested for 5.5 hours at 32°C and subjected to microscopy analysis. (a) Graph plot showing percentage of monopolar spindle formation in endocytosis mutants. Error bars represent standard deviation. [(b) and (c)] Images were captured with 9x0.5µm z-planes for Tub1p-GFP Myo1p-GFP and Spc29p-RFP. The images shown were maximum projection of 9 z-planes. (d) Table showing the percentage monopolar spindle formation and p-values for endocytosis mutants. Student-t test was employed for the statistical analysis.

4.9 GFP-Yck2p colocalizes with Chs2p-mCherry during mitotic exit.

It has been previously shown that retrieval of transmembrane proteins such as Ste2p and Fur4p requires evolutionarily conserved proteins, yeast casein kinases, Yck1/2p activity (Hicke et al., 1998; Marchal et al., 2000). However, the requirement of Yck1/2p activity for the turnover of transmembrane cytokinetic enzymes, Chs2p at the division site has not been directly examined. Upon arrival at division site, Chs2p is rapidly internalized through clathrin mediated endocytosis and targeted to vacuole for degradation (Chuang and Schekman, 1996). Concurrently, actin cytoskeleton rearranges and changes in polarized secretion towards the neck, translocate Yck1/2p from the plasma membrane to the division site at late mitosis (Robinson et al., 1999). Together, this led to the speculation that Chs2p might be a potential substrate for Yck1/2p during mitotic exit.

To investigate the localization of Yck1/2p relative to Chs2p at the end of mitosis, the spatio-temporal localization of Yck2p and Chs2p was examined in *GFP-YCK2 CHS2-mCHERRY* cells using time-lapsed microscopy during Noc release. Upon release from Noc, Chs2p-mCherry was translocated from the ER to the neck and colocalized with GFP-Yck2p [Figure 4.13 (c) 2-12min]. The colocalization of Chs2p-mCherry and GFP-Yck2p was observed in all cells examined [Figure 4.13 (n=104)]. After arrival of Chs2p-mCherry at the neck, Chs2p-mCherry fluorescence intensity decreased gradually as cells progressed through the mitotic exit [Figure 4.13 (b)]. These results show that Yck2p and Chs2p colocalizes at the neck during mitotic exit.

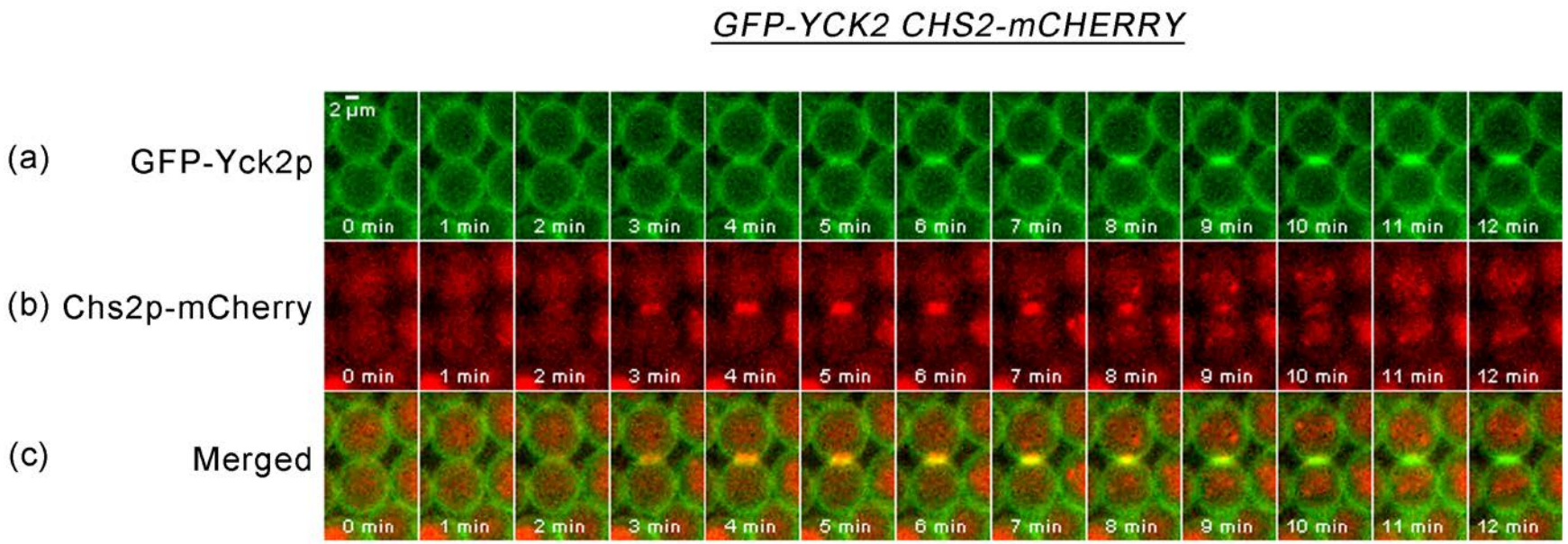

Figure 4.13 Yeast Casein Kinase GFP-Yck2p Colocalizes with Chs2p-mCherry. *GFP-YCK2 CHS2-mCHERRY* cells were arrested in YPD/Noc at 24^{o}C. After 4 hours, cells were released from metaphase into fresh YPD for 30min. Cells were then mounted in SC/Glu agar pad and examined with time-lapsed microscopy (n=104). Images were taken at 1 min interval.

4.10 Chs2p-GFP endocytosis is inhibited in *yck1*Δ *yck2-2* mutant

It has been demonstrated that the thermosensitive allele of *YCK1/2*, *yck1*Δ *yck2-2* cells displayed defects in cytokinesis and aberrant chitin deposition at the division site (Robinson et al., 1999). Furthermore, the data in this study demonstrated that GFP-Yck2p colocalized with Chs2p-mCherry at the neck during mitotic exit (Figure 4.13). These results begged the question if Yck1/2p activity mediates the endocytic retrieval of transmembrane cytokinetic enzymes such as Chs2p at the division site during mitotic exit.

To test this idea, the endocytosis of Chs2p at the neck in *YCK1 YCK2 CHS2-GFP ABP1-mCHERRY* and *yck1*Δ *yck2-2 CHS2-GFP ABP1-mCHERRY* cells were examined during Noc release. In *YCK1 YCK2 CHS2-GFP ABP1-mCHERRY* cells, Chs2p-GFP was rapidly exported out from the ER as evident from the loss of ER signals and appearance of the signals at the neck [Figure 4.14 (b) and (d) 20-40min]. The Chs2p-GFP neck signals peaked at 40min time-point [43.7%, Figure 4.14(g)]. In parallel, Abp1-mCherry (endocytosis marker) also accumulated at the division site. This indicates that endocytosis is highly active at the division site during mitotic exit. Chs2p-GFP neck signals then diminished and vacuolar signals were observed at 60 min onwards [Figure 4.14 (b) and (d) 60-80min]. Likewise, in *yck1*Δ *yck2-2 CHS2-GFP ABP1-mCHERRY* cells, Chs2p-GFP was exported out from the ER and localized to the neck [Figure 4.14 (d) and (h) 20-40min]. However, Chs2p-GFP fluorescence signal remains at the neck for an extended period of time in *yck1*Δ *yck2-2* cells [Figure 4.14 (d) and (h) 20-80min]. At 80min time-point, about 87.5% of Chs2p-GFP signals were retained at the neck even after cells

exited from mitosis as indicated by the decrease in Clb2p level [Figure 4.14 (d), (f) and (h)].

These results imply that Yck1/2p activity is indeed essential for Chs2p endocytosis at the neck during mitotic exit. The abnormal chitin deposition observed in *yck1*Δ *yck2-2* temperature sensitive mutants in previous study might be partly due to the prolonged persistence of Chs2p at the neck (Robinson et al., 1993). However, to validate the possibility that Chs2p internalization is dependent Yck1/2p phosphorylation, Phostag gel analysis (Kinoshita et al., 2009) can be conducted to determine the phosphorylation status of Chs2p in *yck1*Δ *yck2-2* mutant during mitotic exit.

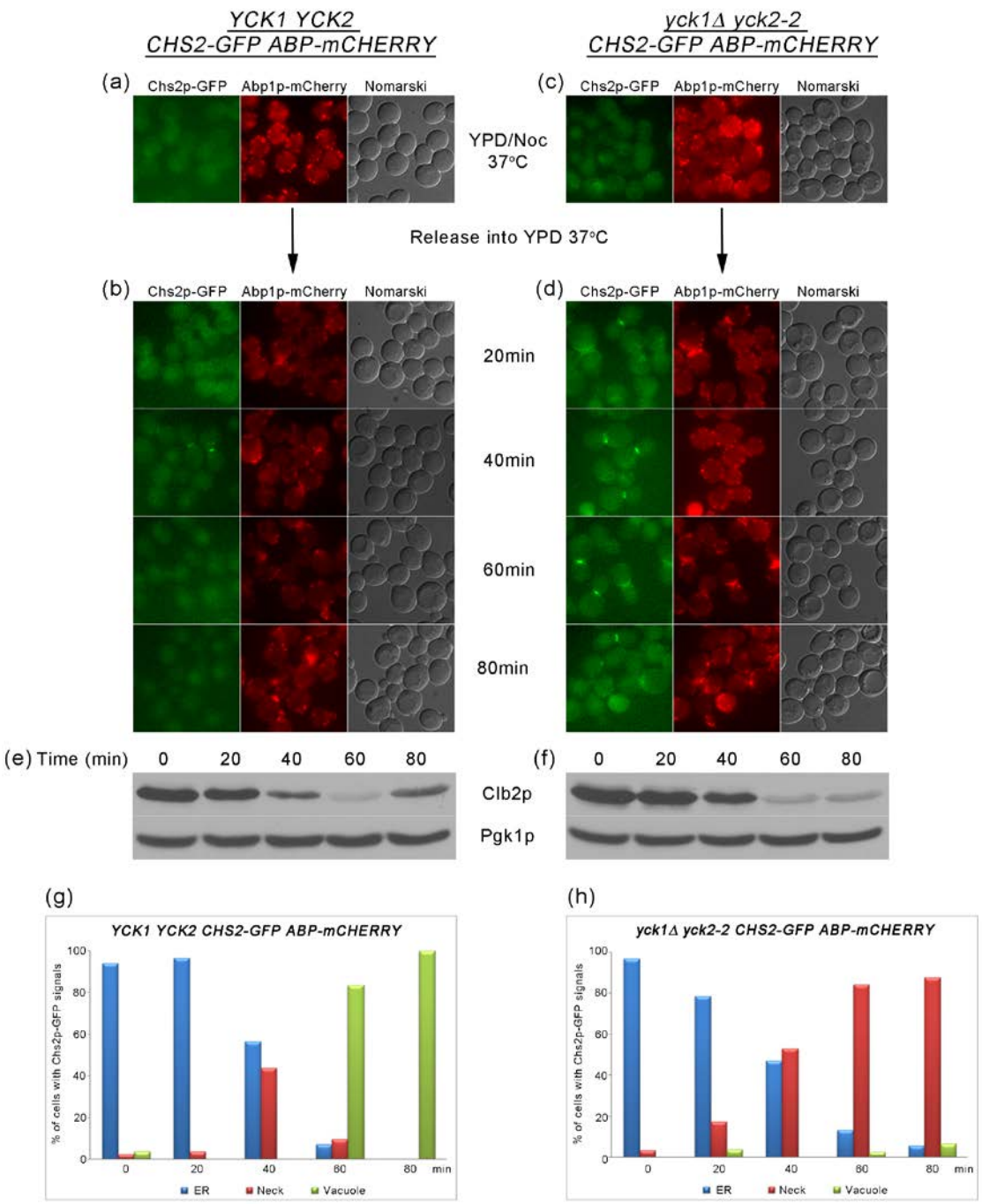

Figure 4.14 Chs2p-GFP endocytosis is inhibited in *yck1Δ yck2-2* mutant. (a) *YCK1 YCK2CHS2-GFP ABP1-mCHERRY* and (c) *yck1Δ yck2-2 CHS2-GFP ABP1-mCHERRY* were arrested in YPD/Noc for 4 hours and shifted up to 37°C for 15min. [(b) and (d)] Cells were washed and released into fresh YPD at 37°C. Samples were harvested every 20min and subjected to fluorescence microscopy and western blot analysis. [(e) and (f)] Western blot analysis of Clb2p and Pgk1p to demonstrate equivalent mitotic exit in Noc released cells. [(g) and (h)] Graph plots showing percentage of cells with Chs2p-GFP signals from 0-80 min time-points (n>100 for each time-point). Chs2p signals were classified as described in Material and Methods section. Graph plots shown were typical representations of three independent experiments.

4.11 Yck1/2p Phospho-deficient Chs2p-YFP failed to be internalized at the division site during mitotic exit.

To further demonstrate that Yck1/2p facilitates the endocytosis of Chs2p at the end of mitosis, *CHS2* mutagenesis study was conducted. Previous studies showed that Yck1/2p activity is essential in phosphorylation of the PEST (Proline/Glutamic Acid/Serine/Threonine rich) region of the permease, Fur4p, which facilitates the ubiquitination and subsequent internalization of the permease from the plasma membrane (Marchal et al., 1998; Marchal et al., 2000). Bioinformatic analysis (EMBOSS-epestfind) revealed that there were three potential PEST like sequence with Yck1/2p consensus sequences (position 3-17, 35-63, 154-174 amino acids) located at the N-terminal end of Chs2p that faces the cytoplasm (1-300 amino acids). In addition, it has been previously established that casein kinase 1 (CK1) recognizes the consensus sequence of S/T-XX-S/T (Flotow et al., 1990). To prevent Yck1/2p phosphorylating the Ser/Thr residues that are not within the PEST region, all of the Ser/Thr residues in the N-terminal end of *CHS2* that contains Yck1/2p consensus motif (inclusive of the serine reside in PEST region) were mutated to alanine. Bioinformatics analysis revealed that there were 15 potential CKI sites at the N-terminal ends of *CHS2*. In this study, all of the 15 potential Yck1/2p serine sites of *CHS2* were mutated to alanine (S11A, S14A, S21A, S24A, S40A, S43A, S112A, S115A, S150A, S153A, S158A, S161A, S167A, S180A and S183A) and fused with YFP [hereafter refer as chs2-(15S-to-15A)-YFP].

It has been previously shown that over-expression of *chs2-4S-4A* mutant kills cells (Teh et al., 2009). Similarly, the expression of Chs2p-15S-15A might

affect the cell viability; as such the localization of Chs2p-YFP and chs2p-(15S-to-15A)-YFP was examined under the control of inducible *GAL* promoter using time-lapsed microscopy during Noc release. Upon arrest in metaphase, 2% Gal was added to induce the expression of Chs2p-YFP and chs2p-(15S-to-15A)-YFP for 45min. Cells were then released from the Noc arrest and subjected to time-lapsed microscopy. In *CHS2-YFP* cells, Chs2p-YFP ER signals were visible at the beginning of the imaging. As cells progress through mitosis, Chs2p-YFP was exported out from the ER and localized to the neck [Figure 4.15 (a) 20-29min]. Next, Chs2p-YFP was rapidly endocytosed at the division site as indicated by the loss of Chs2p neck signals and appearance of vacuolar signals (97%) [Figure 4.15 (a)]. Similarly, chs2p-(15S-to15A)-YFP was also translocated from the ER to the neck during Noc release. However, as opposed to Chs2p-YFP, the chs2p-(15S-to15A)-YFP vacuolar signals were absent in the *chs2* phospho-alanine mutant cells. All of the chs2p-(15S-to15A)-YFP neck signals persisted at the neck throughout the duration of the time-lapsed imaging [Figure 4.15 (b)]. The Chs2p-(15S-to-15A)-YFP neck signals persisted even after the emergence of the new buds [Figure 4.15 (b) 36-45min]. The Chs2p neck persistence observed resembled the defect of Chs2p internalization in *sla2*Δ mutant suggesting that Chs2p failed to be endocytosed from the neck during mitotic exit (Figure 3.5).

This evidence suggests that the Yck1/2p dependent phosphorylation of Chs2p N-terminal serine clusters is essential in triggering timely endocytic retrieval of Chs2p from the division site during mitotic exit.

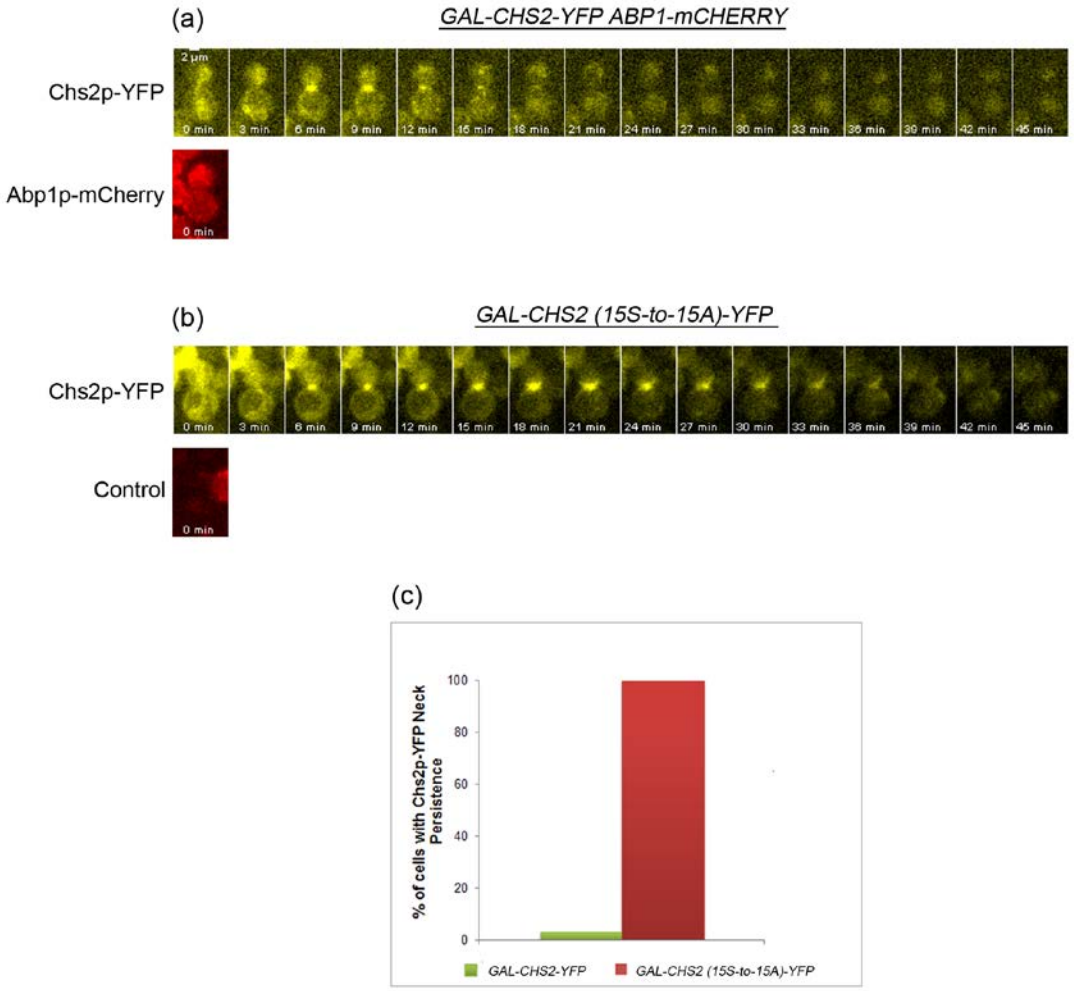

Figure 4.15 Yck1/2p Phospho-deficient Chs2p-YFP failed to be internalized during mitotic exit. (a) *GAL-CHS2-YFP ABP1-mCHERRY* (n=31) and (b) *GAL-CHS2 (15S-to-15A)-YFP* (n=43) cells were mixed and arrested in YPR/Noc for 5 hours at 24^{o}C. 2% of Gal was added into the culture for 45mins. Next, cells were washed and released into fresh YPD for 30min. Cells were then mounted on SC/Glu agar pad and examined with time-lapsed microscopy. Images were captured at 1min interval. Abp1p-mCherry signals were captured at the beginning of the time-lapsed microscopy to mark the *GAL-CHS2-YFP* cells.

Chapter 5 Discussion

Most studies on mitotic exit had emphasized the importance of reducing the mitotic kinase activity as the key condition required for cell to exit from mitosis [reviewed in (Nigg, 2001)]. As such, the idea that phosphorylation on Cdk1p substrates need to be dephosphorylated so that the action of Cdk1p activity can be reversed has not been fully explored till recent times. For instance, at the onset of anaphase, microtubule associated proteins (MAPs) and chromosomal passenger complex component, such as Ask1p, Ase1p, Sli15p, Slk19p and Cin8p are held in check via their phosphorylation by Cdk1p (Avunie-Masala et al., 2011; Khmelinskii et al., 2009; Li and Elledge, 2003; Park et al., 2008). It is only upon their dephosphorylation of Cdk1p sites by Cdc14p that they become activated and competent for executing their respective functions in spindle elongation (Avunie-Masala et al., 2011; Higuchi and Uhlmann, 2005; Khmelinskii et al., 2007; Pereira and Schiebel, 2003). Other studies have since identified further substrates of Cdc14p that are also Cdk1p substrates (Bloom et al., 2011; Ubersax et al., 2003).

In this study, the Cdk1p substrate, Chs2p that is phosphorylated at the N-terminal serine clusters in metaphase (Loog and Morgan, 2005; Martinez-Rucobo et al., 2009; Teh et al., 2009; Ubersax et al., 2003) was shown to be dephosphorylated during mitotic exit by Cdc14p both in-vivo and in-vitro (Figure 3.9). This provides evidence that the transmembrane Chs2p is a previously unidentified substrate of Cdc14p. More significantly, the data provided here show that the dephosphorylation of Chs2p and concomitant export from the ER depend upon the late mitotic liberation of Cdc14p from the nucleolus (Figure 3.1 and 3.2). Such a coordination of Chs2p ER export with

the mitotic exit pathway ensures that the formation of primary septum invariably occurs only after chromosome segregation.

The finding that Chs2p is a late mitotic substrate of Cdc14p lends support to the notion that Cdc14p has differential substrate affinities that allow it to reverse the Cdk1p phosphorylation of its substrate. For instance, Cdc14p has a greater catalytic efficiency for its early substrate, Sli15p as compared to a late substrate Orc6p (Bouchoux and Uhlmann, 2011). The authors suggested that the higher catalytic efficiency of Cdc14p for early substrates is to allow their dephosphorylation despite the persistence of Clb/Cdk activity during early anaphase. This is consistent with the results in this study showing that phosphorylation status of Sli15p was efficiently reversed by ectopic expression of Cdc14p even in the presence of high mitotic kinase (Figure 3.10). Collectively, the data in this study highlight that the interplay between mitotic kinase and Cdc14p phosphatase during mitotic exit might serves as a mechanism to safeguard the sequential execution of late mitotic events.

In addition to the identification of Chs2p as a Cdc14p substrate, the fact that Chs2p is a cargo of the secretory pathway that is regulated in a cell cycle dependent manner (Zhang et al., 2006) provides evidence of possible functional interaction between cell cycle regulators and protein trafficking. Interestingly, the regulated secretion of endogenous transmembrane cargo that involved in cytokinesis has not been previously explored in yeast and mammalian cells. The results in this study highlighted that the Chs2p is regulated secretory cargo and its timely export to the division site is tightly controlled by cell division cycle machinery. This is a striking observation, as secretory cargoes in budding yeast were previously thought to be exported in a

constitutive manner (Makarow, 1988; Nevalainen et al., 1989). A recent report from Schekman's group demonstrated that Cdc14p phosphatase activity was indeed required for Chs2p ER export during mitotic exit, presumably for the selection of Chs2p into COPII vesicles (Jakobsen et al., 2013). The authors noted that Chs2p is accumulated at the ER exit sites (ERES) during metaphase as evident from the colocalization with ERES marker, Sec13p. Unlike other constitutively export secretory cargoes, the phosphorylated Chs2p was not selected by Sec24p and incorporated into COPII vesicles at the ERES. While the underlying mechanism of how phosphorylation of Chs2p prevent its incorporation into COPII vesicles remains unknown, the data taken together suggest that there are potential further interaction between cell cycle regulators and the COPII pathway that could be important in cell division.

Moreover, Chs2p, the chitin synthase responsible for the primary septum, is also needed for AMR constriction (Schmidt et al., 2002; VerPlank and Li, 2005). The tight regulation on its export to the neck to deposit the primary septum should therefore not be surprising, given that premature localization of Chs2p at the division site could lay down the septum (Zhang et al., 2006). In fission yeast, *cut* (cell untimely torn) mutants have been identified that often exhibit an unrestrained cytokinesis and premature septum formation which in turn contributes to the cleavage of undivided nucleus (known as 'cut' phenotype). Further characterization of these mutants revealed that most proteins encoded by '*cut*' genes are essential and generally participated in pre- or post-anaphase events such as chromosome condensation, sister chromatid separation and chromosome segregation [reviewed in (Yanagida, 1998)].

Lesson from fission yeast '*cut*' mutants indicated that after cells have committed to septation, the process can't be delayed or halt ('point of no return') even when the late mitotic events are compromised. Consistent with this notion, budding yeast that exhibit defects in spindle disassembly such as *kip3*Δ mutant cells continue to undergo cytokinesis despite the presence of intact spindle (Woodruff et al., 2010). This result suggests that mitotic arrest is not possible upon initiation of septation due to the absence of surveillance system in post-anaphase. This raised the question of how the cell regulates the septation process to ensure cytokinesis invariably occurs after spindle disassembly.

In budding yeast, such cut mutants have not been isolated, implying that the process of septum formation and AMR constriction are perhaps under control of complex mechanism to prevent premature septation and cytokinesis. This is especially pertinent as Chs2p, which promotes AMR constriction, localizes to the neck prior to spindle disassembly [Figure 4.1, (VerPlank and Li, 2005)] and could potentially lead to premature execution of cytokinesis. However, in wild type cells, only about 5% of mitotic spindle breakage is observed (Figure 4.6, 4.9 and 4.10). The puzzle of how cells avoided mitotic spindle breakage was resolved when it was noted that endocytosis mutants accumulated higher concentration of Chs2p at the division site (Figure 4.3) that is highly correlated with untimely spindle breakage. While it has been previously shown that endocytosis of Chs2p occurred during late mitosis, presumably needed for the removal of Chs2p after it has executed its function, the Chs2p accumulation and spindle breakage in the endocytosis mutants support the idea that endocytosis could be essential in regulating the concentration of

cytokinetic enzymes at the division site throughout the mitotic exit. In agreement to this idea, the increase in uptake of FM4-64 (Figure 4.4) and accumulation of key CME components (Figure 4.5), at the division site when Chs2p arrived at the neck prior to AMR constriction suggesting that the endocytosis is highly active during mitotic exit. By continuously internalizing Chs2p from the division site, this excessive accumulation of Chs2p is prevented, which in turn safeguard the cells from premature constriction of AMR. This regulation ensures the spindle integrity is maintained and avoids the '*cut*' phenotype.

The spindle breakage phenotype observed in endocytosis mutants resembled *kip3*Δ, *cdh1*Δ, *doc1*Δ, *dbf2*Δ mutant cells, which exhibit a hyper-stabilized spindle and abnormal distribution of midzone proteins, Ase1p and Cin8p (Woodruff et al., 2010). However, the spindle breakage observed in *end3*Δ mutant cells was not due to the hyper-stabilized spindle but rather a premature constriction of the AMR (Figure 4.6 and 4.8). Unlike spindle depolymerization mutant cells that showed persistent spindle-halves after breakage (>100min) (Woodruff et al., 2010), the broken spindle was rapidly disassembled after spindle breakage in *end3*Δ mutant cells, excluding the possibility that the spindle breakage phenotype was due to a hyper-stable spindle (Figure 4.6). Interestingly, an increase in spindle breakage events observed in *kip3*Δ *end3*Δ mutant cells as compared to single *kip3*Δ or *end3*Δ mutant cells (Figure 4.9). On the other hand, the spindle breakage phenotype in *end3*Δ mutant cells was rescued by *slk19*Δ which displayed a short and destabilized spindle. The premature spindle disassembly counteracted the effect of accelerated AMR constriction, resulting in a rescue of the spindle

breakage in *end3*Δ mutant cells. These data suggest that spindle disassembly and AMR constriction is tightly coordinated. Failure of spindle disassembly or premature AMR constriction causes mitotic spindle breakage. Loss of coordination between spindle disassembly and AMR constriction compromises the mitotic spindle integrity during mitotic exit (Woodruff et al., 2010; Woodruff et al., 2012).

As a consequence of spindle breakage, the cells failed to establish the bi-polar spindle in the subsequent cell division cycle (Figure 4.12). The spindle breakage and monopolar spindle formation in endocytosis mutant can be rescued by deletion of *CHS2*, *CHS3*, and *FKS1* respectively (Figure 4.9 and 4.12). Although AMR stabilization and constriction is regulated by Chs2p dependent primary septum deposition, the findings of this study suggest that Chs3p and Fks1p might assist the cytokinesis process by providing the additional contractile force for efficient AMR constriction. This speculation is plausible as the initial constriction of the AMR occurs even in the absence of *chs2* or its activator *INN1* (Nishihama et al., 2009; VerPlank and Li, 2005). In addition, the Myo1p motor activity has been shown to be dispensable for AMR constriction (Fang et al., 2010; Lord et al., 2005).

Indeed, the data demonstrated that the deletion of *CHS3* or *FKS1* rescued the spindle breakage phenotype in *end3*Δ mutant cells (Figure 4.9). Furthermore, the spindle breakage observed in *end3*Δ mutant cells also can be rescued by suppressing the activity of Chs3p or Fks1p using specific inhibitors (Figure 4.10). Inhibition of Chs3p or Fks1p activity partially restored the normal dynamics of AMR constriction and rescued the spindle breakage phenotype in *end3*Δ mutant cells (Figure 4.11). These results suggest that premature AMR

constriction in endocytosis mutant cells was partially due to hyperactive Chs3p and Fks1p activity at the neck during cytokinesis. Taken together, these data support the hypothesis that Chs3p and Fks1p play a role in mediating AMR constriction during cytokinesis. However, further studies need to be conducted to confirm this hypothesis.

The results in this study also revealed that the timely retrieval of Chs2p from the division site requires the evolutionarily conserved kinase, yeast casein kinases, Yck1/2p. At late mitosis, the rearrangement of actin cytoskeleton and changes in polarized secretion towards the neck triggers the translocation of Yck1/2p from the plasma membrane to the division site (Robinson et al., 1999). Concurrently, Chs2p is exported from the ER and targeted to the division site to deposit the PS. In this study, GFP-Yck2p was colocalized with Chs2p-mCherry at the neck during Noc release (Figure 4.13). As the Yck1/2p dependent phosphorylation of transmembrane proteins such as Ste2p and Fur4p is prerequisite for endocytosis, the spatio-temporal colocalization of Yck2p and Chs2p might be important for Yck1/2p to phosphorylate Chs2p directly during mitotic exit. The phosphorylation of Chs2p by Yck1/2p might serve as an endocytosis signal which recruits endocytic machinery to facilitate its internalization from the division site (Feng and Davis, 2000; Hicke et al., 1998; Marchal et al., 2000). Consistent with this idea, Chs2p endocytosis was inhibited in the absence of Yck1/2p activity (Figure 4.14). Furthermore, mutagenesis analysis revealed that mutation of Yck1/2p consensus motif of Chs2p to alanine inhibited the retrieval of Chs2p from the division site (Figure 4.15). These results corroborate the hypothesis that the retrieval of Chs2p from the division site requires Yck1/2p activity during mitotic exit.

Collectively, the data gathered in this study highlighted the significance of cell cycle regulated protein trafficking of cytokinetic enzymes during mitotic exit. The high level of mitotic kinase activity during metaphase inhibits the delivery of Chs2p to the division site to prevent premature septation before nuclear division. After the separation of sister chromatids, the inactivation of mitotic kinase together with Cdc14p in the cytoplasm reverses the phosphorylation of Chs2p and permits its timely export to the division site to deposit the primary septum. This tight regulation maintains the genomic stability by ensuring that the septation process is strictly occurs only after the separation of genetic materials.

Upon arrival at the division site, the phosphorylation that is imposed by Yck1/2p on Chs2p serves as a signal to promote continuous endocytosis. The optimal concentration of cytokinetic enzymes at the division site is maintained via the balance between forward trafficking and endocytosis. This is crucial as insufficient amount or absence of cytokinetic enzymes at the division site contributes to failure in AMR constriction that eventually leads to cytokinesis defects. On the contrary, excessive accumulation of cytokinetic enzymes at the neck leads to premature AMR constriction which in turn causes the shearing of mitotic spindle during mitotic exit.

Chapter 6 Conclusion and Future Directions

6.1 Conclusion

The work in this dissertation has provided a new perspective of how the cell coordinates spindle dynamics, trafficking of cytokinetic enzymes, and AMR constriction during late mitosis. A simple yet effective model of how the cell regulates the ordering of late mitotic events was proposed (Figure 6.1).

At metaphase when the mitotic kinase activity is high, Chs2p was retained in the ER due to the phospho-inhibitory action imposed by Cdk1p (Teh et al., 2009). Upon faithful attachment of mitotic spindle microtubules to kinetochores, the spindle assembly checkpoint (SAC) is satisfied, leading to the initial wave of mitotic cyclins destruction by APC^{Cdc20} (Visintin et al., 1997; Yeong et al., 2000). Concurrently, the activation of FEAR pathway promotes the liberation of Cdc14p from the nucleolus to the nucleoplasm [reviewed in (Queralt and Uhlmann, 2008a; Stegmeier and Amon, 2004). Cdc14p in the nucleoplasm reverses the phosphorylation on microtubule binding proteins such as Sli15p that is pivotal in mitotic spindle stabilization and elongation (Pereira and Schiebel, 2003). The elongation of mitotic spindle separates the spindle pole bodies into mother and daughter cell and elicits the activation of MEN. As a result, Cdc14p is dissociated from its nucleolar inhibitor, Net1p, and release into the cytoplasm [reviewed in (Queralt and Uhlmann, 2008a; Stegmeier and Amon, 2004). This drives the exit of the cell from mitosis through Sic1p accumulation and APC^{Cdh1} activation (Visintin et al., 1998; Yeong et al., 2000). The loss of competing mitotic kinase during mitotic exit tips the balance of Cdk1p-Cdc14p activity towards the phosphatase and promotes the Cdc14p dependent dephosphorylations of Chs2p. Alleviation of the phospho-inhibitory signal on Chs2p causes the

incorporation of Chs2p into COPII vesicles and translocation to the neck. Simultaneously, polarized secretion towards the neck delivers Chs3p and Fks1p to the division site.

At this point, the mitotic spindle remains intact even after the arrival of cytokinetic enzymes at the neck. The data in this study demonstrate that excessive accumulation of cytokinetic enzymes at the neck causes premature constriction of AMR which in turn contributes to shearing of the mitotic spindle. Hence, the continuous endocytosis at the division site might serves as a mechanism to maintain the optimal concentration of cytokinetic enzymes at the division site. This mechanism ensures that the execution of AMR constriction strictly occur after spindle disassembly. The data in this study also reveals that the internalization of Chs2p at the division site is dependent on phosphorylation imposed by Yck1/2p.

Collectively, the data gathered in this study suggested that the ordering of late mitotic events is achieved via the balance between Cdk1p-Cdc14p activities. Together with endocytosis at the neck, the cell ensures that the spindle elongation, chromosome segregation and cytokinesis always occur in a sequential manner. The defect in the ordering of late mitotic events is detrimental to cells as premature septation prior to chromosome segregation or mitotic spindle disassembly causes cells death (Teh et al., 2009) and failure in the re-establishment of bi-polar spindle in the subsequent round of cell division cycle.

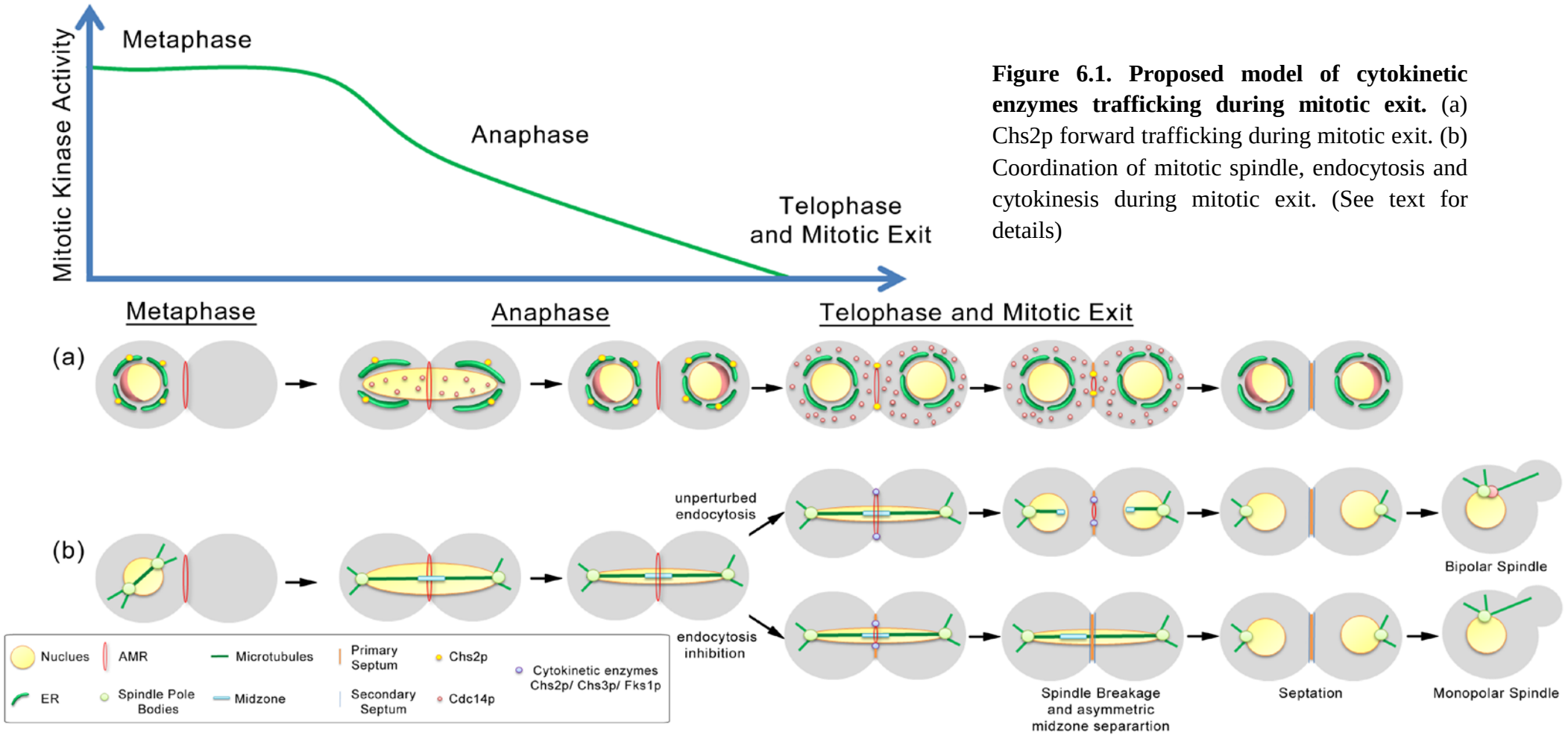

Figure 6.1. Proposed model of cytokinetic enzymes trafficking during mitotic exit. (a) Chs2p forward trafficking during mitotic exit. (b) Coordination of mitotic spindle, endocytosis and cytokinesis during mitotic exit. (See text for details)

6.2 Future directions

Based on the experimental data, discussion presented and conclusion drawn from this dissertation work, several interesting directions that can be further explored are highlighted below:

6.2.1 Cell cycle regulated protein trafficking

6.2.2.1 Understanding the role of mitotic kinase in regulating the spatio-temporal localization of key CME components during mitotic exit.

A direct extension from this work is to investigate the relationship between mitotic kinase destruction and localization of CME components at the division site during mitotic exit. The data from this study showed that the endocytic marker, Abp1p accumulated at the division site at the end of mitosis. Similarly, other CME key components such as Ede1p, Sla2p, Las17p Sla1p, and Rvs167p were also localized to the division shortly after the arrival of Chs2p (Figure 4.5). Consistent with previous study, yeast epsin, Ent2p (mammalian epsin homolog) had been reported to the cortex region throughout the cell cycle and accumulates at the bud neck at the end of mitosis (Mukherjee et al., 2009). Besides, ectopic expression of mitotic kinase inhibitor, Sic1p, in metaphase arrested cells contributed to the premature neck localization of Abp1p-ECFP, Sla1p-mCherry (appendices, Figure S3). These observations have led to the speculation that the reduction in mitotic kinase activity at the end of mitosis affects the distribution of the key CME components.

Indeed, in large scale analysis, Sla1p was shown to be phosphorylated by Cdc28p (Ptacek et al., 2005). Sla1p phosphorylation by Cdc28p has also been reported in pathogenic yeast, *Candida albicans* (Zeng et al., 2012). Moreover,

the in-vitro phosphatase treatment using generic phosphatase, lambda phosphatase on Sla1p that immunoprecipitated from Noc arrested cells lysate revealed that Sla1p was indeed phosphorylated (appendices, Figure S4). Activation of MEN during mitotic exit might alleviate the phosphorylation on CME components which in turn results in their accumulation at the division site to facilitate endocytosis. However, the accumulation of CME components at the division site might be also due to the arrival of endocytic cargo during mitotic exit. It has been proposed that arrival of endocytic cargo into pre-existing endocytic sites initiates the assembly of endocytic machinery (Toshima et al., 2009; Toshima et al., 2006). The premature mitotic exit that is induced by ectopic expression of Sic1p in metaphase arrested cells also led to delivery of endocytic cargoes to the division site such as Chs2p (Zhang et al., 2006). Hence, it is crucial to uncouple the delivery of secretory cargoes and reduction of mitotic kinase in order to understand the relationship between these two events.

To ascertain if arrival of endocytic cargoes at the division site leads to the recruitment of CME components, the secretion mutant such as *sec10-2* can be employed to block the forward protein trafficking during mitotic exit. On the other hand, endocytic cargo can be prematurely delivered to the division site to examine whether CME components are accumulated in high mitotic kinase environment. For instance, Chs2p-(6S-6A)-YFP that is constitutively exported out from the ER during metaphase can be employed to test this idea. However, further research is required to gain better understanding of the regulation of CME components localization at the division site.

6.2.2.2 Identification of molecular factors involved in protein trafficking of Fks1p.

Another interesting area for future exploration is the identification of factors involved in the export of Fks1p from the ER. The protein secretion of Chs3p is well characterized in many studies [reviewed in (Lesage and Bussey, 2006; Orlean, 2012)]. Likewise, the mechanism that triggers Chs2p ER export is also established in this study (Chin et al., 2011). However, the secretion of Fks1p from the ER remains poorly characterized. So far, Soo1p is the only protein identified that played a role in Fks1p ER secretion. Hence, further studies have to be conducted to determine if additional factors are involved in Fks1p ER export.

To isolate mutants that fail to direct Fks1p to the plasma membrane, random mutagenesis using EMS (ethyl-methanesuffonate) can be performed. It has been demonstrated that the deletion or mutation of *FKS1* lead to up-regulation of Chs3p activity which in turn result in elevated chitin content in the cell (Garcia-Rodriguez et al., 2000). This indicates that the failure in secretion of Fks1p to the plasma membrane also should yield similar phenotype. Hence, Calcofluor white (CFW) can be utilized to identify the mutant cells that display hypersensitivity to this compound. CFW is an anti-fungal compound binds specifically to chitin and inhibits the cell growth through interference with cell wall assembly (Roncero and Duran, 1985; Roncero et al., 1988). The mutated gene that confers hypersensitivity to calcofluor can be identified through rescue assay using yeast genomic DNA library or Next-Generation sequencing.

Understanding the trafficking of chitin and glucan synthases provides invaluable information for antifungal drug development. The chitin and glucan synthases are highly conserved among pathogen fungal such as *Candida albicans*, and non-*candida albicans* species, but absent in the human host, rendering these proteins attractive drug targets for treatment of fungal infections such as candidiasis.

6.2.2 Cell division cycle and cytokinesis

6.2.2.1 Investigate the role of MEN components at the mother-daughter neck and its implications in regulating cytokinesis.

Future research should attempt to elucidate the role of MEN components at the neck during mitotic exit. In addition to its role in mediating mitotic exit, MEN components are also involved in facilitating septation and cytokinesis at the division site. Cdc5, Tem1p, Cdc15p, Dbf2p, Dbf20p, Mob1p and Cdc14p have been shown to localize to the division site at the end of mitosis [reviewed in (Yeong et al., 2002)]. However, the role of MEN at the neck during mitotic exit remains poorly characterized.

A recent study from Palani and co-workers demonstrates that the neck localization of Cdc14p is required for the reversal of Cdk1p phosphorylation of Inn1p at the division site. The Cdc14p dependent Inn1p dephosphorylation facilitates the formation of Inn1p-Cyk3 complex that is crucial in activating Chs2p for primary septum formation (Meitinger et al., 2010; Palani et al., 2012). Besides Cdc14p, the role of Dbf2p at the neck is recently revealed in the study from Erfei Bi group. The authors demonstrated that Dbf2p neck

localization phosphorylates the ser-217 residue of Chs2p which in turn triggers its dissociation from the AMR during mitotic exit (Oh et al., 2012).

To gain better understanding in the role of MEN components in regulating cytokinesis, particularly at the division site, the interacting partners or the substrates of MEN components should be identified. However, the identification of the neck specific MEN components binding proteins remained an obstacle due to the fact that most of the co-immunoprecipiation assays coupled with mass spectrometry (MS) analysis were performed using asynchronous culture. For instance, the biochemical pull down screens of Cdc14p substrates were carried out using log culture or G2/M arrested cells (Bloom et al., 2011; Kao et al., 2014). Such experimental approaches might fail to identify MEN component substrates, due to the highly dynamic nature of protein interaction at the neck. Lysates of co-immunoprecipitation assays for mass spectrometry analysis should be harvested from cells released from metaphase block and enriched in mitotic exit phase to increase the probability of isolating MEN components' novel substrates.

6.2.2.2 Identification of Yeast casein kinase 1 substrates during mitosis.

Likewise, co-immunoprecipiation assays coupled with mass spectrometry (MS) analysis approach also can be employed to identify the Yck1/2p substrates at the division site. In budding yeast, it has been shown that in cells lacking Yck1/2p activity displayed a defect in cytokinesis (Robinson et al., 1992; Robinson et al., 1993). The defect in septin organization was proposed to be the main factor that contributed to the cytokinesis defect in *yck1/2* mutant cells. However, the existence of cytokinetic proteins that require post-translational modification by Yck1/2p to facilitate cytokinesis cannot be excluded. In

addition, it has been demonstrated that RNAi knockdown of *Trypanasoma brucei* casein kinase 1 isoform, *TbCK1.2* led to multinucleated cells suggesting that CK1 might play a role in regulating cytokinesis (Urbaniak, 2009).

Apart from its role in regulating cytokinesis, a recent report from Gould group revealed that CK1 in *Schizosaccharomyces pombe* plays a role in delaying cytokinesis upon mitotic checkpoint activation through phospho-priming the scaffolding component of Septation Initiation Network (budding yeast MEN), Sid4p, for Dma1p (an E3 ubiquitin ligase)- mediated ubiquitination. Ubiquitinated Sid4p delays recruitment of SIN activator, Plo1p (Polo-like kinase) to the SPB which in turn resulted in stalling of cytokinesis (Johnson and Gould, 2011). The results from these studies suggest that CK1 might play multiple roles in regulating mitotic events. Hence, the identification of mitotic Yck1/2p substrates is crucial in elucidating the roles of CK1 during mitosis.

6.3 Limitations

The work on cytokinetic enzymes trafficking at the end of mitosis reported in this thesis has two major limitations. Firstly, although Cdc14p dependent Chs2p ER export was identified, the exact mechanism of how the phosphorylation on Chs2p prevents its incorporation into COPII vesicle is not well understood. It is speculated that the phosphorylation on Chs2p could induce the conformational change and eventually mask the signal for COPII coat incorporation. However, this issue has not been addressed due to the lack of information on Chs2p crystal structure. Understanding the crystal structure of transmembrane protein, Chs2p remains obscured due to its highly unstable and plasticity nature (Carpenter et al., 2008). Secondly, the possibility that other unknown proteins might be involved in cytokinesis during mitotic exit cannot be excluded. The spindle breakage phenotype observed in endocytosis mutants might be partly contributed by other unidentified cytokinetic proteins that regulate AMR constriction at the end of mitosis.

Appendices

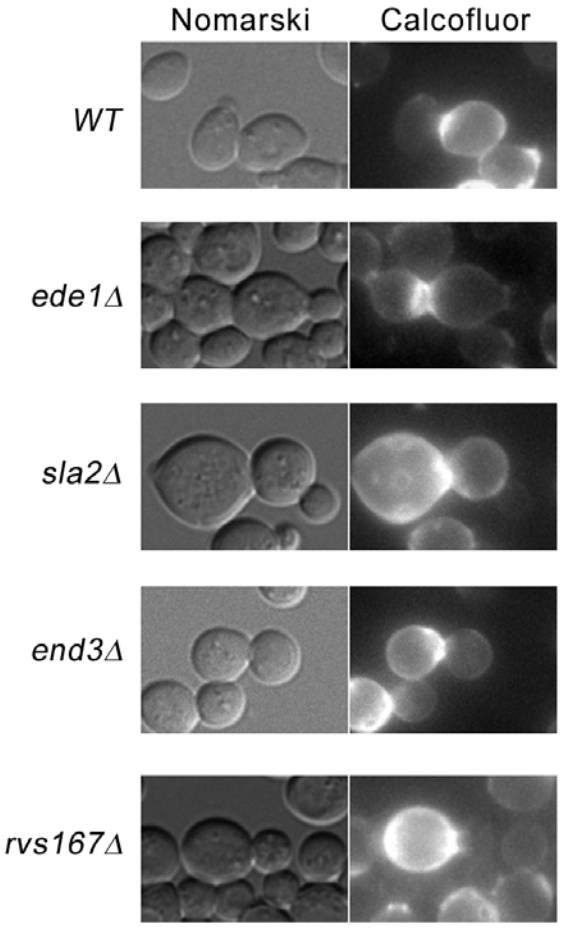

Figure S1. Aberrant chitin deposition at the division site in key CME deletion mutant. Cells were cycling at 32^{o}C in YPD for 3 hours. The cells were then harvested, stained with calcofluor white and subjected to fluorescence microscopy analysis.

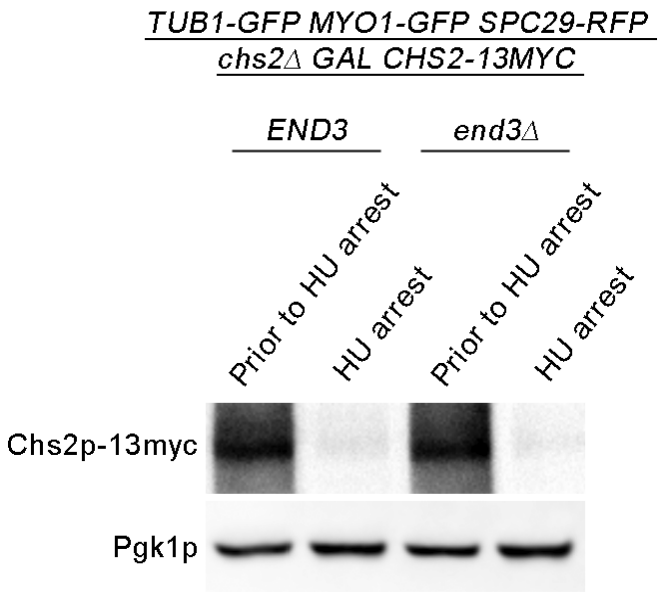

Figure S2. Mitotic spindle breakage in endocytosis mutants contributes to failure in spindle re-establishment in progeny cells. *TUB1-GFP MYO1-GFP SPC29-RFP chs2Δ GAL-CHS2-13MYC* cells harbouring *END3* and *end3*Δ respectively were cultured in YPR/0.1% Gal overnight. Cells were cycling in YPD for 2 hours at 32^{o}C. Hydroxyurea was added to final concentration of 0.2M. Cells were then arrested for 5.5 hours at 32^{o}C, harvested and subjected to western blot analysis.

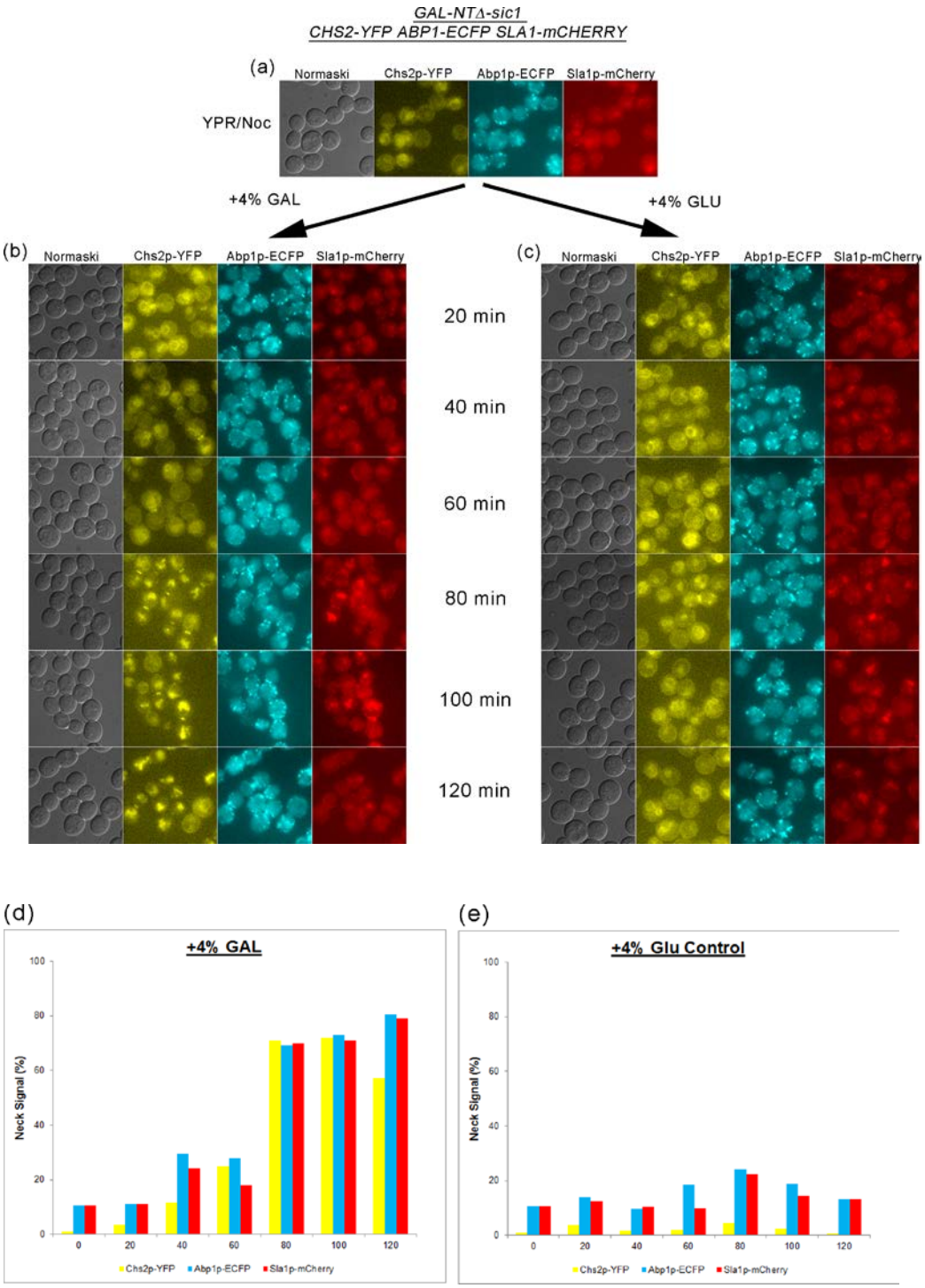

Figure S3. Ectopic expression of Cdk1 inhibitor, Sic1p, triggers the accumulation of Abp1p-ECFP and Sla1p-mCherry at the neck. (a) Cells harbouring *GAL-SIC1-MYC (4-copies) CHS2-YFP ABP1-ECFP SLA1-mCHERRY* were arrested in YP/Raff/Noc for 5 hours at 24^{o}C. (b) 4% Gal and (c) 4% Glu was added into the culture to induce the expression of Sic1p-myc. Cells were then harvested at 20min intervals and subjected to fluorescence microscopy analysis. [(d) and (e)] Graph plots showing percentage of cells with Chs2p-YFP, Abp1p-ECFP and Sla1p-mCherry neck signals (>50 cells were counted for each time-point).

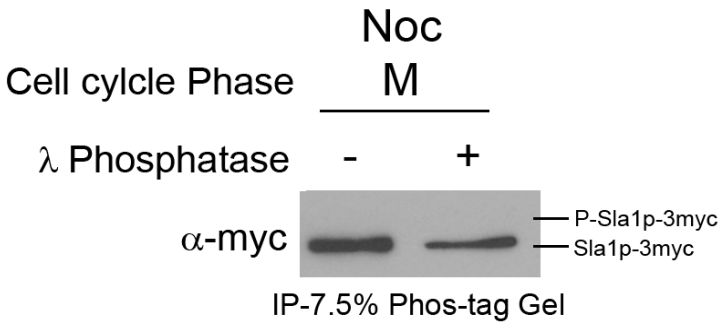

Figure S4. Sla1p is phosphorylated during metaphase. Sla1p-3myc was immunoprecipitated using anti-myc beads from Noc arrested TCA cell lysates. Sla1p-3myc bound beads were treated with lambda phosphatase at 30^{o}C for 30min.

Bibliography

Adams, D.J. 2004. Fungal cell wall chitinases and glucanases. *Microbiology*. 150:2029-2035.

Avunie-Masala, R., N. Movshovich, Y. Nissenkorn, A. Gerson-Gurwitz, V. Fridman, M. Koivomagi, M. Loog, M.A. Hoyt, A. Zaritsky, and L. Gheber. 2011. Phospho-regulation of kinesin-5 during anaphase spindle elongation. *J Cell Sci*. 124:873-878.

Azzam, R., S.L. Chen, W. Shou, A.S. Mah, G. Alexandru, K. Nasmyth, R.S. Annan, S.A. Carr, and R.J. Deshaies. 2004. Phosphorylation by cyclin B-Cdk underlies release of mitotic exit activator Cdc14 from the nucleolus. *Science*. 305:516-519.

Bacon, J.S., E.D. Davidson, D. Jones, and I.F. Taylor. 1966. The location of chitin in the yeast cell wall. *Biochem J*. 101:36C-38C.

Bähler. 2005. Cell-cycle control of gene expression in budding and fission yeast. *Annu Rev Genet.* 39:69-94.

Baladron, V., S. Ufano, E. Duenas, A.B. Martin-Cuadrado, F. del Rey, and C.R. Vazquez de Aldana. 2002. Eng1p, an endo-1,3-beta-glucanase localized at the daughter side of the septum, is involved in cell separation in Saccharomyces cerevisiae. *Eukaryot Cell*. 1:774-786.

Balasubramanian, M.K., E. Bi, and M. Glotzer. 2004. Comparative analysis of cytokinesis in budding yeast, fission yeast and animal cells. *Curr Biol*. 14:R806-818.

Bannykh, S.I., T. Rowe, and W.E. Balch. 1996. The organization of endoplasmic reticulum export complexes. *J Cell Biol*. 135:19-35.

Bardin, A.J., R. Visintin, and A. Amon. 2000. A mechanism for coupling exit from mitosis to partitioning of the nucleus. *Cell*. 102:21-31.

Barlowe, C., C. d'Enfert, and R. Schekman. 1993. Purification and characterization of SAR1p, a small GTP-binding protein required for transport vesicle formation from the endoplasmic reticulum. *J Biol Chem*. 268:873-879.

Barlowe, C.K., and E.A. Miller. 2013. Secretory protein biogenesis and traffic in the early secretory pathway. *Genetics*. 193:383-410.

Baro, B., J.A. Rodriguez-Rodriguez, I. Calabria, M.L. Hernaez, C. Gil, and E. Queralt. 2013. Dual Regulation of the Mitotic Exit Network (MEN) by PP2A-Cdc55 Phosphatase. *PLoS Genet*. 9:e1003966.

Bembenek, J., J. Kang, C. Kurischko, B. Li, J.R. Raab, K.D. Belanger, F.C. Luca, and H. Yu. 2005. Crm1-mediated nuclear export of Cdc14 is required for the completion of cytokinesis in budding yeast. *Cell Cycle*. 4:961-971.

Berben, G., J. Dumont, V. Gilliquet, P.A. Bolle, and F. Hilger. 1991. The YDp plasmids: a uniform set of vectors bearing versatile gene disruption cassettes for Saccharomyces cerevisiae. *Yeast*. 7:475-477.

Bi, E. 2001. Cytokinesis in budding yeast: the relationship between actomyosin ring function and septum formation. *Cell Struct Funct*. 26:529-537.

Bi, E., P. Maddox, D.J. Lew, E.D. Salmon, J.N. McMillan, E. Yeh, and J.R. Pringle. 1998. Involvement of an actomyosin contractile ring in Saccharomyces cerevisiae cytokinesis. *J Cell Biol*. 142:1301-1312.

Bi, E., and H.-O. Park. 2012a. Cell polarization and cytokinesis in budding yeast. *Genetics*. 191:347-387.

Bi, E., and H.O. Park. 2012b. Cell polarization and cytokinesis in budding yeast. *Genetics*. 191:347-387.

Bi, X., R.A. Corpina, and J. Goldberg. 2002. Structure of the Sec23/24-Sar1 pre-budding complex of the COPII vesicle coat. *Nature*. 419:271-277.

Blondel, M.O., J. Morvan, S. Dupre, D. Urban-Grimal, R. Haguenauer-Tsapis, and C. Volland. 2004. Direct sorting of the yeast uracil permease to the endosomal system is controlled by uracil binding and Rsp5p-dependent ubiquitylation. *Mol Biol Cell*. 15:883-895.

Bloom, J., I.M. Cristea, A.L. Procko, V. Lubkov, B.T. Chait, M. Snyder, and F.R. Cross. 2011. Global analysis of Cdc14 phosphatase reveals diverse roles in mitotic processes. *J Biol Chem*. 286:5434-5445.

Boettner, D.R., R.J. Chi, and S.K. Lemmon. 2011. Lessons from yeast for clathrin-mediated endocytosis. *Nat Cell Biol*. 14:2-10.

Booher, R.N., R.J. Deshaies, and M.W. Kirschner. 1993. Properties of Saccharomyces cerevisiae wee1 and its differential regulation of p34CDC28 in response to G1 and G2 cyclins. *Embo J*. 12:3417-3426.

Bouchoux, C., and F. Uhlmann. 2011. A quantitative model for ordered Cdk substrate dephosphorylation during mitotic exit. *Cell*. 147:803-814.

Bouck, D.C., and K.S. Bloom. 2005. The kinetochore protein Ndc10p is required for spindle stability and cytokinesis in yeast. *Proc Natl Acad Sci U S A*. 102:5408-5413.

Brandizzi, F., and C. Barlowe. 2013. Organization of the ER-Golgi interface for membrane traffic control. *Nat Rev Mol Cell Biol*. 14:382-392.

Cabib, E., and B. Bowers. 1971. Chitin and yeast budding. Localization of chitin in yeast bud scars. *J Biol Chem*. 246:152-159.

Cabib, E., D.H. Roh, M. Schmidt, L.B. Crotti, and A. Varma. 2001. The yeast cell wall and septum as paradigms of cell growth and morphogenesis. *J Biol Chem*. 276:19679-19682.

Cabib, E., and M. Schmidt. 2003. Chitin synthase III activity, but not the chitin ring, is required for remedial septa formation in budding yeast. *FEMS Microbiol Lett*. 224:299-305.

Carpenter, E.P., K. Beis, A.D. Cameron, and S. Iwata. 2008. Overcoming the challenges of membrane protein crystallography. *Curr Opin Struct Biol*. 18:581-586.

Chang, J.S., K. Henry, B.L. Wolf, M. Geli, and S.K. Lemmon. 2002. Protein phosphatase-1 binding to scd5p is important for regulation of actin organization and endocytosis in yeast. *J Biol Chem*. 277:48002-48008.

Chin, C.F., A.M. Bennett, W.K. Ma, M.C. Hall, and F.M. Yeong. 2011. Dependence of Chs2 ER export on dephosphorylation by cytoplasmic Cdc14 ensures that septum formation follows mitosis. *Mol Biol Cell*.

Cho, R.J., M.J. Campbell, E.A. Winzeler, L. Steinmetz, A. Conway, L. Wodicka, T.G. Wolfsberg, A.E. Gabrielian, D. Landsman, D.J. Lockhart, and R.W. Davis. 1998. A genome-wide transcriptional analysis of the mitotic cell cycle. *Mol Cell*. 2:65-73.

Chuang, J.S., and R.W. Schekman. 1996. Differential trafficking and timed localization of two chitin synthase proteins, Chs2p and Chs3p. *J Cell Biol*. 135:597-610.

Civelekoglu-Scholey, G., and J.M. Scholey. 2010. Mitotic force generators and chromosome segregation. *Cell Mol Life Sci*. 67:2231-2250.

Cohen-Fix, O., J.M. Peters, M.W. Kirschner, and D. Koshland. 1996. Anaphase initiation in Saccharomyces cerevisiae is controlled by the APC-dependent degradation of the anaphase inhibitor Pds1p. *Genes Dev*. 10:3081-3093.

D'Amours, D., and A. Amon. 2004. At the interface between signaling and executing anaphase--Cdc14 and the FEAR network. *Genes Dev*. 18:2581-2595.

De Souza, C.P., and S.A. Osmani. 2007. Mitosis, not just open or closed. *Eukaryot Cell*. 6:1521-1527.

Devrekanli, A., M. Foltman, C. Roncero, A. Sanchez-Diaz, and K. Labib. 2012. Inn1 and Cyk3 regulate chitin synthase during cytokinesis in budding yeasts. *J Cell Sci*. 125:5453-5466.

Dobbelaere, J., and Y. Barral. 2004. Spatial coordination of cytokinetic events by compartmentalization of the cell cortex. *Science*. 305:393-396.

Douglas, L.M., F.J. Alvarez, C. McCreary, and J.B. Konopka. 2005. Septin function in yeast model systems and pathogenic fungi. *Eukaryot Cell*. 4:1503-1512.

Dunn, R., and L. Hicke. 2001. Domains of the Rsp5 ubiquitin-protein ligase required for receptor-mediated and fluid-phase endocytosis. *Mol Biol Cell*. 12:421-435.

Engqvist-Goldstein, A.E., and D.G. Drubin. 2003. Actin assembly and endocytosis: from yeast to mammals. *Annu Rev Cell Dev Biol*. 19:287-332.

Enserink, J.M., and R.D. Kolodner. 2010. An overview of Cdk1-controlled targets and processes. *Cell Div*. 5:11.

Epp, J.A., and J. Chant. 1997. An IQGAP-related protein controls actin-ring formation and cytokinesis in yeast. *Curr Biol*. 7:921-929.

Fang, X., J. Luo, R. Nishihama, C. Wloka, C. Dravis, M. Travaglia, M. Iwase, E.A. Vallen, and E. Bi. 2010. Biphasic targeting and cleavage furrow ingression directed by the tail of a myosin II. *J Cell Biol*. 191:1333-1350.

Feng, B., H. Schwarz, and S. Jesuthasan. 2002. Furrow-specific endocytosis during cytokinesis of zebrafish blastomeres. *Exp Cell Res*. 279:14-20.

Feng, Y., and N.G. Davis. 2000. Akr1p and the type I casein kinases act prior to the ubiquitination step of yeast endocytosis: Akr1p is required for kinase localization to the plasma membrane. *Mol Cell Biol*. 20:5350-5359.

Fielding, A.B., A.K. Willox, E. Okeke, and S.J. Royle. 2012. Clathrin-mediated endocytosis is inhibited during mitosis. *Proc Natl Acad Sci U S A*. 109:6572-6577.

Fitch, I., C. Dahmann, U. Surana, A. Amon, K. Nasmyth, L. Goetsch, B. Byers, and B. Futcher. 1992. Characterization of four B-type cyclin genes of the budding yeast Saccharomyces cerevisiae. *Mol Biol Cell*. 3:805-818.

Flotow, H., P.R. Graves, A.Q. Wang, C.J. Fiol, R.W. Roeske, and P.J. Roach. 1990. Phosphate groups as substrate determinants for casein kinase I action. *J Biol Chem*. 265:14264-14269.

Foley, E.A., and T.M. Kapoor. 2013. Microtubule attachment and spindle assembly checkpoint signalling at the kinetochore. *Nat Rev Mol Cell Biol*. 14:25-37.

Friesen, H., C. Humphries, Y. Ho, O. Schub, K. Colwill, and B. Andrews. 2006. Characterization of the yeast amphiphysins Rvs161p and

Rvs167p reveals roles for the Rvs heterodimer in vivo. *Mol Biol Cell*. 17:1306-1321.

Gachet, Y., and J.S. Hyams. 2005. Endocytosis in fission yeast is spatially associated with the actin cytoskeleton during polarised cell growth and cytokinesis. *J Cell Sci*. 118:4231-4242.

Garcia-Rodriguez, L.J., J.A. Trilla, C. Castro, M.H. Valdivieso, A. Duran, and C. Roncero. 2000. Characterization of the chitin biosynthesis process as a compensatory mechanism in the fks1 mutant of Saccharomyces cerevisiae. *FEBS Lett*. 478:84-88.

Gardner, M.K., J. Haase, K. Mythreye, J.N. Molk, M. Anderson, A.P. Joglekar, E.T. O'Toole, M. Winey, E.D. Salmon, D.J. Odde, and K. Bloom. 2008. The microtubule-based motor Kar3 and plus end-binding protein Bim1 provide structural support for the anaphase spindle. *J Cell Biol*. 180:91-100.

Gaughran, J.P., M.H. Lai, D.R. Kirsch, and S.J. Silverman. 1994. Nikkomycin Z is a specific inhibitor of Saccharomyces cerevisiae chitin synthase isozyme Chs3 in vitro and in vivo. *J Bacteriol*. 176:5857-5860.

Gietz, R.D., and A. Sugino. 1988. New yeast-Escherichia coli shuttle vectors constructed with in vitro mutagenized yeast genes lacking six-base pair restriction sites. *Gene*. 74:527-534.

Gietz, R.D., and R.A. Woods. 2006. Yeast transformation by the LiAc/SS Carrier DNA/PEG method. *Methods Mol Biol*. 313:107-120.

Glotzer, M. 2009. The 3Ms of central spindle assembly: microtubules, motors and MAPs. *Nat Rev Mol Cell Biol*. 10:9-20.

Gray, C.H., V.M. Good, N.K. Tonks, and D. Barford. 2003. The structure of the cell cycle protein Cdc14 reveals a proline-directed protein phosphatase. *Embo J*. 22:3524-3535.

Gupta, M.L., Jr., P. Carvalho, D.M. Roof, and D. Pellman. 2006. Plus end-specific depolymerase activity of Kip3, a kinesin-8 protein, explains its role in positioning the yeast mitotic spindle. *Nat Cell Biol*. 8:913-923.

Hall, M.C., D.E. Jeong, J.T. Henderson, E. Choi, S.C. Bremmer, A.B. Iliuk, and H. Charbonneau. 2008. Cdc28 and Cdc14 control stability of the anaphase-promoting complex inhibitor Acm1. *J Biol Chem*. 283:10396-10407.

Hammond, A.T., and B.S. Glick. 2000. Dynamics of transitional endoplasmic reticulum sites in vertebrate cells. *Mol Biol Cell*. 11:3013-3030.

Hanahan, D. 1983. Studies on transformation of Escherichia coli with plasmids. *J Mol Biol*. 166:557-580.

Hardwick, K.G., R.C. Johnston, D.L. Smith, and A.W. Murray. 2000. MAD3 encodes a novel component of the spindle checkpoint which interacts with Bub3p, Cdc20p, and Mad2p. *J Cell Biol*. 148:871-882.

Hartwell, L.H. 1967. Macromolecule synthesis in temperature-sensitive mutants of yeast. *J Bacteriol*. 93:1662-1670.

Hartwell, L.H., J. Culotti, and B. Reid. 1970. Genetic control of the cell-division cycle in yeast. I. Detection of mutants. *Proc Natl Acad Sci U S A*. 66:352-359.

Henry, K.R., K. D'Hondt, J.S. Chang, D.A. Nix, M.J. Cope, C.S. Chan, D.G. Drubin, and S.K. Lemmon. 2003. The actin-regulating kinase Prk1p negatively regulates Scd5p, a suppressor of clathrin deficiency, in actin organization and endocytosis. *Curr Biol*. 13:1564-1569.

Hicke, L., and H. Riezman. 1996. Ubiquitination of a yeast plasma membrane receptor signals its ligand-stimulated endocytosis. *Cell*. 84:277-287.

Hicke, L., B. Zanolari, and H. Riezman. 1998. Cytoplasmic tail phosphorylation of the alpha-factor receptor is required for its ubiquitination and internalization. *J Cell Biol*. 141:349-358.

Higuchi, T., and F. Uhlmann. 2005. Stabilization of microtubule dynamics at anaphase onset promotes chromosome segregation. *Nature*. 433:171-176.

Hildebrandt, E.R., and M.A. Hoyt. 2001. Cell cycle-dependent degradation of the Saccharomyces cerevisiae spindle motor Cin8p requires APC(Cdh1) and a bipartite destruction sequence. *Mol Biol Cell*. 12:3402-3416.

Holt, L.J., B.B. Tuch, J. Villen, A.D. Johnson, S.P. Gygi, and D.O. Morgan. 2009. Global analysis of Cdk1 substrate phosphorylation sites provides insights into evolution. *Science*. 325:1682-1686.

Hsu, S.C., A.E. Ting, C.D. Hazuka, S. Davanger, J.W. Kenny, Y. Kee, and R.H. Scheller. 1996. The mammalian brain rsec6/8 complex. *Neuron*. 17:1209-1219.

Huang, B., G. Zeng, A.Y. Ng, and M. Cai. 2003. Identification of novel recognition motifs and regulatory targets for the yeast actin-regulating kinase Prk1p. *Mol Biol Cell*. 14:4871-4884.

Huckaba, T.M., A.C. Gay, L.F. Pantalena, H.C. Yang, and L.A. Pon. 2004. Live cell imaging of the assembly, disassembly, and actin cable-dependent movement of endosomes and actin patches in the budding yeast, Saccharomyces cerevisiae. *J Cell Biol*. 167:519-530.

Irniger, S., S. Piatti, C. Michaelis, and K. Nasmyth. 1995. Genes involved in sister chromatid separation are needed for B-type cyclin proteolysis in budding yeast. *Cell*. 81:269-278.

Jakobsen, M.K., Z. Cheng, S.K. Lam, E. Roth-Johnson, R.M. Barfield, and R. Schekman. 2013. Phosphorylation of Chs2p regulates interaction with COPII. *J Cell Sci*. 126:2151-2156.

Janke, C., M.M. Magiera, N. Rathfelder, C. Taxis, S. Reber, H. Maekawa, A. Moreno-Borchart, G. Doenges, E. Schwob, E. Schiebel, and M. Knop. 2004. A versatile toolbox for PCR-based tagging of yeast genes: new fluorescent proteins, more markers and promoter substitution cassettes. *Yeast*. 21:947-962.

Jaspersen, S.L., J.F. Charles, R.L. Tinker-Kulberg, and D.O. Morgan. 1998. A late mitotic regulatory network controlling cyclin destruction in Saccharomyces cerevisiae. *Mol Biol Cell*. 9:2803-2817.

Jenness, D.D., and P. Spatrick. 1986. Down regulation of the alpha-factor pheromone receptor in S. cerevisiae. *Cell*. 46:345-353.

Jin, F., H. Liu, F. Liang, R. Rizkallah, M.M. Hurt, and Y. Wang. 2008. Temporal control of the dephosphorylation of Cdk substrates by mitotic exit pathways in budding yeast. *Proc Natl Acad Sci U S A*. 105:16177-16182.

Johnson, A.E., and K.L. Gould. 2011. Dma1 ubiquitinates the SIN scaffold, Sid4, to impede the mitotic localization of Plo1 kinase. *Embo J*. 30:341-354.

Juang, Y.L., J. Huang, J.M. Peters, M.E. McLaughlin, C.Y. Tai, and D. Pellman. 1997. APC-mediated proteolysis of Ase1 and the morphogenesis of the mitotic spindle. *Science*. 275:1311-1314.

Kaksonen, M., Y. Sun, and D.G. Drubin. 2003. A pathway for association of receptors, adaptors, and actin during endocytic internalization. *Cell*. 115:475-487.

Kang, J., I.M. Cheeseman, G. Kallstrom, S. Velmurugan, G. Barnes, and C.S. Chan. 2001. Functional cooperation of Dam1, Ipl1, and the inner centromere protein (INCENP)-related protein Sli15 during chromosome segregation. *J Cell Biol*. 155:763-774.

Kao, L., Y.T. Wang, Y.C. Chen, S.F. Tseng, J.C. Jhang, Y.J. Chen, and S.C. Teng. 2014. Global analysis of cdc14 dephosphorylation sites reveals essential regulatory role in mitosis and cytokinesis. *Mol Cell Proteomics*. 13:594-605.

Kaur, S., A.B. Fielding, G. Gassner, N.J. Carter, and S.J. Royle. 2014. An unmet actin requirement explains the mitotic inhibition of clathrin-mediated endocytosis. *Elife*. 3:e00829.

Khmelinskii, A., C. Lawrence, J. Roostalu, and E. Schiebel. 2007. Cdc14-regulated midzone assembly controls anaphase B. *J Cell Biol*. 177:981-993.

Khmelinskii, A., J. Roostalu, H. Roque, C. Antony, and E. Schiebel. 2009. Phosphorylation-dependent protein interactions at the spindle midzone mediate cell cycle regulation of spindle elongation. *Dev Cell*. 17:244-256.

Kinoshita, E., E. Kinoshita-Kikuta, and T. Koike. 2009. Separation and detection of large phosphoproteins using Phos-tag SDS-PAGE. *Nat Protoc*. 4:1513-1521.

Kuranda MJ, R.P. 1991. Chitinase is required for cell separation during growth of Saccharomyces cerevisiae. *J Biol Chem*. 266:19758-19767.

Kurtz, M.B., and C.M. Douglas. 1997. Lipopeptide inhibitors of fungal glucan synthase. *J Med Vet Mycol*. 35:79-86.

Larson, D.R., D. Zenklusen, B. Wu, J.A. Chao, and R.H. Singer. 2011. Real-time observation of transcription initiation and elongation on an endogenous yeast gene. *Science*. 332:475-478.

Lau, D.T., and A.W. Murray. 2012. Mad2 and Mad3 cooperate to arrest budding yeast in mitosis. *Curr Biol*. 22:180-190.

Lederkremer, G.Z., Y. Cheng, B.M. Petre, E. Vogan, S. Springer, R. Schekman, T. Walz, and T. Kirchhausen. 2001. Structure of the Sec23p/24p and Sec13p/31p complexes of COPII. *Proc Natl Acad Sci U S A*. 98:10704-10709.

Lee, D.W., G.W. Ahn, H.G. Kang, and H.M. Park. 1999. Identification of a gene, SOO1, which complements osmo-sensitivity and defect in in vitro beta1,3-glucan synthase activity in Saccharomyces cerevisiae. *Biochim Biophys Acta*. 1450:145-154.

Lee, S.E., L.M. Frenz, N.J. Wells, A.L. Johnson, and L.H. Johnston. 2001. Order of function of the budding-yeast mitotic exit-network proteins Tem1, Cdc15, Mob1, Dbf2, and Cdc5. *Curr Biol*. 11:784-788.

Lesage, G., and H. Bussey. 2006. Cell wall assembly in Saccharomyces cerevisiae. *Microbiol Mol Biol Rev*. 70:317-343.

Lesage, G., J. Shapiro, C.A. Specht, A.M. Sdicu, P. Menard, S. Hussein, A.H. Tong, C. Boone, and H. Bussey. 2005. An interactional network of

genes involved in chitin synthesis in Saccharomyces cerevisiae. *BMC Genet*. 6:8.

Li, Y., and S.J. Elledge. 2003. The DASH complex component Ask1 is a cell cycle-regulated Cdk substrate in Saccharomyces cerevisiae. *Cell Cycle*. 2:143-148.

Lippincott, J., and R. Li. 1998. Sequential assembly of myosin II, an IQGAP-like protein, and filamentous actin to a ring structure involved in budding yeast cytokinesis. *J Cell Biol*. 140:355-366.

Liu, H., F. Liang, F. Jin, and Y. Wang. 2008. The coordination of centromere replication, spindle formation, and kinetochore-microtubule interaction in budding yeast. *PLoS Genet*. 4:e1000262.

Loog, M., and D.O. Morgan. 2005. Cyclin specificity in the phosphorylation of cyclin-dependent kinase substrates. *Nature*. 434:104-108.

Looke, M., K. Kristjuhan, and A. Kristjuhan. 2011. Extraction of genomic DNA from yeasts for PCR-based applications. *Biotechniques*. 50:325-328.

Lord, M., E. Laves, and T.D. Pollard. 2005. Cytokinesis depends on the motor domains of myosin-II in fission yeast but not in budding yeast. *Mol Biol Cell*. 16:5346-5355.

Mah, A.S., J. Jang, and R.J. Deshaies. 2001. Protein kinase Cdc15 activates the Dbf2-Mob1 kinase complex. *Proc Natl Acad Sci U S A*. 98:7325-7330.

Makarow, M. 1988. Secretion of invertase in mitotic yeast cells. *Embo J*. 7:1475-1482.

Manzoni, R., F. Montani, C. Visintin, F. Caudron, A. Ciliberto, and R. Visintin. 2010. Oscillations in Cdc14 release and sequestration reveal a circuit underlying mitotic exit. *J Cell Biol*. 190:209-222.

Marchal, C., R. Haguenauer-Tsapis, and D. Urban-Grimal. 1998. A PEST-like sequence mediates phosphorylation and efficient ubiquitination of yeast uracil permease. *Mol Cell Biol*. 18:314-321.

Marchal, C., R. Haguenauer-Tsapis, and D. Urban-Grimal. 2000. Casein kinase I-dependent phosphorylation within a PEST sequence and ubiquitination at nearby lysines signal endocytosis of yeast uracil permease. *J Biol Chem*. 275:23608-23614.

Martinez-Rucobo, F.W., L. Eckhardt-Strelau, and A.C. Terwisscha van Scheltinga. 2009. Yeast chitin synthase 2 activity is modulated by proteolysis and phosphorylation. *Biochem J*. 417:547-554.

Matsuoka, K., L. Orci, M. Amherdt, S.Y. Bednarek, S. Hamamoto, R. Schekman, and T. Yeung. 1998. COPII-coated vesicle formation reconstituted with purified coat proteins and chemically defined liposomes. *Cell*. 93:263-275.

Mazur, P., N. Morin, W. Baginsky, M. el-Sherbeini, J.A. Clemas, J.B. Nielsen, and F. Foor. 1995. Differential expression and function of two homologous subunits of yeast 1,3-beta-D-glucan synthase. *Mol Cell Biol*. 15:5671-5681.

Meitinger, F., B. Petrova, I.M. Lombardi, D.T. Bertazzi, B. Hub, H. Zentgraf, and G. Pereira. 2010. Targeted localization of Inn1, Cyk3 and Chs2 by the mitotic-exit network regulates cytokinesis in budding yeast. *J Cell Sci*. 123:1851-1861.

Miller, E., B. Antonny, S. Hamamoto, and R. Schekman. 2002. Cargo selection into COPII vesicles is driven by the Sec24p subunit. *Embo J*. 21:6105-6113.

Miller, E.A., T.H. Beilharz, P.N. Malkus, M.C. Lee, S. Hamamoto, L. Orci, and R. Schekman. 2003. Multiple cargo binding sites on the COPII subunit Sec24p ensure capture of diverse membrane proteins into transport vesicles. *Cell*. 114:497-509.

Mohl, D.A., M.J. Huddleston, T.S. Collingwood, R.S. Annan, and R.J. Deshaies. 2009. Dbf2-Mob1 drives relocalization of protein phosphatase Cdc14 to the cytoplasm during exit from mitosis. *J Cell Biol*. 184:527-539.

Montpetit, B., T.R. Hazbun, S. Fields, and P. Hieter. 2006. Sumoylation of the budding yeast kinetochore protein Ndc10 is required for Ndc10 spindle localization and regulation of anaphase spindle elongation. *J Cell Biol*. 174:653-663.

Mukherjee, D., B.G. Coon, D.F. Edwards, 3rd, C.B. Hanna, S.A. Longhi, J.M. McCaffery, B. Wendland, L.A. Retegui, E. Bi, and R.C. Aguilar. 2009. The yeast endocytic protein Epsin 2 functions in a cell-division signaling pathway. *J Cell Sci*. 122:2453-2463.

Mulholland, J., A. Wesp, H. Riezman, and D. Botstein. 1997. Yeast actin cytoskeleton mutants accumulate a new class of Golgi-derived secretary vesicle. *Mol Biol Cell*. 8:1481-1499.

Nevalainen, L.T., J. Louhelainen, and M. Makarow. 1989. Post-translational modifications in mitotic yeast cells. *Eur J Biochem*. 184:165-172.

Nevalainen, L.T., and M. Makarow. 1991. Uptake of endocytic markers into mitotic yeast cells. *FEBS Lett*. 282:166-169.

Nigg, E.A. 2001. Mitotic kinases as regulators of cell division and its checkpoints. *Nat Rev Mol Cell Biol*. 2:21-32.

Nishihama, R., J.H. Schreiter, M. Onishi, E.A. Vallen, J. Hanna, K. Moravcevic, M.F. Lippincott, H. Han, M.A. Lemmon, J.R. Pringle, and E. Bi. 2009. Role of Inn1 and its interactions with Hof1 and Cyk3 in promoting cleavage furrow and septum formation in S. cerevisiae. *J Cell Biol*. 185:995-1012.

Noton, E., and J.F. Diffley. 2000. CDK inactivation is the only essential function of the APC/C and the mitotic exit network proteins for origin resetting during mitosis. *Mol Cell*. 5:85-95.

Novick, P., C. Field, and R. Schekman. 1980. Identification of 23 complementation groups required for post-translational events in the yeast secretory pathway. *Cell*. 21:205-215.

Oh, Y., K.J. Chang, P. Orlean, C. Wloka, R. Deshaies, and E. Bi. 2012. Mitotic exit kinase Dbf2 directly phosphorylates chitin synthase Chs2 to regulate cytokinesis in budding yeast. *Mol Biol Cell*. 23:2445-2456.

Orlean, P. 2012. Architecture and biosynthesis of the Saccharomyces cerevisiae cell wall. *Genetics*. 192:775-818.

Palani, S., F. Meitinger, M.E. Boehm, W.D. Lehmann, and G. Pereira. 2012. Cdc14-dependent dephosphorylation of Inn1 contributes to Inn1-Cyk3 complex formation. *J Cell Sci*. 125:3091-3096.

Pammer, M., P. Briza, A. Ellinger, T. Schuster, R. Stucka, H. Feldmann, and M. Breitenbach. 1992. DIT101 (CSD2, CAL1), a cell cycle-regulated yeast gene required for synthesis of chitin in cell walls and chitosan in spore walls. *Yeast*. 8:1089-1099.

Park, C.J., J.E. Park, T.S. Karpova, N.K. Soung, L.R. Yu, S. Song, K.H. Lee, X. Xia, E. Kang, I. Dabanoglu, D.Y. Oh, J.Y. Zhang, Y.H. Kang, S. Wincovitch, T.C. Huffaker, T.D. Veenstra, J.G. McNally, and K.S. Lee. 2008. Requirement for the budding yeast polo kinase Cdc5 in proper microtubule growth and dynamics. *Eukaryot Cell*. 7:444-453.

Pereira, G., T. Hofken, J. Grindlay, C. Manson, and E. Schiebel. 2000. The Bub2p spindle checkpoint links nuclear migration with mitotic exit. *Mol Cell*. 6:1-10.

Pereira, G., and E. Schiebel. 2003. Separase regulates INCENP-Aurora B anaphase spindle function through Cdc14. *Science*. 302:2120-2124.

Peters, J.M. 2006. The anaphase promoting complex/cyclosome: a machine designed to destroy. *Nat Rev Mol Cell Biol*. 7:644-656.

Pfau, S.J., and A. Amon. 2012. Chromosomal instability and aneuploidy in cancer: from yeast to man. *EMBO Rep*. 13:515-527.

Pruyne, D., and A. Bretscher. 2000. Polarization of cell growth in yeast. *J Cell Sci*. 113 (Pt 4):571-585.

Pruyne, D.W., D.H. Schott, and A. Bretscher. 1998. Tropomyosin-containing actin cables direct the Myo2p-dependent polarized delivery of secretory vesicles in budding yeast. *J Cell Biol*. 143:1931-1945.

Ptacek, J., G. Devgan, G. Michaud, H. Zhu, X. Zhu, J. Fasolo, H. Guo, G. Jona, A. Breitkreutz, R. Sopko, R.R. McCartney, M.C. Schmidt, N. Rachidi, S.J. Lee, A.S. Mah, L. Meng, M.J. Stark, D.F. Stern, C. De Virgilio, M. Tyers, B. Andrews, M. Gerstein, B. Schweitzer, P.F. Predki, and M. Snyder. 2005. Global analysis of protein phosphorylation in yeast. *Nature*. 438:679-684.

Queralt, E., C. Lehane, B. Novak, and F. Uhlmann. 2006. Downregulation of PP2A(Cdc55) phosphatase by separase initiates mitotic exit in budding yeast. *Cell*. 125:719-732.

Queralt, E., and F. Uhlmann. 2008a. Cdk-counteracting phosphatases unlock mitotic exit. *Curr Opin Cell Biol*. 20:661-668.

Queralt, E., and F. Uhlmann. 2008b. Separase cooperates with Zds1 and Zds2 to activate Cdc14 phosphatase in early anaphase. *J Cell Biol*. 182:873-883.

Robinson, L.C., C. Bradley, J.D. Bryan, A. Jerome, Y. Kweon, and H.R. Panek. 1999. The Yck2 yeast casein kinase 1 isoform shows cell cycle-specific localization to sites of polarized growth and is required for proper septin organization. *Mol Biol Cell*. 10:1077-1092.

Robinson, L.C., E.J. Hubbard, P.R. Graves, A.A. DePaoli-Roach, P.J. Roach, C. Kung, D.W. Haas, C.H. Hagedorn, M. Goebl, M.R. Culbertson, and et al. 1992. Yeast casein kinase I homologues: an essential gene pair. *Proc Natl Acad Sci U S A*. 89:28-32.

Robinson, L.C., M.M. Menold, S. Garrett, and M.R. Culbertson. 1993. Casein kinase I-like protein kinases encoded by YCK1 and YCK2 are required for yeast morphogenesis. *Mol Cell Biol*. 13:2870-2881.

Roncero, C., and A. Duran. 1985. Effect of Calcofluor white and Congo red on fungal cell wall morphogenesis: in vivo activation of chitin polymerization. *J Bacteriol*. 163:1180-1185.

Roncero, C., M.H. Valdivieso, J.C. Ribas, and A. Duran. 1988. Effect of calcofluor white on chitin synthases from Saccharomyces cerevisiae. *J Bacteriol*. 170:1945-1949.

Russell, P., S. Moreno, and S.I. Reed. 1989. Conservation of mitotic controls in fission and budding yeasts. *Cell*. 57:295-303.

Schekman, R. 2010. Charting the secretory pathway in a simple eukaryote. *Mol Biol Cell*. 21:3781-3784.

Schmidt, M., B. Bowers, A. Varma, D.H. Roh, and E. Cabib. 2002. In budding yeast, contraction of the actomyosin ring and formation of the primary septum at cytokinesis depend on each other. *J Cell Sci*. 115:293-302.

Schultz, M. 2008. Rudolf Virchow. *Emerg Infect Dis*. Vol. 14:1480-1481.

Schweitzer, J.K., E.E. Burke, H.V. Goodson, and C. D'Souza-Schorey. 2005. Endocytosis resumes during late mitosis and is required for cytokinesis. *J Biol Chem*. 280:41628-41635.

Sheff, M.A., and K.S. Thorn. 2004. Optimized cassettes for fluorescent protein tagging in Saccharomyces cerevisiae. *Yeast*. 21:661-670.

Shou, W., R. Azzam, S.L. Chen, M.J. Huddleston, C. Baskerville, H. Charbonneau, R.S. Annan, S.A. Carr, and R.J. Deshaies. 2002. Cdc5 influences phosphorylation of Net1 and disassembly of the RENT complex. *BMC Mol Biol*. 3:3.

Shou, W., J.H. Seol, A. Shevchenko, C. Baskerville, D. Moazed, Z.W. Chen, J. Jang, H. Charbonneau, and R.J. Deshaies. 1999. Exit from mitosis is triggered by Tem1-dependent release of the protein phosphatase Cdc14 from nucleolar RENT complex. *Cell*. 97:233-244.

Silverman, S.J., A. Sburlati, M.L. Slater, and E. Cabib. 1988. Chitin synthase 2 is essential for septum formation and cell division in Saccharomyces cerevisiae. *Proc Natl Acad Sci U S A*. 85:4735-4739.

Smythe, E., and K.R. Ayscough. 2006. Actin regulation in endocytosis. *J Cell Sci*. 119:4589-4598.

Spellman, P.T., G. Sherlock, M.Q. Zhang, V.R. Iyer, K. Anders, M.B. Eisen, P.O. Brown, D. Botstein, and B. Futcher. 1998. Comprehensive identification of cell cycle-regulated genes of the yeast Saccharomyces cerevisiae by microarray hybridization. *Mol Biol Cell*. 9:3273-3297.

Stegmeier, F., and A. Amon. 2004. Closing mitosis: the functions of the Cdc14 phosphatase and its regulation. *Annu Rev Genet*. 38:203-232.

Tacheva-Grigorova, S.K., A.J. Santos, E. Boucrot, and T. Kirchhausen. 2013. Clathrin-mediated endocytosis persists during unperturbed mitosis. *Cell Rep*. 4:659-668.

Taxis, C., and M. Knop. 2006. System of centromeric, episomal, and integrative vectors based on drug resistance markers for Saccharomyces cerevisiae. *Biotechniques*. 40:73-78.

Teh, E.M., C.C. Chai, and F.M. Yeong. 2009. Retention of Chs2p in the ER requires N-terminal CDK1-phosphorylation sites. *Cell Cycle*. 8:2964-2974.

TerBush, D.R., T. Maurice, D. Roth, and P. Novick. 1996. The Exocyst is a multiprotein complex required for exocytosis in Saccharomyces cerevisiae. *Embo J*. 15:6483-6494.

Tirnauer, J.S., E. O'Toole, L. Berrueta, B.E. Bierer, and D. Pellman. 1999. Yeast Bim1p promotes the G1-specific dynamics of microtubules. *J Cell Biol*. 145:993-1007.

Tomson, B.N., R. Rahal, V. Reiser, F. Monje-Casas, K. Mekhail, D. Moazed, and A. Amon. 2009. Regulation of Spo12 phosphorylation and its essential role in the FEAR network. *Curr Biol*. 19:449-460.

Toshima, J.Y., J. Nakanishi, K. Mizuno, J. Toshima, and D.G. Drubin. 2009. Requirements for recruitment of a G protein-coupled receptor to clathrin-coated pits in budding yeast. *Mol Biol Cell*. 20:5039-5050.

Toshima, J.Y., J. Toshima, M. Kaksonen, A.C. Martin, D.S. King, and D.G. Drubin. 2006. Spatial dynamics of receptor-mediated endocytic trafficking in budding yeast revealed by using fluorescent alpha-factor derivatives. *Proc Natl Acad Sci U S A*. 103:5793-5798.

Traverso, E.E., C. Baskerville, Y. Liu, W. Shou, P. James, R.J. Deshaies, and H. Charbonneau. 2001. Characterization of the Net1 cell cycle-dependent regulator of the Cdc14 phosphatase from budding yeast. *J Biol Chem*. 276:21924-21931.

Ubersax, J.A., E.L. Woodbury, P.N. Quang, M. Paraz, J.D. Blethrow, K. Shah, K.M. Shokat, and D.O. Morgan. 2003. Targets of the cyclin-dependent kinase Cdk1. *Nature*. 425:859-864.

Uhlmann, F., D. Wernic, M.A. Poupart, E.V. Koonin, and K. Nasmyth. 2000. Cleavage of cohesin by the CD clan protease separin triggers anaphase in yeast. *Cell*. 103:375-386.

Urbaniak, M.D. 2009. Casein kinase 1 isoform 2 is essential for bloodstream form Trypanosoma brucei. *Mol Biochem Parasitol*. 166:183-185.

Vancura, A., A. Sessler, B. Leichus, and J. Kuret. 1994. A prenylation motif is required for plasma membrane localization and biochemical function of casein kinase I in budding yeast. *J Biol Chem*. 269:19271-19278.

Varga, V., J. Helenius, K. Tanaka, A.A. Hyman, T.U. Tanaka, and J. Howard. 2006. Yeast kinesin-8 depolymerizes microtubules in a length-dependent manner. *Nat Cell Biol*. 8:957-962.

VerPlank, L., and R. Li. 2005. Cell cycle-regulated trafficking of Chs2 controls actomyosin ring stability during cytokinesis. *Mol Biol Cell*. 16:2529-2543.

Visintin, C., B.N. Tomson, R. Rahal, J. Paulson, M. Cohen, J. Taunton, A. Amon, and R. Visintin. 2008. APC/C-Cdh1-mediated degradation of the Polo kinase Cdc5 promotes the return of Cdc14 into the nucleolus. *Genes Dev*. 22:79-90.

Visintin, R., K. Craig, E.S. Hwang, S. Prinz, M. Tyers, and A. Amon. 1998. The phosphatase Cdc14 triggers mitotic exit by reversal of Cdk-dependent phosphorylation. *Mol Cell*. 2:709-718.

Visintin, R., E.S. Hwang, and A. Amon. 1999. Cfi1 prevents premature exit from mitosis by anchoring Cdc14 phosphatase in the nucleolus. *Nature*. 398:818-823.

Visintin, R., S. Prinz, and A. Amon. 1997. CDC20 and CDH1: a family of substrate-specific activators of APC-dependent proteolysis. *Science*. 278:460-463.

Wang, P.C., A. Vancura, T.G. Mitcheson, and J. Kuret. 1992. Two genes in Saccharomyces cerevisiae encode a membrane-bound form of casein kinase-1. *Mol Biol Cell*. 3:275-286.

Wang, Y., F. Hu, and S.J. Elledge. 2000. The Bfa1/Bub2 GAP complex comprises a universal checkpoint required to prevent mitotic exit. *Curr Biol*. 10:1379-1382.

Wang, Y., and T.Y. Ng. 2006. Phosphatase 2A negatively regulates mitotic exit in Saccharomyces cerevisiae. *Mol Biol Cell*. 17:80-89.

Weinberg, J., and D.G. Drubin. 2012. Clathrin-mediated endocytosis in budding yeast. *Trends Cell Biol*. 22:1-13.

Weiss, E.L. 2012. Mitotic exit and separation of mother and daughter cells. *Genetics*. 192:1165-1202.

Winey, M., and K. Bloom. 2012. Mitotic spindle form and function. *Genetics*. 190:1197-1224.

Wloka, C., R. Nishihama, M. Onishi, Y. Oh, J. Hanna, J.R. Pringle, M. Krauss, and E. Bi. 2011. Evidence that a septin diffusion barrier is dispensable for cytokinesis in budding yeast. *Biol Chem*. 392:813-829.

Woodbury, E.L., and D.O. Morgan. 2007. Cdk and APC activities limit the spindle-stabilizing function of Fin1 to anaphase. *Nat Cell Biol*. 9:106-112.

Woodruff, J.B., D.G. Drubin, and G. Barnes. 2010. Mitotic spindle disassembly occurs via distinct subprocesses driven by the anaphase-promoting complex, Aurora B kinase, and kinesin-8. *J Cell Biol*. 191:795-808.

Woodruff, J.B., D.G. Drubin, and G. Barnes. 2012. Spindle assembly requires complete disassembly of spindle remnants from the previous cell cycle. *Mol Biol Cell*. 23:258-267.

Wurzenberger, C., and D.W. Gerlich. 2011. Phosphatases: providing safe passage through mitotic exit. *Nat Rev Mol Cell Biol*. 12:469-482.

Yanagida, M. 1998. Fission yeast cut mutations revisited: control of anaphase. *Trends Cell Biol*. 8:144-149.

Yellman, C.M., and D.J. Burke. 2006. The role of Cdc55 in the spindle checkpoint is through regulation of mitotic exit in Saccharomyces cerevisiae. *Mol Biol Cell*. 17:658-666.

Yeong, F.M. 2005. Severing all ties between mother and daughter: cell separation in budding yeast. *Mol Microbiol*. 55:1325-1331.

Yeong, F.M., H.H. Lim, C.G. Padmashree, and U. Surana. 2000. Exit from mitosis in budding yeast: biphasic inactivation of the Cdc28-Clb2 mitotic kinase and the role of Cdc20. *Mol Cell*. 5:501-511.

Yeong, F.M., H.H. Lim, and U. Surana. 2002. MEN, destruction and separation: mechanistic links between mitotic exit and cytokinesis in budding yeast. *Bioessays*. 24:659-666.

Yoshida, S., S. Bartolini, and D. Pellman. 2009. Mechanisms for concentrating Rho1 during cytokinesis. *Genes Dev*. 23:810-823.

Yoshihisa, T., C. Barlowe, and R. Schekman. 1993. Requirement for a GTPase-activating protein in vesicle budding from the endoplasmic reticulum. *Science*. 259:1466-1468.

Yu, H. 2002. Regulation of APC-Cdc20 by the spindle checkpoint. *Curr Opin Cell Biol*. 14:706-714.

Zeng, G., B. Huang, S.P. Neo, J. Wang, and M. Cai. 2007. Scd5p mediates phosphoregulation of actin and endocytosis by the type 1 phosphatase Glc7p in yeast. *Mol Biol Cell*. 18:4885-4898.

Zeng, G., Y.M. Wang, and Y. Wang. 2012. Cdc28-Cln3 phosphorylation of Sla1 regulates actin patch dynamics in different modes of fungal growth. *Mol Biol Cell*. 23:3485-3497.

Zeng, G., X. Yu, and M. Cai. 2001. Regulation of yeast actin cytoskeleton-regulatory complex Pan1p/Sla1p/End3p by serine/threonine kinase Prk1p. *Mol Biol Cell*. 12:3759-3772.

Zeng, X., J.A. Kahana, P.A. Silver, M.K. Morphew, J.R. McIntosh, I.T. Fitch, J. Carbon, and W.S. Saunders. 1999. Slk19p is a centromere protein that functions to stabilize mitotic spindles. *J Cell Biol*. 146:415-425.

Zhai, Y., P.Y. Yung, L. Huo, and C. Liang. 2010. Cdc14p resets the competency of replication licensing by dephosphorylating multiple initiation proteins during mitotic exit in budding yeast. *J Cell Sci*. 123:3933-3943.

Zhang, G., R. Kashimshetty, K.E. Ng, H.B. Tan, and F.M. Yeong. 2006. Exit from mitosis triggers Chs2p transport from the endoplasmic reticulum to mother-daughter neck via the secretory pathway in budding yeast. *J Cell Biol*. 174:207-220.

Ziman, M., J.S. Chuang, M. Tsung, S. Hamamoto, and R. Schekman. 1998. Chs6p-dependent anterograde transport of Chs3p from the chitosome to the plasma membrane in Saccharomyces cerevisiae. *Mol Biol Cell*. 9:1565-1576.

Zimniak, T., K. Stengl, K. Mechtler, and S. Westermann. 2009. Phosphoregulation of the budding yeast EB1 homologue Bim1p by Aurora/Ipl1p. *J Cell Biol*. 186:379-391.